Integrated Watershed and River Modeling Study of the Pawtuxet River, Rhode Island

M Reza Hashemi [1,2], Soroush Kouhi [1], Rozita Kian [1], Malcolm Spaulding [1,5], Stephanie Steele [1], Chris Damon [4] and James Boyd [3]

[1] *Department of Ocean Engineering, University of Rhode Island, Narragansett, RI*

[2] *Graduate School of Oceanography, University of Rhode Island, Narragansett, RI*

[3] *Rhode Island Coastal Resources Management Council, Wakefield, RI*

[4] *Environmental Data Center, University of Rhode Island, Kingston, RI*

[5] *Spaulding Environmental Associates, LLC, RI*

August 24, 2017

University of Rhode Island, 215 S Ferry Rd, Narragansett, RI, USA

Prepared for RI Coastal Resources Management Council (CRMC)

Acknowledgements

This study was carried out under a cooperative agreement with the Rhode Island Coastal Resources Council with funding from the U.S. Department of Housing and Urban Development Community Development Block Grant administered by the Rhode Island Office of Housing and Community Development. Many thanks to David Vallee (NWS), Steve Soito (Providence Water Supply), Gardner Bent (USGS), John Fonseca (Flat River Reservoir), Alisa Richardson (RI DEM), J. Matthew Bellisle (Pare Corporation), and Art Gold (URI) for their providing data, help, and information. We thank Laura Sullivan, Disaster Recovery Program Manager, Office of Housing and Community Development, RI for supporting this project.

Contents

Abbreviations **17**

1 Executive Summary **19**

Executive Summary **19**

2 Introduction **22**

2.1 Motivation 22
2.2 Objectives 26
2.3 Deliverables 26

3 Watershed and River Data **28**

3.1 Units and Datum 28
3.2 Geospatial Data 29
3.2.1 The Pawtuxet River Watershed 29
3.2.2 Digital Elevation Model 31
3.2.3 Land Use/Land Cover Data 31
3.2.4 Soil Type Data 31
3.2.5 Scituate Reservoir 36
3.2.6 The Flat River Reservoir 39
3.2.7 River Structures 40
3.3 Precipitation Data 40
3.3.1 Precipitation Data 40
3.3.2 Hindcast Precipitation Data 42
3.3.3 Spatial Variability of Rainfall Over Watershed 43
3.3.4 Intensity-Duration-Frequency Curves 47
3.3.5 Climate Change Effects on Precipitation in New England 49
3.4 Flow Data 50
3.4.1 Observed Data 50
3.4.2 Annual Exceedance Probability of Flood Peaks 52
3.4.3 Contributions of the Subbasin Branches of the Pawtuxet River to the Discharge Values 54

4 Methodology **56**

4.1 Overview 56

4.2 HEC-GeoHMS . . . 57
4.3 HEC-HMS . . . 58
4.3.1 Runoff/Infiltration Formulation . . . 58
4.3.2 Calibration Process . . . 59
4.3.3 Uncertainty Analysis . . . 60
4.3.4 Hydrologic Reservoir Routing . . . 61
4.4 HEC-GeoRAS . . . 62
4.5 HEC-RAS . . . 62
4.5.1 Steady State Flow Simulation . . . 64
4.5.2 Unsteady Flow Formulation . . . 65
4.5.3 Simulation of Dams in HEC-RAS . . . 66

5 Development of Hydrologic/Hydraulic models 68
5.1 Watershed Model . . . 68
5.1.1 Terrain Processing . . . 68
5.1.2 Subbasin Delineation . . . 70
5.1.3 Infiltration Map . . . 72
5.1.4 Rainfall-Runoff Modeling . . . 73
5.2 River Model . . . 75
5.2.1 River Structures . . . 75
5.2.2 River Geometry . . . 76
5.2.3 Updating River Cross Sections . . . 78
5.2.4 Steady Flow Simulation . . . 79
5.2.5 Event Profiles . . . 81
5.2.6 Unsteady Flow Simulation Settings . . . 82

6 Results and Discussion 84
6.1 HEC-HMS Model Results . . . 84
6.1.1 HEC-HMS Model Calibration . . . 84
6.1.2 Validation . . . 85
6.1.3 Uncertainty Analysis . . . 87
6.1.4 Effect of the Scituate Reservoir on Flooding . . . 91
6.1.5 Effect of the Flat River Reservoir . . . 95
6.2 River Modeling Results . . . 97
6.2.1 Comparison with the FEMA Maps . . . 97
6.2.2 HEC-RAS Unsteady Flow Results . . . 97
6.2.3 Integration of floodmaps to STORMTOOLS . . . 100

6.2.4 Effect of Historical Dams on Flooding 102
6.2.4.1 Analysis of Dam Removals in the Main Branch 102
6.2.4.2 Analysis of the Removal of the Dams in the North Branch . 109
6.2.4.3 Analysis of Dam Removal in the South Branch 115
6.2.4.4 Summary of Effect of Dams on Flooding 117
6.2.5 Effects of Debris on Flooding 124
6.2.6 Effect of Sea Level Rise and Storm Surge on Flooding 130
6.2.7 Flood Mitigation at the Warwick Wastewater Treatment Facility . . . 133

7 Summary and Conclusions **138**
7.1 Overview of the Results 138
7.2 Main Contributions 138
7.3 Recommendations 140

Appendix A Streamflow Data in Selected USGS Stations **141**

List of Figures

1 Map of the Pawtuxet River watershed. Top map shows watershed border outlined in red, Flat River Reservoir highlighted in blue, and Scituate Reservoir highlighted in cyan. Bottom map shows zoomed-out view of the watershed, in and the surrounding states. 22
2 A textile factory along the South Branch of the Pawtuxet River in Coventry, RI. 23
3 Warwick Mall flooded in 2010, Source: NOAA 24
4 Flood history at the USGS streamgauge location in Cranston, RI on the Pawtuxet River from 1940-2013. The color of the bar indicates the severity of the flood. Notice the dramatic increase in both frequency of flooding since the late 1960's, the frequency of multiple floods in a given year, and the severity of these floods. Floods in the major category approximate the 100 year base flood elevation based on FEMA Flood Insurance Rate Maps (FIRMs), Source: David Vallee NOAA NWS NERFC 25
5 NAVD 88, MHW and NGVD 29 datums difference in Providence Station 8454000 at -71.4133° longitude and 41.8239° latitude. 28
6 Pawtuxet River Watershed with surface area (left) area upstream of the Scituate Reservoir outlined and shaded in green (A), area upstream of the USGS 01116000 in the South Branch outlined and shaded in pink (B), rest of the watershed are outlined in orange (C); (right) upstream of the Cranston USGS station gauge shaded and outlined in cyan (D), and downstream area of the Cranston gauge outlined in purple (E). See Table 1. 30
7 Pawtuxet River Watershed Digital Elevation Model (DEM in NAVD 88), Source: RIGIS. 32
8 Land cover of the Pawtuxet River Watershed in 2011, Source: RIGIS. See Table 2 for legend decsription. 33
9 Map of the Pawtuxet Watershed soil type data. Yellow depicts water areas. . 35
10 The Scituate Reservoir. The photo is taken from the Scituate Avenue looking toward NW. 36
11 Elevation-storage graph of the Scituate Reservoir; Source: Providence Water Supply. 37
12 Scituate Reservoir cross section details, source: Providence Water Supply. . . 38
13 The Flat River Reservoir and Spillway. 39

14 Location of precipitation station/nodes used for the watershed model. Red star shows the observational precipitation gauge and yellow shows the CFSR model nodes. . . . 41
15 Precipitation data recorded in March 2010 from the hourly observed gauge at T.F. Green Airport, RI (1 mm = 0.039 in). . . . 42
16 Daily precipitation (2008-2012) at CFSR model nodes 1, 2, 3, 4, 5, 6, 7, 8 and 9. See Figure 14 for node locations (1 mm = 0.039 in). . . . 44
17 Comparison of daily observed precipitation data of Warwick land-based station with daily CFSR model precipitation in nodes 2, 4, 5, and 8. . . . 45
18 Comparison of spatial distribution of daily precipitation at CFSR model nodes a) 2 & 5, b) 4 & 5, c) 6 & 5 and d) 8 & 5. . . . 46
19 Annual Intensity-Duration-Frequency (IDF) curves at Warwick, RI. . . . 48
20 Rhode Island average precipitation from 1960, projected to 2099. Two projections are shown: one based on lower emissions and the other based on the higher emissions scenario; a) summer and b) winter precipitation averages. Source: CSNE . . . 49
21 USGS stream gauge stations in the Pawtuxet River Watershed, RI. . . . 51
22 Hourly streamflow 2008–2013 at (a) Cranston, The Main Branch of the Pawtuxet River, RI and (b) Washington in the South Branch of the Pawtuxet River, RI. . . . 52
23 Peak discharge (left) and peak discharge ratios (right) the North Branch, South Branch, and Main Branch of the Pawtuxet River, for 10-, 50-, 100-, and 500-year return period flood events. Discharge ratios are the peak flow discharges of the North Branch and South Branch divided by the observed flow in Cranston along the Main Branch. . . . 54
24 Hydrologic processes from precipitation to discharge in a watershed (Feldman, 2000). . . . 56
25 Flowchart of distributed hydrologic and hydraulic modeling of flow in watersheds (Knebl et al., 2005). . . . 57
26 Calibration process in a hydrological model (Feldman, 2000). . . . 60
27 Inflow and outflow hydrograph from a reservoir spillway crest. . . . 61
28 Flowchart of HEC-RAS and HEC-GeoRAS for flood simulation (Ackerman, 2009). . . . 63
29 Energy equation terms (Brunner, 2016). . . . 64
30 Cross section divisions in HEC-RAS model (Brunner, 2016). . . . 65
31 Control volume for mass and momentum conservation (Brunner, 2016). . . . 66

32 Discharge coefficient of an ogee spillway as a function of energy head, H_e. C is the coefficient of discharge for an arbitrary energy head (i.e., H_e), C_0 is the coefficient of discharge at the design head H_o (corresponding to the design discharge, e.g., 200-year) (USBR, 1977). 67
33 Preliminary steps in preparing data for the terrain analysis, prior to subbasin delineation in HEC-GeoHMS (1 m = 3.28 ft). 69
34 Subbasin delineation for watershed model with 24 and 9 subbasins. Locations of USGS stream gauges are shown in yellow circles. 70
35 Modeling of the Pawtuxet River watershed with 24 and 9 subbasins in HEC-HMS. 72
36 Curve Number (CN) map of the Pawtuxet River Watershed. 74
37 Pawtuxet Falls Dam partial removal, Fall 2011, Source: NBEP. 76
38 Warwick Waste Water Treatment flooded during spring 2010. 77
39 Examples of bridge structures models. The Pawtuxet Village Bridge (left), and I-295 West Ramp Bridge (right). 77
40 Comparing topography and bathymetry data from HEC-RAS and LiDAR DEM for a non-surveyed channel on the North Branch, as an example. . . . 78
41 Comparing topography and bathymetry data from HEC-RAS and LiDAR DEM for a surveyed channel on the North Branch, as an example. 78
42 Missed inundation areas caused by short cross sections in HEC-RAS model (original USGS) in North Branch of the Pawtuxet River (top) and the revised model (this study) including elongated cross sections (bottom). 80
43 Updating cross sections in the North Branch of the Pawtuxet River: before (left), and after (right) lengthening of cross section cutlines. 81
44 Updating cross sections in the South Branch of the Pawtuxet River: before (left), and after (right) lengthening of cross section cutlines. 81
45 Hydrographs for the original model, observed data, and calibrated model for Event #1 at USGS stations 01116500 in Cranston and 01116000 in the South Branch. 86
46 Hydrographs for the original model, observed data, and calibrated model for Event #2 at USGS stations 01116500 in Cranston and 01116000 in the South Branch. 86
47 Validation of the calibrated watershed model using events in Jun 1982 and Jun 2006 at Cranston station 01116500. Errors are calculated based on the observed and modeled peak flow in each event : $Er = \left(|Q_p^{Obs} - Q_p^{Mod}|\right)/Q_p^{Obs}$. The precipitation data were daily for these simulations. 87

48 Daily precipitation data for mid-March through early April, 2010 from Warwick meteorological station as well as NWS, CSFR, and ECMWF hindcasts. 88
49 (a) 90% confidence intervals for the daily precipitation data and (b) precipitation from observed, ECMWF, CFSR, and NWS sources, along with upper and lower 90% confidence limits, mid-March through early April 2010. 89
50 (a) 80% confidence intervals for the daily precipitation data and (b) precipitation from observed, ECMWF, CFSR, and NWS sources, along with upper and lower 80% confidence limits, during mid-March through early April 2010. 89
51 (a) HEC-HMS outflow results for the precipitation at 90% confidence interval and (b) outflow results when forced with observed, ECMWF, CFSR, NWS, upper 90% limit, and lower 90% limit. Observed outflow at Cranston are also plotted for comparison. 90
52 (a) HEC-HMS outflow results for the precipitation at 80% confidence interval and (b) outflow results when forced with observed, ECMWF, CFSR, NWS, upper 80% limit, and lower 80% limit. Observed outflow at the Cranston gauge are also plotted for comparison. 90
53 Volume of runoff generated upstream of the Scituate Reservoir versus cumulative precipitation is shown in the bottom plot. The maximum water elevation that is required to trap the runoff (below the spillway crest) in the reservoir is shown on the top plot. The flood capacity is provided by the difference of the spillway crest elevation (284 ft) and water elevation. Datum is MHW. Reservoir drainage area is 91 mi^2 and the surface area of the reservoir is 5.3 mi^2. Note that at 284.0 ft (MHW) the volume is zero (MHW=NAVD88-2.12 at this location). 91
54 Photo of flashboards in the Scituate Reservoir spillway. Red arrows show the flashboards. 92
55 Comparison of flow over Gainer Dam Spillway versus water elevation in the reservoir for three scenarios: without flashboard, one flashboard, and two flashboards. Source of data: Providence Water Supply. 93
56 Comparison of Gainer Dam spillway outflow using HEC-HMS, data provided by the dam authorities, and ogee spillway formula. The spillway crest elevation is 286.12 ft (NAVD88). 93

57 Inflow and outflow of the ogee spillway in the Scituate Reservoir when the reservoir is assumed at the full capacity. Inflow is based on hourly data of Event #1, March 28 – April 4, 2010 from Table 16. Inflow and outflow modeled by HEC-HMS. The red line shows the start of runoff, and blue dashed line shows the estimated 500-yr peak flow. 94
58 Inflow and outflow over the ogee spillway in the Scituate Reservoir when the initial water level at the reservoir is 4 ft below the spillway crest. Inflow is based on hourly data of Event #1, March 28 – April 4, 2010 from Table 16. The red line shows the start of runoff, and blue dashed line shows the estimated 500-yr peak flow.. 95
59 Simulated inflow and outflow to the Flat River when the reservoir is full in Event #1. The spillway crest elevation was approximately considered 237 ft (NAVD88). 96
60 Comparison of the FEMA FIRMs (bottom) and our HEC-RAS model flood map (top) in the Main Branch of the Pawtuxet River for a 100-year return period flood event. Note that the HEC-RAS generated map only includes the Pawtuxet River, whereas FIRMs includes other rivers in addition to the Pawtuxet River. 98
61 Comparison of the FEMA FIRMs (bottom) and our updated HEC-RAS model flood map (top) for a 100-year event around Warwick Mall. 99
62 Comparison of the HEC-RAS unsteady flow results, observed data, and HEC-HMS results at (a) Cranston in the Main Branch, and (b) Washington in the South Branch. 100
63 Pawtuxet River online inundation map integrated into STORMTOOLS (a) compared with FEMA FIRMs (b). 101
64 Location of the dams in the Main Branch of the Pawtuxet River. 1-Natick Pond Dam, 2-Pontiac Dam, 3-Pontiac Downstream Dam, 4- Pawtuxet Falls Dam. 103
65 Photos of the dams in the Main Branch of the Pawtuxet River. 103
66 Pontiac Dam in the Main Branch of the Pawtuxet River during March 2010 flood, Source: Alisa Richardson (RIDEM), 2016, personal communication. . 104

67 Removal of Pontiac Dam on the Main Branch. Left column: flood water depth in blue contour (after removal) and reduced flooding areas due to dam removal in yellow. Right column shows the flood water elevation change (i.e., water elevation before removal minus water elevation after removal). The reduced flooding area due to removal is shown in dark purple in the right column. The top row shows results for a 50-year event, the middle row for a 100-year event, and the bottom row for a 500-year event. 105
68 Effect of removing Pontiac Dam on the water surface profile in the Main Branch for a 100-year event. Water levels with and without dam are shown using blue line with x markers, and in orange line with square markers, respectively. Vertical dotted red line shows the location of Pontiac Dam along river length. 106
69 Water surface elevation (WSE) reduction after removing the Pontiac Dam from the HEC-RAS model for a 50, 100, and 500-year event. Vertical dotted red line is at location of Pontiac Dam along river length. 106
70 Removal of Pawtuxet Falls Dam at Pawtuxet Village. Left column: flood water depth in blue contour (after removal) and reduced flooding areas due to dam removal in yellow. Right column shows the flood water elevation change (i.e., water elevation before removal minus water elevation after removal). The reduced flooding area due to removal is shown in dark purple in the right column. The top row shows results for a 50-year event, the middle row for a 100-year event, and the bottom row for a 500-year event. 107
71 Effect of removing Pawtuxet Falls Dam on the Main Branch of the Pawtuxet River profile for a 100-year event. Water levels with and without dam are shown using blue line with x markers, and in orange line with square markers, respectively. Vertical dotted red line shows the location of the dam along river length. 108
72 Water surface elevation reduction after removal of the Pawtuxet Falls Dam for 50-, 100-, and 500-year events. Vertical dotted red line shows the location of the Pawtuxet Falls Dam. 108

73 Removal of all dams on the Main Branch. Left column: flood water depth in blue contour (after removal) and reduced flooding areas due to dam removal in yellow. Right column shows the flood water elevation change (i.e., water elevation before removal minus water elevation after removal). The reduced flooding area due to removal is shown in dark purple in the right column. The top row shows results for a 50-year event, the middle row for a 100-year event, and the bottom row for a 500-year event. 110
74 North Branch dam locations: 1. Scituate Reservoir Dam, 2. Hope Dam, 3. Low Head Weir, 4. Arkwright Dam, 5. Harris Pond Dam, 6. Phoenix Dam, 7. Breached Dam. 111
75 Photos of the 6 dams on the North Branch of the Pawtuxet River. 112
76 Removal of Hope Dam on the North Branch. Left column: flood water depth in blue contour (after removal) and reduced flooding areas due to dam removal in yellow. Right column shows the flood water elevation change (i.e., water elevation before removal minus water elevation after removal). The reduced flooding area due to removal is shown in dark purple in the right column. The top row shows results for a 50-year event, the middle row for a 100-year event, and the bottom row for a 500-year event. 113
77 Removal of all dams in the North Branch. Left column: flood water depth in blue contour (after removal) and reduced flooding areas due to dam removal in yellow. Right column shows the flood water elevation change (i.e., water elevation before removal minus water elevation after removal). The reduced flooding area due to removal is shown in dark purple in the right column. The top row shows results for a 50-year event, the middle row for a 100-year event, and the bottom row for a 500-year event. 114
78 Location of the dams on the South Branch of the Pawtuxet River. 115
79 Photos of the dams in the South Branch of the Pawtuxet River. 116
80 Removal of Washington Pond Dam on the South Branch. Left column: flood water depth in blue contour (after removal) and reduced flooding areas due to dam removal in yellow. Right column shows the flood water elevation change (i.e., water elevation before removal minus water elevation after removal). The reduced flooding area due to removal is shown in dark purple in the right column. The top row shows results for a 50-year event, the middle row for a 100-year event, and the bottom row for a 500-year event. 118

81 Modeled effect of removing Washington Upper Pond Dam on the South Branch of the Pawtuxet River profile for a 100-year event. Water levels with and without dam are shown using blue line with x markers, and in orange line with square markers, respectively. Vertical dotted red line shows the location of the dam along river length. 119
82 Water surface elevation reduction after removal of the Washington Upper Pond Dam in for 50, 100, and 500-year events. Vertical dotted red line is at location of Washington Upper Pond Dam. 119
83 Removal of Mill Pond Dam on the South Branch. Left column: flood water depth in blue contour (after removal) and reduced flooding areas due to dam removal in yellow. Right column shows the flood water elevation change (i.e., water elevation before removal minus water elevation after removal). The reduced flooding area due to removal is shown in dark purple in the right column. The top row shows results for a 50-year event, the middle row for a 100-year event, and the bottom row for a 500-year event. 120
84 Modeled effect of removing Mill Pond Dam on the South Branch of the Pawtuxet River profile for a 100-year event. Water levels with and without dam are shown using blue line with x markers, and in orange line with square markers, respectively. Vertical dotted red line shows the location of the dam along river length. 121
85 Water surface elevation reduction after removal of the Mill Pond Dam based on the HEC-RAS river model for 50, 100, and 500-year events. Vertical dotted red line is at location of Mill Pond Dam. 121
86 A broken tree (debris) in North Branch of the Pawtuxet River. 124
87 Idealized dimensions of rectangular modeled debris accumulations, Source: Lagasse et al. (2010). 125
88 Location of the 17 bridges in the Main Branch of the Pawtuxet River. See Figures 89 and 90 for photos of the bridges and the names. 125
89 Photos of the bridges in the Main Branch of the Pawtuxet River. See Figure 88 for location of each bridge along the Pawtuxet River. 1- Route 33 (Providence St.), 2- East Ave., 3- Washington Secondary Trail (Old Roadrail), 4- Route 2 Ramp 5- Route 2/Bald Hill Road Northwest Span, 6- Route 2/Bald Hill Road Southeast Span, 7- I-295 West Span, 8- I 295 East Span, 9- Route 5 (Greenwich Ave.), and 10- Route 37 South Span. 127

90 Photos of the bridges in the Main Branch of the Pawtuxet River (continued). See Figure 88 for location of each bridge along the Pawtuxet River. 11- Route 37 North Span, 12- I-95, 13- Conrail Bridge No. 1 (Old Railroad), 14- Elmwood Ave., 15- Conrail No. 2 (Old Roadrail), 16- Warwick Ave., and 17- Pawtuxet Village. 128
91 Flood water depth (left column) and water elevation change (right column) after adding debris to the Pawtuxet Village Bridge for 50 (top row), 100 (middle row), and 500-year (bottom row) event scenarios. 129
92 NOAA 2017 relative sea level change scenarios for Providence. (1 m = 3.28 ft). 131
93 NOAA's estimated storm surge values for various return periods at the Providence Station. 131
94 100-year flood water depth and the increased extent of flooding for three scenarios in the Main Branch: 12 ft SLR plus 2.7 ft of tide (a); 12 ft SLR plus 2.7 ft tide plus 7.2 ft (50-yr) surge (b); 12 ft SLR plus 2.7 ft tide plus 8.8 ft (100-yr) surge (c). The yellow areas show the increased flooded area due to tide, SLR, and surge. 133
95 Warwick Wastewater Treatment Facility during the flood in March 2010. . . 134
96 Warwick Wastewater Treatment Facility Levees (Pare Corporation, 2016) . . 134
97 Location of the Warwick Wastewater Treatment Facility, outlined in red. Levee structures are within Warwick Wastewater Treatment Facility perimeter. Green lines show river cross section locations, labeled with cross section identifier numbers. Blue line outlining Pawtuxet River, dark blue arrow showing flow direction of the river. 135
98 Elevation plots for a 500-year flooding event, at cross sections 31385.16 and 32037.30 adjacent to the Wastewater Treatment Facility. Levee structure location marked, as well as corresponding freeboard. 136
99 The Warwick Wastewater Treatment Facility is protected by its levee for a 100-year event (left) and a 500-year event (right). 136

List of Tables

1 Overview of the Pawtuxet River Watershed. Areas A-E are shown in Figure 6. 29
2 Description of land cover data, 2011 in Figure 8, Source: RIGIS. 34
3 Scituate Reservoir spillway details. 37
4 Estimated dimensions of the Flat River Reservoir Spillway. 40
5 CFSR model nodes used to analyze the spatial variability of rainfall in RI . . 43
6 Intensity-duration-frequency (in/hr) values for Warwick, RI (Lat:41.7°, Lon:-71.44°). 47
7 Historical peak flows at USGS stream gauges in the Pawtuxet River Watershed, Source: USGS. The stations on river reaches are highlighted. 52
8 Peak flow at selected USGS Gauges before and after March 2010 event (Zarriello and Bent, 2011). 53
9 Estimated magnitude of flood flows and Annual Exceedance Probability (AEP) at USGS 01116500 in North Branch, USGS 01116000 in South Branch, and in North Branch at confluence with South Branch of the Pawtuxet River for the period of record through 2010 (Zarriello et al., 2012) 53
10 Drainage area and discharge ratios of the South and North Branches relative to Cranston gauge. See Figure 6. 54
11 Typical Overflow Weir Coefficients (Brunner, 2016). 67
12 Subbasin parameters for the Pawtuxet River watershed model with nine subbasins. 71
13 CN look-up table for re-classified land cover data. 73
14 Summary of structures, dams, and river cross sections. 75
15 AEP flood flows (cfs) specified for the Pawtuxet River hydraulic model (Zarriello et al., 2012). 82
16 Selected hourly flooding events. 84
17 Some extreme flooding events since 1978 based on daily data available from Cranston stream gauge station. 87
18 Maximum elevation reduction by removing all dams in the Main Branch of the Pawtuxet River. 109
19 Maximum elevation reduction by removing all dams in the North Branch of the Pawtuxet River. 115
20 Maximum elevation reduction by removing dams in the South Branch of the Pawtuxet River. 122

21 Flood extent areas before and after dam removal, and percent reduction, for 50, 100, and 500-year return flood scenarios. Rows, separated by horizontal lines: top 3 dams located in the Main Branch, middle 6 dams in the North Branch, and bottom 10 dams in the South Branch. 123
22 Debris data used in the modeling. 126
23 Maximum elevation increase by adding debris to bridge piers in the Main Branch of the Pawtuxet River model. 130
24 Tide, surge and SLR at the downstream point of the Main Branch for three extreme scenarios (1 m = 3.28 ft). 132
25 Maximum water elevation in the vicinity of the Warwick Warwick Wastewater Treatment Facility. The levee elevation is 33.66 ft (NAVD88). 135
26 Availability of hourly data at selected stream gauge stations. See Figure 21 for gauge locations. 141
27 Availability of daily data at selected stream gauge stations. See Figure 21 for gauge locations. 142
28 Availability of monthly data at selected stream gauge stations. See Figure 21 for gauge locations. 143

Abbreviations

AEP: Annual Exceedance Probability
AHPS: Advanced Hydrological Prediction Service
CDO: Climate Data Online
CFSR: Climate Forecast System Reanalysis
CRMC: Coastal Management Resources Council
CSNE: Climate Solutions New England
DEM: Digital Elevation Model
ECMWF: European Centre for Medium-Range Weather Forecasts
FEMA: Federal Emergency Management Agency
FIPS: Federal Information Processing Standards
FIRMs: Flood Insurance Rate Maps
GCS: Geographic Coordinate System
GHCN: Global Historical Climate Network
GIS: Geographic Information System
HEC-GeoHMS: Geographic Support for HEC-RAS
HEC-GeoRAS: Geographic Support for HEC-HMS
HEC-HMS: Hydrologic Engineering Center developed Hydrologic Modeling System
HEC-RAS: Hydrologic Engineering Center developed River Analysis System
HWM: High Water Mark
HSG: Hydrologic Soil Groups
LiDAR: Light Detection and Ranging
LULC: Land Use/Land Cover
MCM: Million Cubic Meters
MHW: Mean High Water
NAD: North American Datum
NAVD: North American Vertical Datum
NBEP: Narragansett Bay Estuary Program
NCAR :National Center for Atmospheric Research
NCEI: National Centers for Environmental Information
NCEP: National Centers for Environmental Prediction
NOAA: National Oceanic and Atmospheric Administration
NERFC: Northeast River Forecast Center
NGVD: North Geodetic Vertical Datum
NRCS: Natural Resources Conservation Service

NWS: National Weather Service
PRISM: Parameter-elevation Regression on Independent Slopes Model
RIGIS: Rhode Island Geographic Information System
RISPF: Rhode Island State Plane Feet
URI: University of Rhode Island
USDA: United States Department of Agriculture
USGS: United States Geological Survey
USACE: US Army Corps of Engineers
UTM: Universal Transverse Mercator
WGS: World Geodetic Survey
WSS: Web Soil Survey

1 Executive Summary

The purpose of this study was to develop a spatially distributed model for the Pawtuxet River and its watershed to better understand and predict flood risks. The Pawtuxet River is located on the western side of Narragansett Bay in Rhode Island, and is the only watershed that is entirely within the state borders. The Pawtuxet River watershed includes three branches, with many structures such as dams and bridges on each of the branches. The North Branch originates at the Scituate Reservoir in Scituate. The South Branch originates at Flat River Reservoir and connects to the North River Branch in Warwick. The Main Branch begins at the confluence of the South and North Branches and drains to the Providence River in upper Narragansett Bay. In March 2010, three major rainfall events in New England resulted in the worst recorded flood in 200 years, and caused major damage to communities near the river. After this extreme event, several initiatives, including this study, were undertaken to assess the risk of flood, and prepare for future events.

This study applied a state of the art watershed and river model (Hec-HMS/Hec-GeoHMS, and Hec-Ras/Hec-GeoRas developed by the US Army Corps of Engineers) to evaluate the flooding risk. The model includes river/watershed structures (e.g., Scituate and Flat River Reservoirs, historical dams, and bridges), and was able to map the flood extent continuously (steady/unsteady) in the river floodplain for historical events. The model was calibrated and validated by application to the March 2010, and other selected major flood events. The model can also generate maps for specific return periods such as 50-, 100-, and 500-year events. The study also assessed the effect of hydraulic structures, such as dams and reservoirs, on flooding.

This report presents the watershed, river and meteorological data that were used in the development of model, the details and setting of the watershed and river models, calibration/validation of the model and results/discussions. The main contributions of the study are summarized as follows:

The watershed and river model can predict flood the extent of flooding for a particular rainfall event, and provide a public web-based access to flood maps through the STORMTOOLS website: www.beachsamp.org/stormtools. The model showed a very good ability to predict the flooding from the March 2010 events including both the timing, the magnitude of the peak flow, and the extent of flooding.

The model can be also used as a framework for real-time flood forecasting. The results showed that the model is highly sensitive to the uncertainty in the precipitation data. An ensemble approach to represent rainfall event in the forecasting mode is highly recommended.

The simulation of the Scituate Reservoir in the watershed model showed that the reservoir water elevation can be controlled to effectively manage downstream flooding. For example, a

4 feet capacity in the reservoir (e.g., below the spillway crest, or above the spillway crest with the installation of gates) reduces the peak outflow discharge by about 60% for a 500-year flood event in the North Branch. Using the storage capacity of the reservoir is the most effective way to control flooding for areas downstream of the dam. More study is suggested to design a regulating structure which has minimum impact on the dam and upstream areas, and meets the water supply needs for which the reservoir was designed. It should be added that even when there is no capacity in the reservoir, the flood peak discharge is being reduced significantly by flow routing in the reservoir. The Flat River Reservoir, located on the South Branch, also reduces flooding in the South and consequently the Main Branch, but is much less effective, compared to the Scituate Reservoir, because its area is significantly smaller.

The systematic study of the effect of the removal of small diversion dams on flooding were found to reduce flooding and to have a largely local, and not cumulative impact. For flood mitigation, it was shown that removal of the Pontiac Dam in the Main Branch of the Pawtuxet River would decrease the flood inundation areas by 31.8%, 26.1%, and 5.4% in 50-, 100-, and 500-year floods, respectively. As noted earlier, the Scituate Reservoir can mitigate flood throughout the river, and is more effective for the flood risk management. Model predictions showed that the presence of debris significantly increases the flooding extent. We strongly recommend that the effect of debris be considered in flood risk assessments. These are not currently included in Federal Emergency Management Agency (FEMA) FIRMs (Flood Insurance Rate Maps).

Model simulations show that projected sea level rise can lead to increased inland flooding in the Pawtuxet River (particularly, in downstream areas near the Providence River) during concurrent coastal and inland flooding. This is an additional risk associated with hurricanes that contain considerable rain (i.e., wet hurricanes).

The following recommendations are made based on the results of this study:

An operational flood forecasting model for the Pawtuxet River watershed area should be setup based on the current model. The methodology presented here can also be applied to other rivers and watersheds in Rhode Island. We recommend online maps for inland and coastal flooding for the entire RI within an integrated framework (e.g., STORMTOOLS) to communicate the risk of inland and coastal flooding in the state.

The consequences of possible catastrophic dam failures during major floods, including effects on water quality, flooding, and negative impacts on river ecosystems and Narragansett Bay should be studied.

Recent studies show that the extreme rainfall events and average precipitation rate in RI are increasing due to climate change. Simulating the impacts of climate change on the watershed-river flooding risk should be able to better assess the risks of flooding in the future.

To provide better observational data for future studies, it is recommended to install a station downstream of the Scituate Reservoir to measure streamflow and meteorological data. Conditions in the Scituate Reservoir have a significant impact on the flooding in the watershed. It is also recommended to install a meteorological station in the upland area of the watershed. Currently, the only precipitation gauge in the Pawtuxet River watershed is located at the T.F. Green Airport in Warwick, RI. Adding another gauge would allow for more accurate prediction of flooding and decrease the uncertainty in the spatial and temporal variation in precipitation.

Finally, simulations of concurrent wet hurricanes in the presence of sea level rise should be performed to more fully explore the interaction of inland and coastal flooding.

2 Introduction

2.1 Motivation

The Pawtuxet River is located on the western side of Narragansett Bay in Rhode Island. The longitude range is -71.75° to -71.38°, and the latitude range is 41.57° to 41.92° for the area (Figure 1).

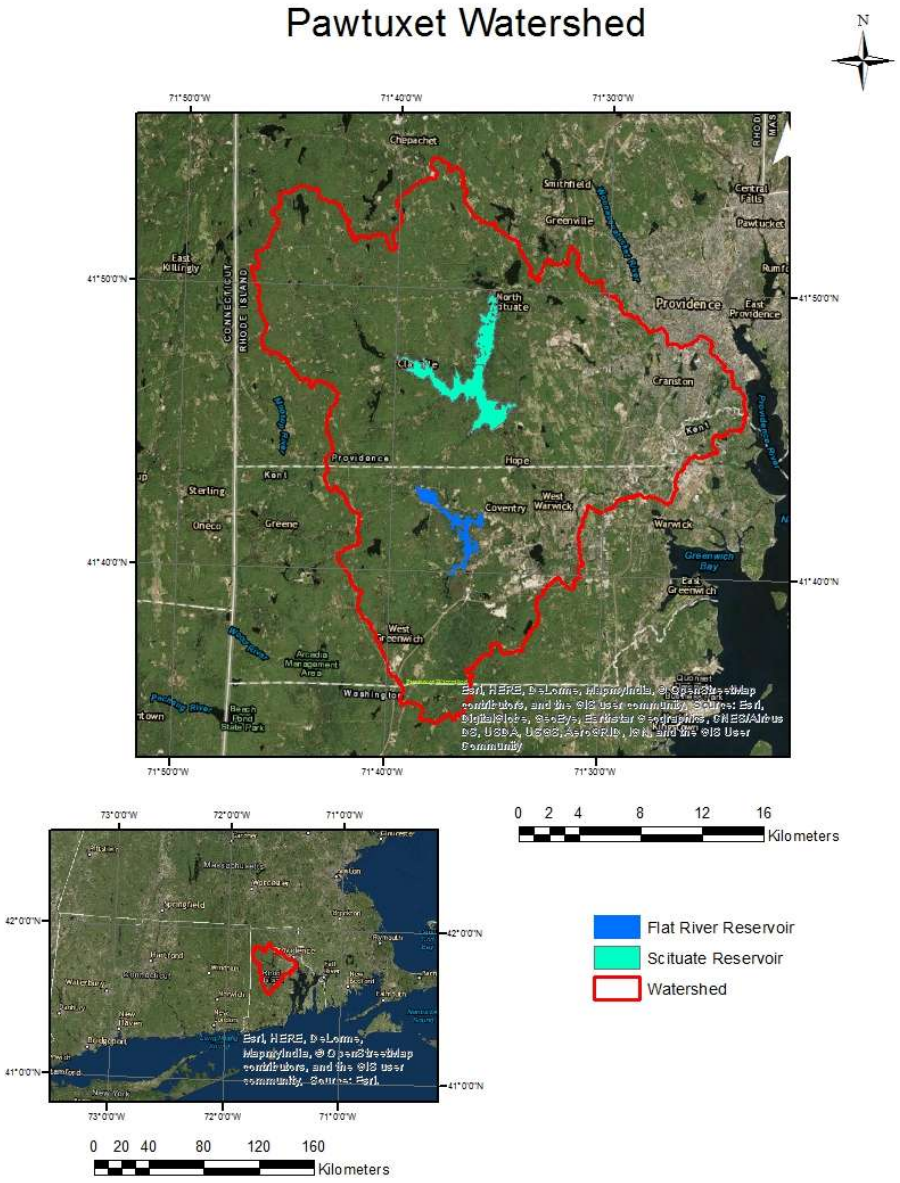

Figure 1: Map of the Pawtuxet River watershed. Top map shows watershed border outlined in red, Flat River Reservoir highlighted in blue, and Scituate Reservoir highlighted in cyan. Bottom map shows zoomed-out view of the watershed, in and the surrounding states.

The Pawtuxet River drains a watershed of 229.2 mi^2, or almost 600 km^2, into the Providence River next to Narragansett Bay. The Pawtuxet River watershed is the largest in Rhode Island, includes 12 Rhode Island communities, and is the only watershed in Rhode Island entirely within state borders.

The North and South Branches of the Pawtuxet River originate in the hills of western Rhode Island, with the confluence of both branches at River Point Village in West Warwick. From the confluence, the Main Branch of the Pawtuxet River continues roughly east through West Warwick, Warwick, and Cranston, emptying into the Providence River at Pawtuxet Village. There are four historical diversion dams along the river's length below the confluence; one in Natick at Providence Street, two at Pontiac Mill, and one in Pawtuxet Village in Warwick. Within the watershed there are 64 ponds, 93 brooks, 7 tributary rivers, and 22 dams. Interstate highways I–95 and I–295 and route RI–2 also traverse the watershed. The Pawtuxet River watershed became a center of textile manufacturing in the 19th and 20th centuries, with many dams created along the river and its tributaries (Coleman, 1963). An example of a textile factory along the river is shown in Figure 2.

Figure 2: A textile factory along the South Branch of the Pawtuxet River in Coventry, RI.

Every year, floods are a major cause for significant loss of life and property damage in the US and around the world. Floods are common occurrences along many rivers and an important part of the natural water cycle. According to Knebl et al. (2005), for the six year period of 1989–1994, 80% of national disasters were due to weather related events including flooding. [1]

[1]The tropical storms flooding losses were $161 bn during 1997 to 2016: www.iii.org

Runoff, in general, is generated by rainstorms, and the quantity of runoff depends on characteristics of the precipitation, such as duration, intensity and distribution, as well as land use and soil type. In March of 2010, there were three major rainfall and runoff events in New England that resulted in over 16 inches of rainfall. Declared a severe storm and flooding emergency on March 30, 2010, the flooding was the worst recorded in 200 years and resulted in hundreds of million dollars of damage.[2] The Pawtuxet River was also extremely impacted during the March 2010 flooding events; the Scituate Reservoir on the North Branch of the Pawtuxet River was almost at the full capacity, resulting in large flood impacts downstream of the reservoir. The Warwick Mall, which is close to the Main Branch of the Pawtuxet River, was also impacted by flooding. Figure 3 shows the flooded Warwick Mall during the March 2010 flooding.

Figure 3: Warwick Mall flooded in 2010, Source: NOAA

After the March 2010 flooding disaster, the U.S. Department of Homeland Security's Federal Emergency Management Agency (FEMA) required the implementation of flood analyses to assess damages as well as minimize future damages (Zarriello et al., 2012). To help inform future forecasting and management, post-flood analysis required the determination of flood peaks. To that end, in April 2010 the U.S. Geological Survey (USGS) and the U.S. Army Corps of Engineers (USACE) measured the high water marks (HWMs) in flooded areas along the Pawtuxet River.

The USGS has thirteen streamgauges in the Pawtuxet River watershed, the Cranston station in the Pawtuxet River being the one farthest downstream with a drainage area of 220 mi^2. Additionally, the National Oceanic and Atmospheric Administration's (NOAA) National Weather Service (NWS) at the Northeast River Forecast Center (NERFC) has

[2] www.fema.gov

provided forecast values of the river stage at the Cranston location. The frequency of floods at Cranston, RI on the Pawtuxet River at the USGS streamgauge location is shown in Figure 4. As this figure shows, after the late 1960's, the frequency of flooding, the frequency of multiple floods over a given year, and severity of floods have been increasing, coinciding with increased precipitation, the development of large shopping malls and highway construction.

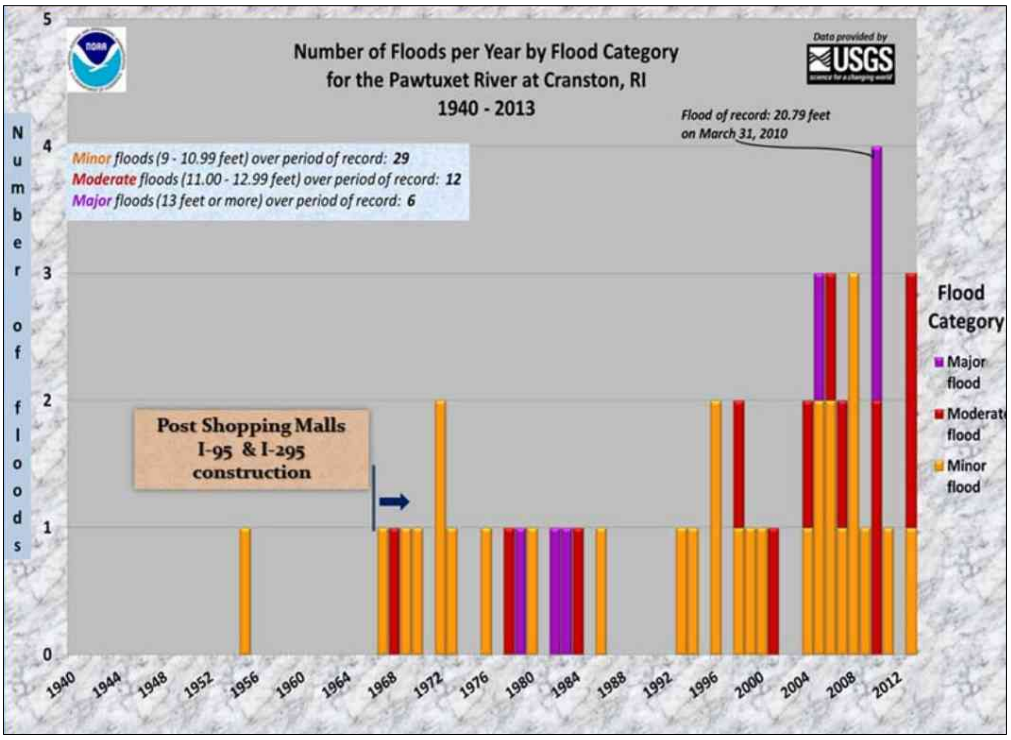

Figure 4: Flood history at the USGS streamgauge location in Cranston, RI on the Pawtuxet River from 1940-2013. The color of the bar indicates the severity of the flood. Notice the dramatic increase in both frequency of flooding since the late 1960's, the frequency of multiple floods in a given year, and the severity of these floods. Floods in the major category approximate the 100 year base flood elevation based on FEMA Flood Insurance Rate Maps (FIRMs), Source: David Vallee NOAA NWS NERFC

Apart from NWS station at the Cranston Gauge, no predictions are available to estimate discharges and water elevations in the branches of the river, along the river floodplain, or in the areas impacted by flooding when flood events occur. This work focuses on developing predictive tools for the Pawtuxet River watershed in Rhode Island, to simulate flooding along the river.

Another aspect of this study, is the interaction of inland and coastal flooding. The Pawtuxet River drains to the Providence River which is connected to the Narragansett Bay. Accordingly, the interaction of coastal and inland flooding is potentially important (e.g. dur-

ing wet hurricanes). In a comprehensive flooding study, meteorologists provide precipitation data. This data is implemented by hydrologists to develop a watershed model. The outcome of the watershed model is used by river/civil engineers to calculate the water elevation in a river and its floodplains. Further, oceanographers provide data for ocean models to predict water elevations at a coast as well as nearshore, coastal, and estuary flooding. Developing a unified dynamic model of watershed, river and ocean that provides a precise flood prediction tool for various scenarios of storms requires a close collaboration of multiple disciplines.

For the state of Rhode Island, an online map tool called STORMTOOLS (Spaulding et al., 2016) has been developed, which provides predictive flooding maps for coastal Rhode Island.[3] Flooding extent and water elevation predictions for scenarios such as 25-, 50-, and 100-year return period events are available. It would be very helpful for flood risk assessment purposes to add riverine flooding to this tool.

2.2 Objectives

The purpose of this study is to develop a spatially distributed watershed/river model for the Pawtuxet River watershed, which includes the river structures and geometry, to allow for an analysis of the watershed/river system in flood events. The developed model maps the flood extent continuously for the river floodplain for past events and for specific scenarios, such as for 50-, 100-, and 500-year events. We also assess the effect of hydraulic structures, such as dams and reservoirs, on flooding at present conditions and in dam removal scenarios. The results from our model can be used to inform recommendations with regards to flood mitigation, reservoir management, and dam management along the Pawtuxet River. This project is also a stepping stone for a real time forecasting tool, which we envision to predict stage levels at selected locations as well as inundated area extent along the floodplain. Further, the interaction of inland and coastal flooding can be assessed using the developed model.

2.3 Deliverables

The deliverables of this project are listed as follows:

1. A validated geographic information system (GIS) based integrated watershed and river model for the Pawtuxet River that provides flood maps with online access.

2. Assessment of the watershed flooding including,

[3] http://www.beachsamp.org/stormtools/stormtools-interactive-maps/

(a) Modeling of the Scituate and the Flat River Reservoirs, and their effects on the flooding.

(b) Analysis of the effect of historical dams and debris at bridges on floods.

(c) The impact of sea level rise on flooding near the Narragansett Bay.

3. This report which describes the methodology, data, model parameters, and results of the project.

3 Watershed and River Data

In this section, we describe the sources of data gathered to be used to develop the Pawtuxet River and Watershed models. We discuss the watershed and river data that informs our model parameters, including data on the watershed, Scituate Reservoir, Flat River Reservoir, and structures along the river. The observed data includes rainfall, streamflow, LiDAR ground elevations, land use, and soil type data. Hindcast (modeled) data includes reanalysis of precipitation, rainfall distribution, rainfall intensities, annual exceedance probabilities, and climate change predictions regarding precipitation in the watershed.

3.1 Units and Datum

For development and validation of watershed and river models, many types of data are required, including watershed Digital Elevation Model (DEM), land use, soil type, rainfall data, river geometry, geometry of river structures, and streamflow data. This project uses the most recent available data; no surveying or field data collection have been included in this effort. Data are reported in the original units of the sources. As much of the data are in U.S. customary units which may give the public as well as stakeholders a better sense of the data, we used this system and tried to provid the equivalent metric values.

For this project, the horizontal coordinate system is based on the North American Datum 1983 system (NAD 83) in the hydrological modeling, and on the Rhode Island State Plane Feet projection system (RISPF) in the hydraulic modeling. The digital elevation model (DEM) data is downloaded in the RISPF, Federal Information Processing Standards (FIPS) Zone 3800 horizontal projection system. The soil property and land use original source data are in the World Geodetic Survey 1984 (WGS84) Geographic Coordinate System. All source data were re-projected to NAD 83 Universal Transverse Mercator (UTM) Zone 19N in our

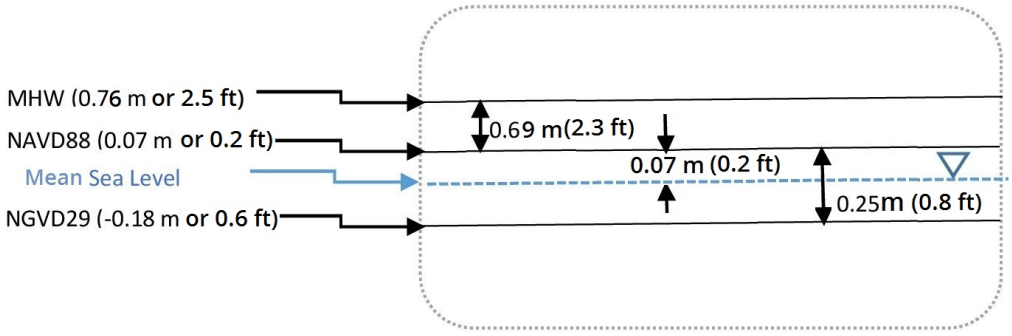

Figure 5: NAVD 88, MHW and NGVD 29 datums difference in Providence Station 8454000 at -71.4133° longitude and 41.8239° latitude.

hydrological modeling and to the RISPF in our hydraulic modeling, using the ArcToolbox projection utility.

The vertical coordinate system for our hydrological and hydraulic modeling is referenced to the North American Vertical Datum of 1988 (NAVD88). The DEM is in NAVD88. The Scituate Reservoir source data was originally reported referenced to the Mean High Water (MHW) datum in Providence. The difference between MHW and NAVD 88 is locally dependent; in Providence MHW is 2.12 ft (0.69 m) higher than NAVD 88.[4] It should be noted that the tidal Station 8454000 in Providence is the nearest to the Pawtuxet River Watershed, and was used as the reference for the datum conversion. Stream gauge source data from Cranston and Coventry are reported with respect to the North Geodetic Vertical Datum (NGVD29). At the Cranston stream gauge station, NAVD88 is 0.836 ft (0.25 m) higher than NGVD 29.[5] Figure 5 shows the NAVD88, MHW, and NGVD29 datum differences in Providence at 41.8239° latitude and -71.4133° longitude relative to MSL. All source data for our hydrological and hydraulic modeling were re-projected to be based on NAVD88.

3.2 Geospatial Data

3.2.1 The Pawtuxet River Watershed

The geographical focus area in this study is the Pawtuxet River Watershed shown in Figure 1, encompassing the Main Branch of the Pawtuxet River, the North Branch of the Pawtuxet River, and the South Branch of the Pawtuxet River. The Main Branch runs 11.2 miles, the North Branch runs 6.6 miles, and the South Branch runs 9.1 miles long. Inside the watershed are two major reservoirs: the Scituate Reservoir and the Flat River Reservoir, as well as several hydraulic structures along the river.

Table 1: Overview of the Pawtuxet River Watershed. Areas A-E are shown in Figure 6.

District	Area (mi^2)	Area Ratio
Total Watershed	229.2	100%
Upstream of the Scituate Reservoir (A)	90.8	40%
Upstream of the USGS 01116000 gauge at South Branch (B)	62.6	27%
Rest of the watershed (C)	75.8	33%
Upstream of the USGS 01116500 gauge at Cranston (D)	220.0	96%
Downstream of the Cranston gauge (E)	9.2	4%

[4] https://tidesandcurrents.noaa.gov

[5] https://www.ngs.noaa.gov/TOOLS/Vertcon/vertcon.html

The Pawtuxet River Watershed includes thirteen USGS stream gauges, among those USGS Station 01116500 at Cranston in the Main Branch and USGS Station 01116000 at Washington in the South Branch are located in the main river branches. Table 1 lists the drainage area of the entire Pawtuxet River Watershed, the area upstream of the USGS stream gauge at Cranston in the Main Branch, downstream of the Cranston gauge, upstream of the Scituate Reservoir, and upstream of the USGS gauge at Washington in the South Branch. Figure 6 shows the areas corresponding to the figures in Table 1. Figure 6a show the areas upstream of the Scituate Reservoir in green, upstream of the Flat River Reservoir in pink, and downstream of both reservoirs in orange. Figure 6b shows the Pawtuxet River Watershed upstream of Cranston in cyan, and downstream in purple.

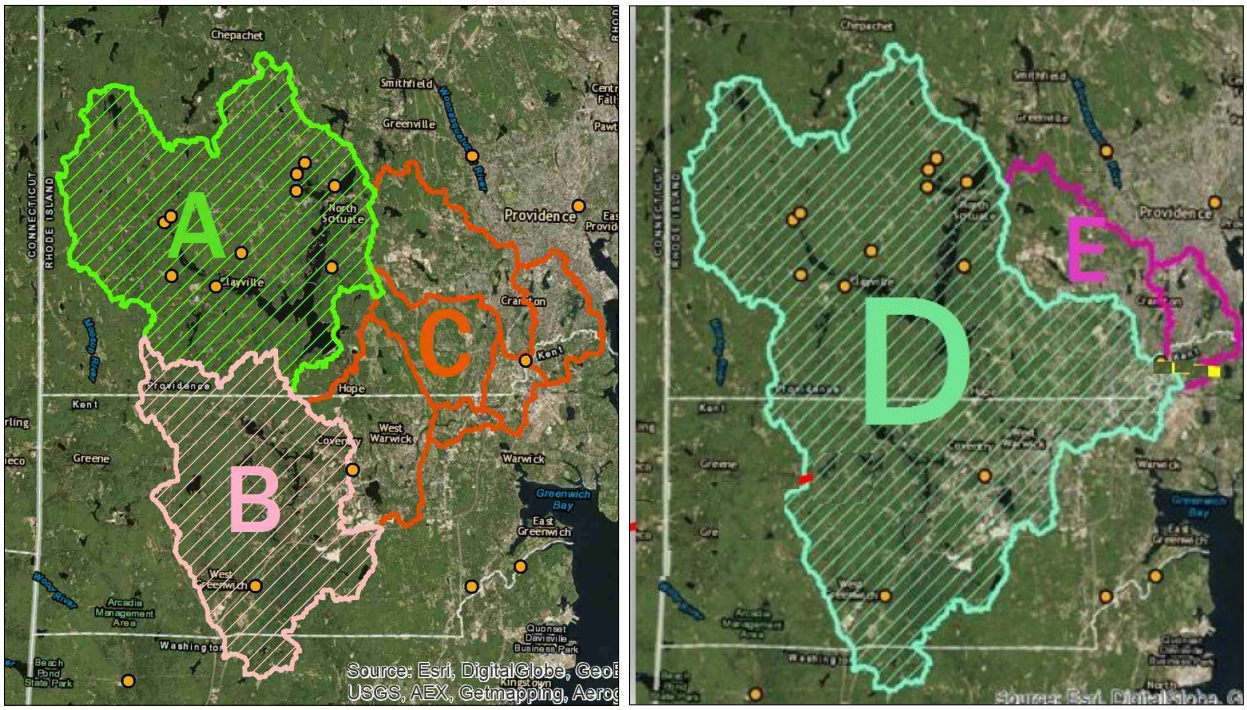

(a) *(b)*

Figure 6: Pawtuxet River Watershed with surface area (left) area upstream of the Scituate Reservoir outlined and shaded in green (A), area upstream of the USGS 01116000 in the South Branch outlined and shaded in pink (B), rest of the watershed are outlined in orange (C); (right) upstream of the Cranston USGS station gauge shaded and outlined in cyan (D), and downstream area of the Cranston gauge outlined in purple (E). See Table 1.

3.2.2 Digital Elevation Model

Airborne LiDAR technology was applied to collect elevation data for the state of Rhode Island in detail from April 22 to May 6, 2011. The data collection in the state of Rhode Island was part of the Northeast LiDAR Project.[6]

The original data are in the RISPF FIPS 3800 horizontal coordinate system, and the NAVD 88 vertical coordinate system. DEM data are re-projected to the UTM coordinate system for the watershed modeling in this project.

Figure 7 depicts DEM information of the Pawtuxet River Watershed. The highest elevation in the Pawtuxet River Watershed is 807 ft or 246 m (NAVD 88) in the western part of the watershed.

3.2.3 Land Use/Land Cover Data

Land Use and Land Cover (LULC) data affect the infiltration and runoff of water during precipitation. The data will be used to estimate runoff in the hydrologic model.

The LULC data applied in this project for the watershed modeling originally comes from the statewide digital dataset for the state of Rhode Island for spring 2011.[7] The scale of this land use data is 1:5000, meeting the National Mapping Standards accuracy. The resolution of the data is 0.5 ft, and the resolution of its derivatives is 3 ft spacing. The classification scheme is similar to the previous LULC datasets (Anderson Level III modified coding) in Rhode Island in 1988, 2003 and 2004. This dataset is also transformed into the Geographic Information System (GIS) database and is available to the public.

Figure 8 shows the LULC map of the Pawtuxet River Watershed, classified into 34 groups as described in Table 2. In the hydrology model, the groups are re-classified into 13 groups for calibration purposes, and explained in Section 5.1.3.

The LULC map of the Pawtuxet River Watershed shows that most of the industrial, commercial and dense residential structures are located in the eastern part of the watershed, making the area more critical in flooding situations.

3.2.4 Soil Type Data

The rate of precipitation and infiltration directly determine the amount of runoff during an event. Infiltration rates depend on soil type and its moisture level, prior precipitation, and surface imperviousness/retention capacity (USDA, 1986).

[6] http://rigis.org
[7] http://rigis.org

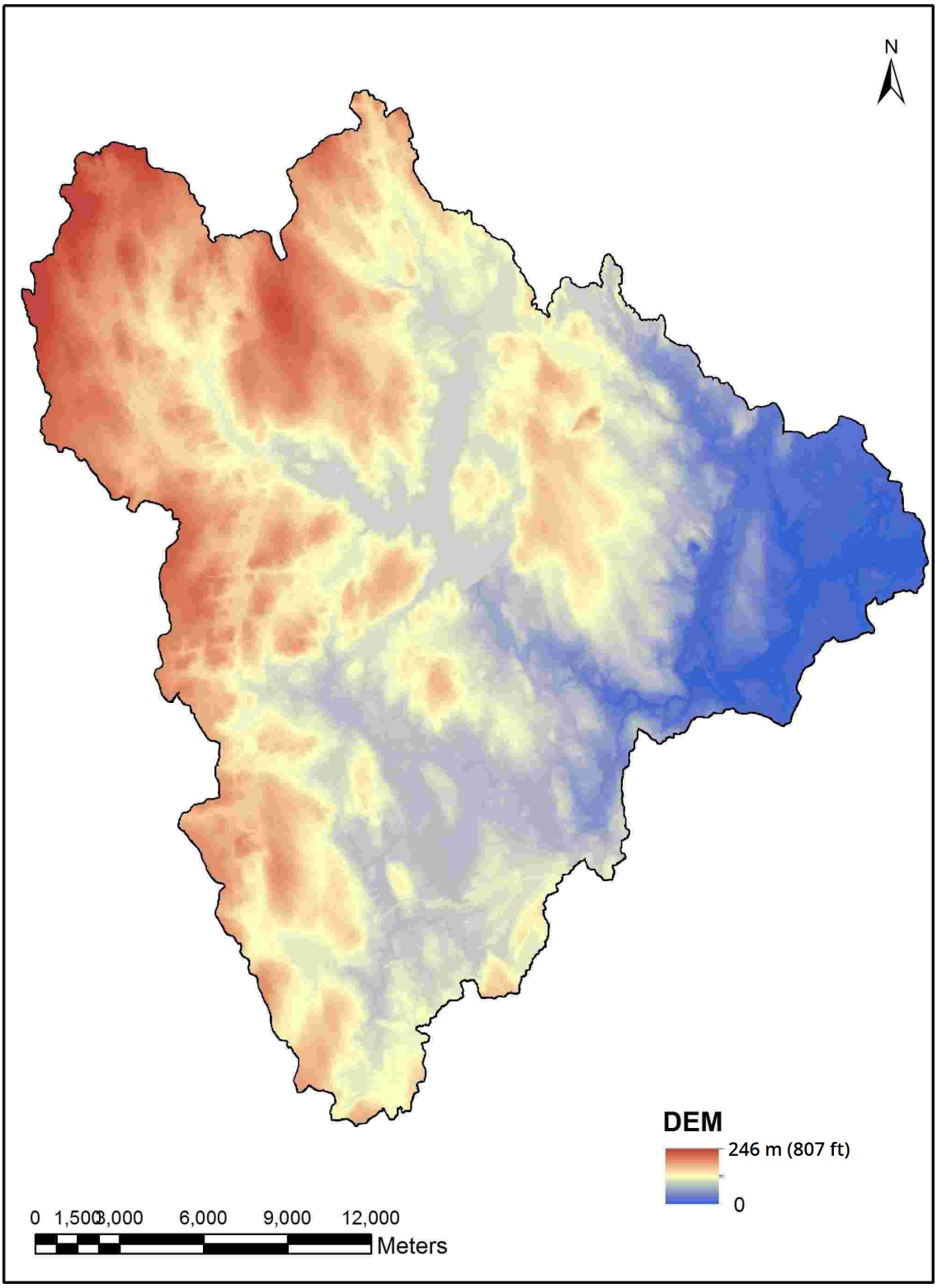

Figure 7: Pawtuxet River Watershed Digital Elevation Model (DEM in NAVD 88), Source: RIGIS.

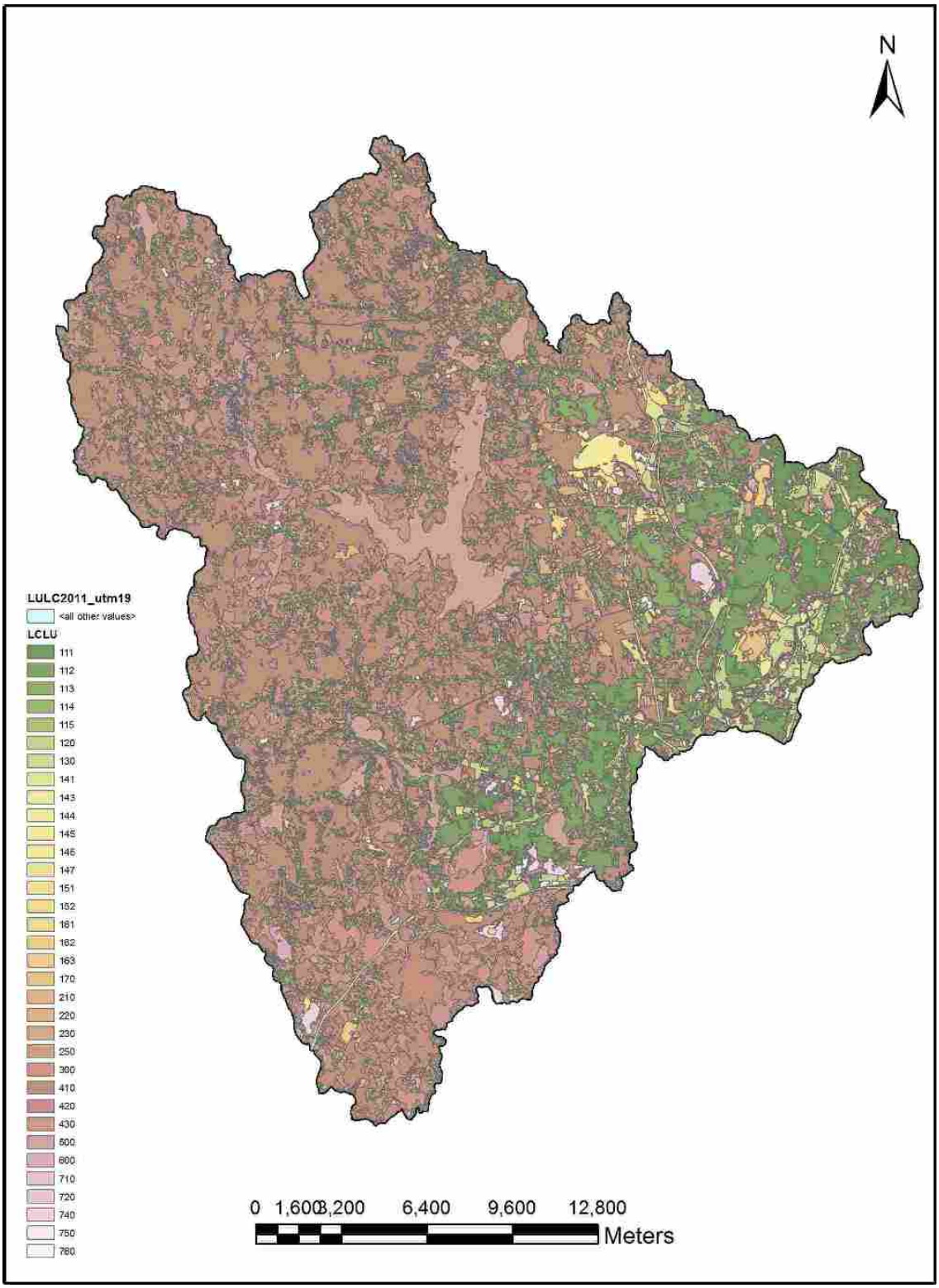

Figure 8: Land cover of the Pawtuxet River Watershed in 2011, Source: RIGIS. See Table 2 for legend decsription.

Table 2: Description of land cover data, 2011 in Figure 8, Source: RIGIS.

LCLU	Description
111	High Density Residential (< 1/8 acre lots)
112	Medium High Density Residential (1/4 to 1/8 acre lots)
113	Medium Density Residential (1 to 1/4 acre lots)
114	Medium Low Density Residential (1 to 2 acre lots)
115	Low Density Residential (> 2 acre lots)
120	Commercial (sale of products and services)
130	Industrial (manufacturing, design, assembly, etc.)
141	Roads (divided highways > 200' plus related facilities)
143	Railroads (and associated facilities)
144	Water and Sewage Treatment
145	Waste Disposal (landfills, junkyards, etc.)
146	Power Lines (100' or more width)
147	Other Transportation (terminals, docks, etc.)
151	Commercial/Residential Mixed
152	Commercial/Industrial Mixed
161	Developed Recreation (all recreation)
162	Vacant Land
163	Cemeteries
170	Institutional (schools, hospitals, churches, etc.)
210	Pasture (agricultural not suitable for tillage)
220	Cropland (tillable)
230	Orchards, Groves, Nurseries
250	Idle Agriculture (abandoned fields and orchards)
300	Brushland (shrub and brush areas, reforestation)
410	Deciduous Forest (> 80% hardwood)
420	Softwood Forest (> 80% softwood)
430	Mixed Forest
500	Water
600	Wetland
710	Beaches
720	Sandy Areas (not beaches)
740	Mines, Quarries and Gravel Pits
750	Transitional Areas (urban open)
760	Mixed Barren Areas

Soil type data are provided by the Web Soil Survey (WSS), produced by the National Cooperative Soil Survey. The United States Department of Agriculture (USDA) Natural Resources Conservation Service (NRCS) has provided soil maps and online data for more than 95% of the nation's counties.[8]

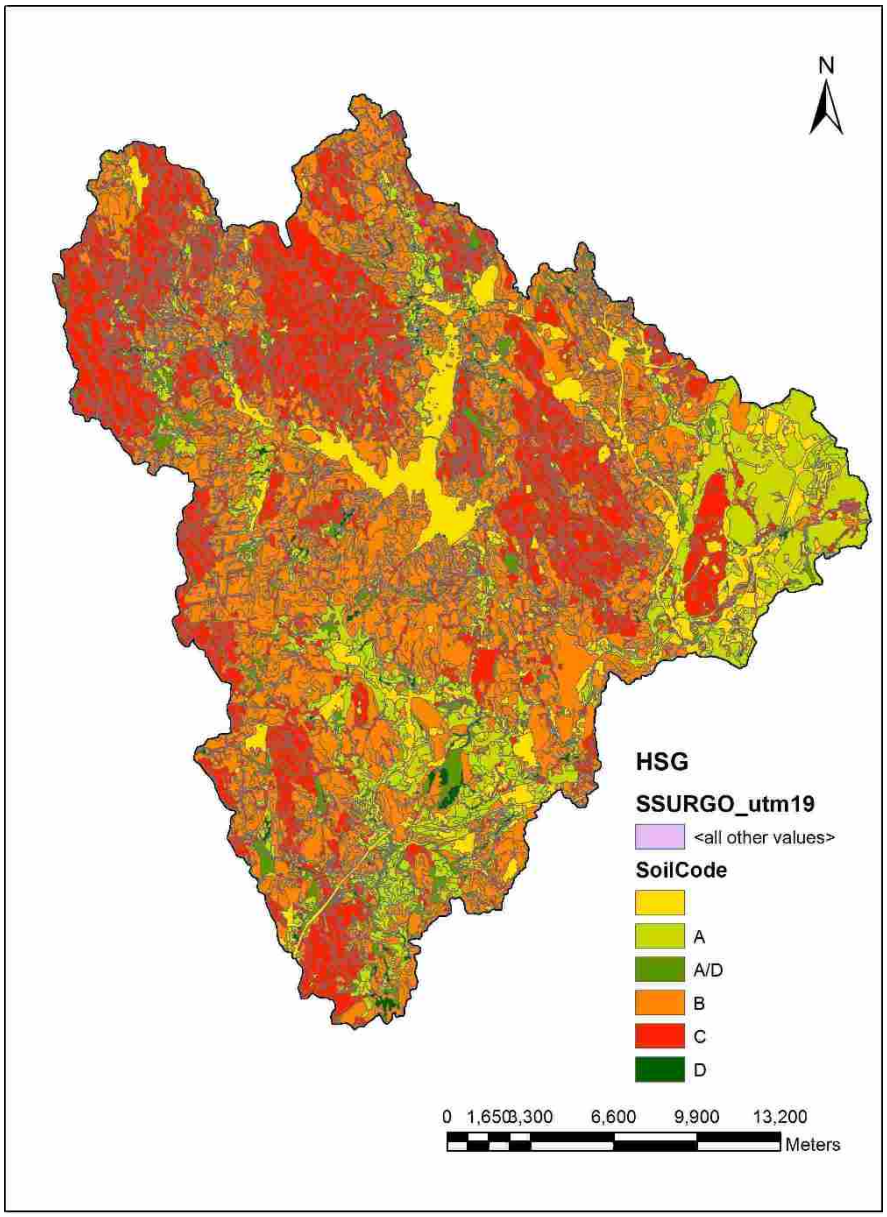

Figure 9: Map of the Pawtuxet Watershed soil type data. Yellow depicts water areas.

The NRCS classifies soils into four different Hydrologic Soil Groups (HSG): A, B, C, and D. Group A soils absorb water readily, sand for an example. The subsequent groups have lower and lower infiltration rates. On the other extreme of the spectrum, Group D soils, like

[8] http://websoilsurvey.nrcs.usda.gov

clay, do not allow much water to infiltrate, causing more runoff.[9]

Figure 9 shows the HSG distribution in the Pawtuxet River Watershed.[10] In general, the northern part of the watershed is mostly covered by soils classified as HSG C, the western part by HSG B, the eastern part by HSG A, and the southern parts by a mixture of all the types. The yellow color on the map shows the water area (rivers, lakes, ponds, reservoirs, etc) in the watershed.

3.2.5 Scituate Reservoir

Referring to Figure 1, the Scituate Reservoir is located in the middle of the northern part of the Pawtuxet River Watershed; an image of the reservoir is shown in Figure 10. The Scituate Reservoir provides over 60% of the state's drinking water.[11]

Figure 10: The Scituate Reservoir. The photo is taken from the Scituate Avenue looking toward NW.

An earth-filled dam spanning the North Branch of the Pawtuxet River forms the Scituate Reservoir. The dam dimensions are approximately 3200 ft in length and 100 ft in height (975 m in length and 30 m in height), with a surface area of 5.3 mi^2(13.7 km^2), and a drainage area of about 91 mi^2(235.5 km^2). Figure 11 shows the elevation-storage graph of the Scituate Reservoir; data provided by Providence Water Supply. The reservoir has a 37000 million US gallon capacity at the spillway crest line elevation of 286.12 ft, with reference to the NAVD88

[9] http://www.mrlc.gov
[10] http://www.nrcs.usda.gov
[11] www.HEALTH.ri.gov/environment/dwq/Home.htm

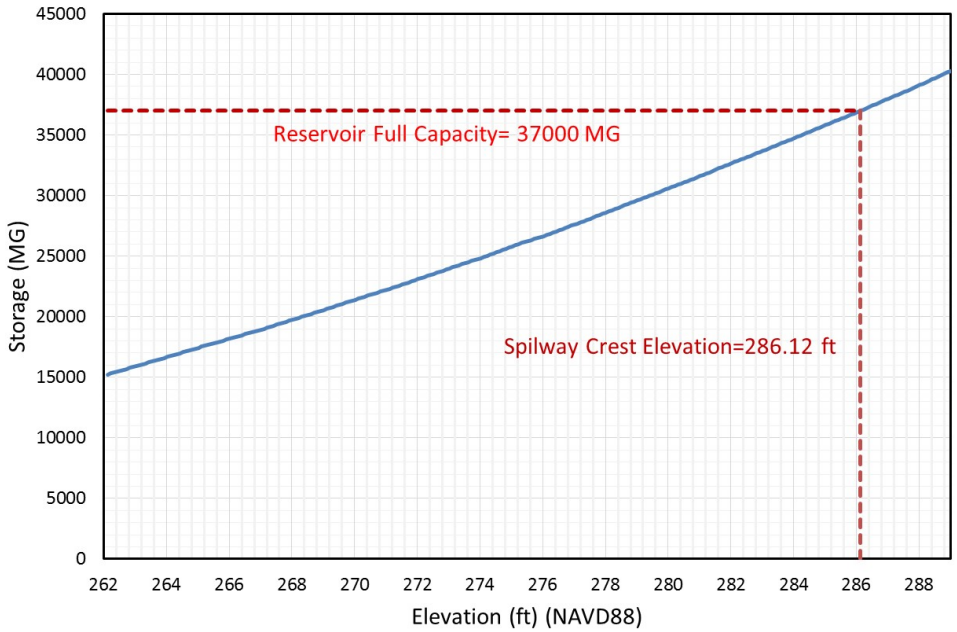

Figure 11: Elevation-storage graph of the Scituate Reservoir; Source: Providence Water Supply.

datum. Figure 12 depicts the cross section of the spillway for this dam. The dimensions of the spillway in the Scituate Reservoir that are applied in the Pawtuxet River Watershed model are summarized in Table 3.

Table 3: Scituate Reservoir spillway details.

Spillway Type	Ogee†
Abutments	2
Abutment Type	Concrete
Vertical Datum/Unit	NAVD1988/ft
Approach Loss	0.00
Crest Elevation	286.12
Crest Length	440.00
Apron Elevation	267.12
Apron Length	200.00
Design Head	8.00
Spillway Coefficient (C)	3.35 ($ft^{1/2}/s$)

† An ogee spillway section follows an ogee curve (Chen, 2015).

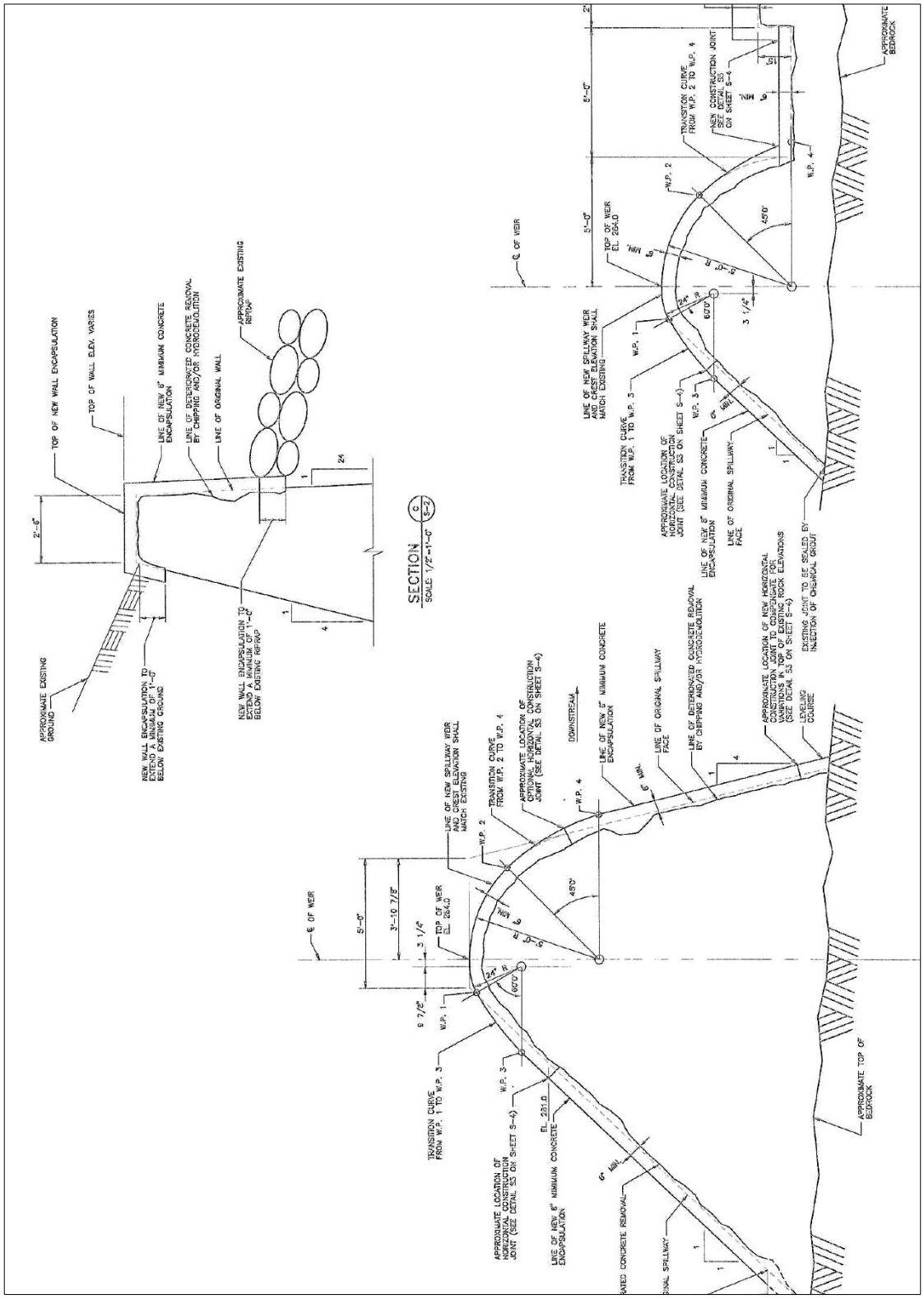

Figure 12: Scituate Reservoir cross section details, source: Providence Water Supply.

3.2.6 The Flat River Reservoir

Figure 13 shows the spillway of the Flat River Reservoir from various angles. Looking at Figure 1, we see that the Flat River Reservoir is located in the middle of the southern part of the Pawtuxet River Watershed. The South Branch of the Pawtuxet River is formed by the confluence of the Flat and other Rivers in the Flat River Reservoir area. Flat River Reservoir is on the Quidnick Brook in Kent County, Rhode Island and is used for recreation purposes (Halberg et al., 1961). The flow regulation of the Flat River Reservoir, other reservoirs, and diversion from Carr Pond have all affected the flow of the South Branch of the Pawtuxet River.

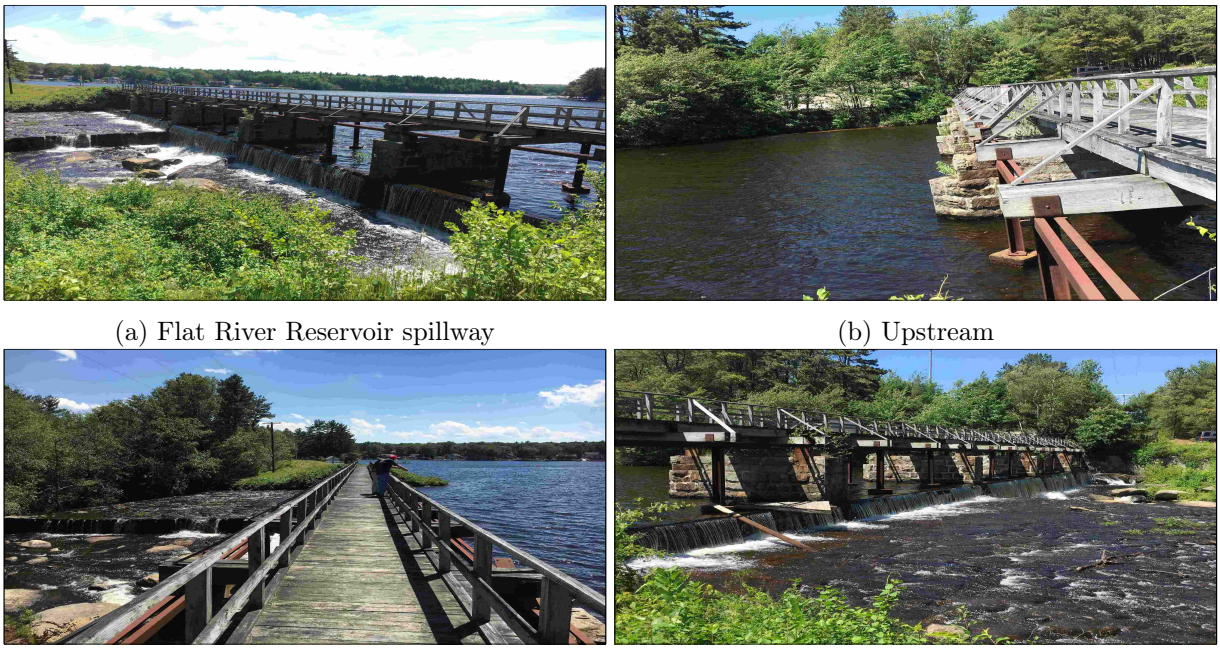

(a) Flat River Reservoir spillway

(b) Upstream

(c) On the spillway

(d) Downstream

Figure 13: The Flat River Reservoir and Spillway.

Quidnick Reservoir Dam is a gravity dam, of earthen construction with a broad crested spillway. Its height is 14 feet, its length 700 feet. Maximum discharge from the dam reported as 495 cfs.[12] The capacity of the Flat River Reservoir is 1,870 million gallons, or about 7 million m^3, and it was constructed about 1875.[13]

Since dimensions for Flat River Reservoir were not available, we estimated the dimensions, summarized in Table 4, by in-situ measurements.

[12] http://www.lakefrontliving.com.ri

[13] https://pubs.usgs.gov

Table 4: Estimated dimensions of the Flat River Reservoir Spillway.

Spillway Type	Broad-Crested
Crest Elevation (ft, NAVD88)	237
Crest Length (ft)	177

3.2.7 River Structures

There have been several site visits by project team to assess the latest condition of river structures along the Pawtuxet River including dams and bridges. In the Main Branch 4 dams and 17 bridges, in the North Branch 7 dams including the Scituate Reservoir Dam and 7 bridges, and in the South Branch 11 dams including the Flat Reservoir Dam and 11 bridges are located along the river that will be discussed in the next chapters. Two recent changes are partial removal of Pawtuxet Falls Dam in 2011 and the construction of new levees around a wastewater treatment facility in Warwick, which are discussed in Sections 6.2.4.1 and 6.2.7, respectively.

3.3 Precipitation Data

3.3.1 Precipitation Data

NOAA's National Centers for Environmental Information (NCEI) preserves, observes, assesses, and prepares public access to the nation's climate and historical weather data and information, providing access to oceanic, atmospheric, and geophysical data. The NCEI provides an archive of global historical weather, climate data, and historical information of land-based observation stations available through Climate Data Online (CDO).[14] The data include hourly, daily, monthly, seasonal, and yearly temperature, precipitation, wind as well as radar data and 30-year climate normals[15] .

For the watershed model, there is NCEI hourly precipitation data available for one land-based station inside the Pawtuxet River Watershed. The rainfall gauge station location is shown in Figure 14, highlighted by the red star. The land-based station is located at the T.F. Green Airport in Warwick, RI at 41.7225° latitude and -71.4325° longitude.[16] Though there is only one station which provides observational precipitation data, we will show in Section

[14] https://www.ncdc.noaa.gov

[15] Climate Normals are three-decade averages of climatological variables including temperature and precipitation. For more information, visit: https://www.ncdc.noaa.gov/data-access

[16] https://gis.ncdc.noaa.gov

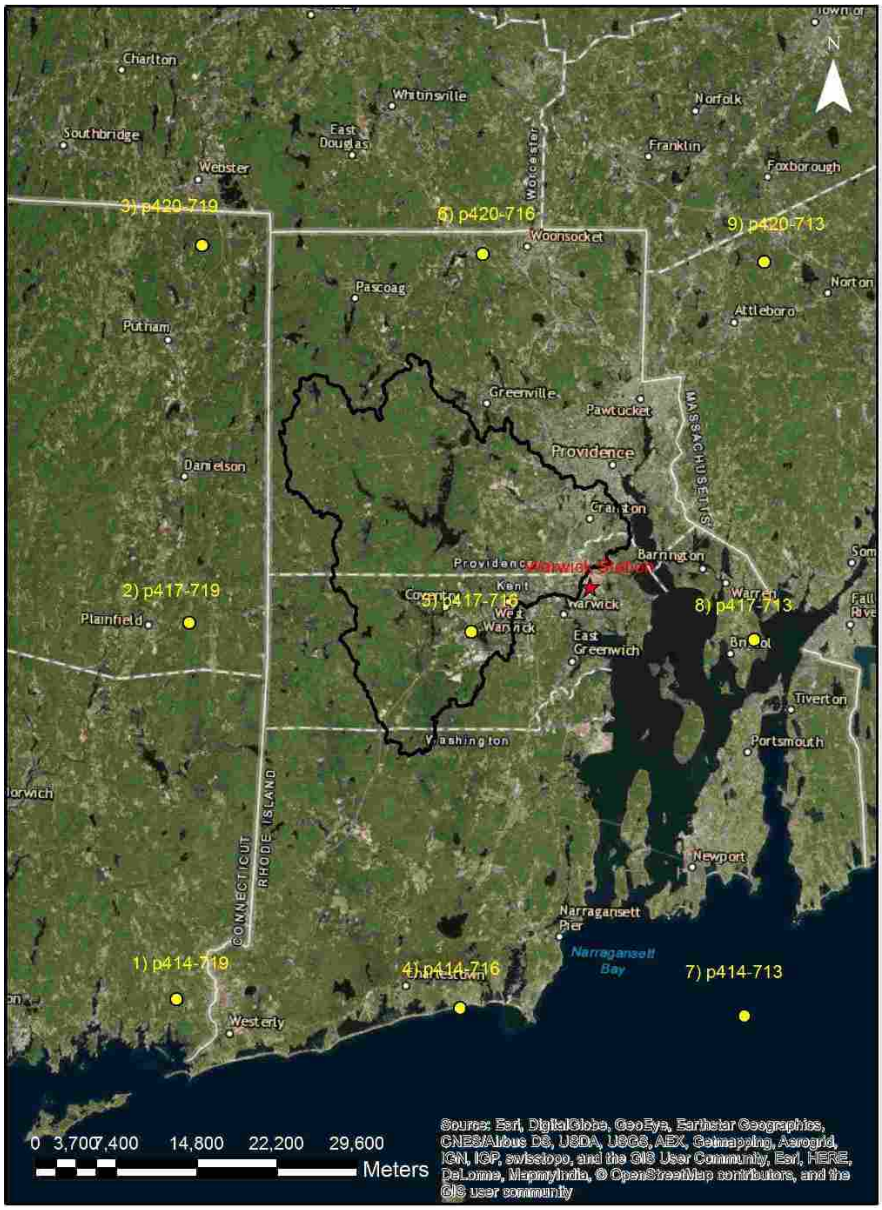

Figure 14: Location of precipitation station/nodes used for the watershed model. Red star shows the observational precipitation gauge and yellow shows the CFSR model nodes.

3.3.3 that the variability of rainfall in the watershed is not significant in this relatively small watershed, and assume a uniform distribution of rainfall for the Pawtuxet River Watershed model. Therefore, we have used the hourly rainfall at the T.F. Green Airport station as the primary input data for our Pawtuxet River Watershed model along with other modeled precipitation data.

During March 2010, 3 major rainfall events occurred in Rhode Island. Figure 15 shows the observed precipitation data recorded at the precipitation gauge in T.F. Green Airport,

RI for March 2010. We note that the heaviest rainfall peaked on March 30, 2010.

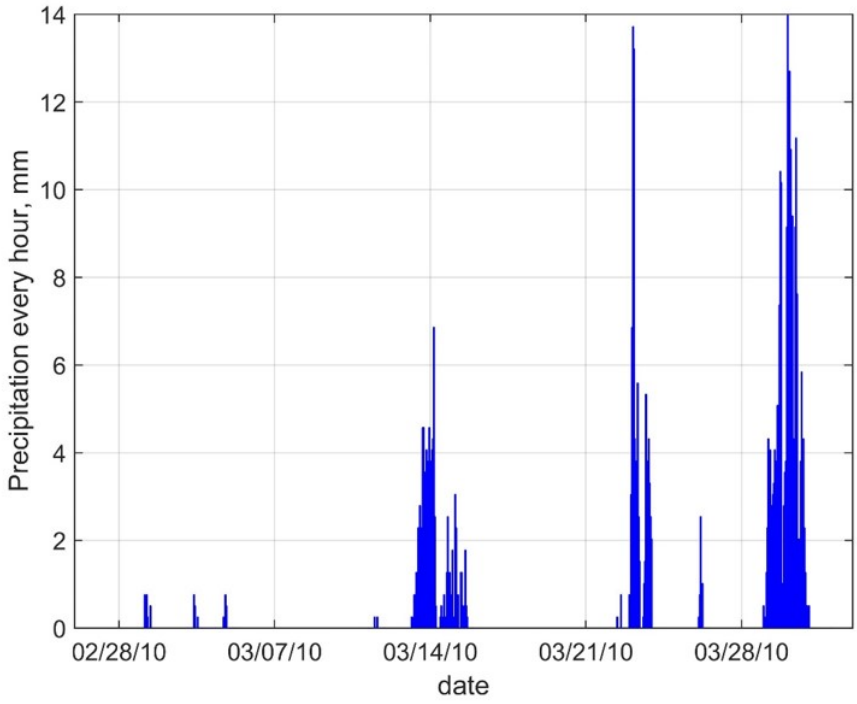

Figure 15: Precipitation data recorded in March 2010 from the hourly observed gauge at T.F. Green Airport, RI (1 mm = 0.039 in).

We also utilized mean area precipitation data for subbasins of the watershed, provided by National Weather Service (NWS).[17] The provided data is from NWS historical time series, as 6 hourly averages, from 1961–2012. The data are also used for the NWS 90 day ensemble streamflow predictions, available through the NWS Advanced Hydrological Prediction Service (AHPS).[18] We also note that the NWS data also uses modeled rainfall data of PRISM (Parameter-elevation Relationships on Independent Slopes Model) interpolation method from the 1971–2000 to calibrate the mean area precipitation data.[19] We used the NWS mean area precipitation data as a data source for our uncertainty analysis, discussed in Section 6.1.3.

3.3.2 Hindcast Precipitation Data

Hindcast precipitation data are used to fill gaps in historical events and mainly for flood forecasting. Modeled meteorological data are available from NOAA's National Centers for

[17] Dave Vallee 2017, personal communication
[18] https://water.weather.gov/precip/
[19] http://www.prism.oregonstate.edu/

Environmental Prediction (NCEP) Climate Forecast System Reanalysis (CFSR). The reanalysis data is available through NCEI and National Center for Atmospheric Research (NCAR) data archives.[20] The reanalysis provides a high-fidelity model output estimation of ocean-atmosphere interaction for the years 1979 through 2014, with hourly time resolution and high spatial resolution of the re-forecast weather conditions.[21] The CFSR dataset is used in our precipitation spatial distribution analysis, discussed in Section 3.3.3.

Climate re-analysis datasets for precipitation are also available from the European Centre for Medium-Range Weather Forecasts (ECMWF) archives.[22] The ECMWF dataset are global datasets with high temporal and spatial resolution, and are another source of precipitation data. The ECMWF dataset is used in our uncertainty analysis, and discussed in Section 6.1.3.

3.3.3 Spatial Variability of Rainfall Over Watershed

As mentioned in Section 3.3.1, the only precipitation station in the Pawtuxet River Watershed is located at the T.F.Green Airport in Warwick, in the eastern part of the watershed. We check here the spatial variability of precipitation over the watershed, using the CFSR data to provide additional information. From the reanalysis dataset, we look specifically at daily precipitation data from 2008–2012 at nine different output nodes located in Rhode Island, from the CFSR model. The locations of these nine CFSR model nodes, along with the

Table 5: CFSR model nodes used to analyze the spatial variability of rainfall in RI

No.	Node Name	Latitude	Longitude
1	p414-719	41.37	-71.875
2	p417-719	41.682	-71.875
3	p420-719	41.995	-71.875
4	p414-716	41.37	-71.563
5	p417-716	41.682	-71.563
6	p420-716	41.995	-71.563
7	p414-713	41.37	-71.25
8	p417-713	41.682	-71.25
9	p420-713	41.995	-71.25

[20] https://globalweather.tamu.edu/
[21] http://cfs.ncep.noaa.gov/cfsr/
[22] http://www.ecmwf.int/en/forecasts/datasets

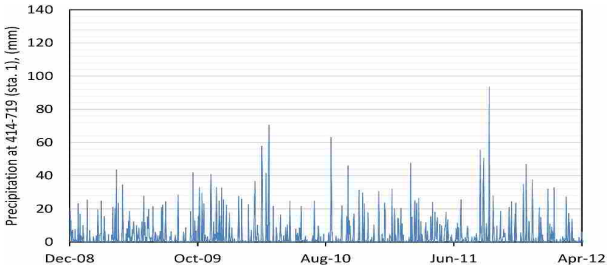

(a) Node 1

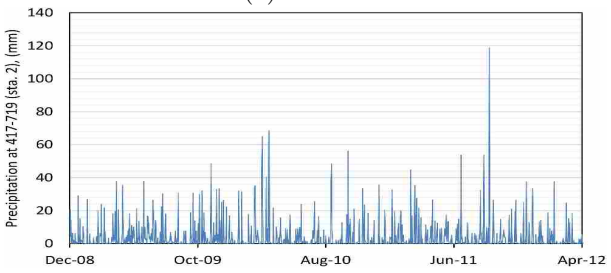

(b) Node 2

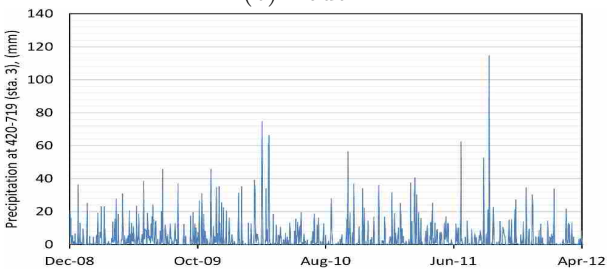

(c) Node 3

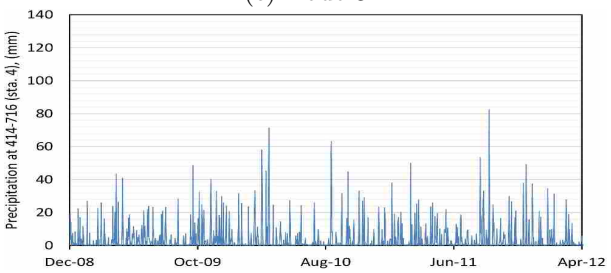

(d) Node 4

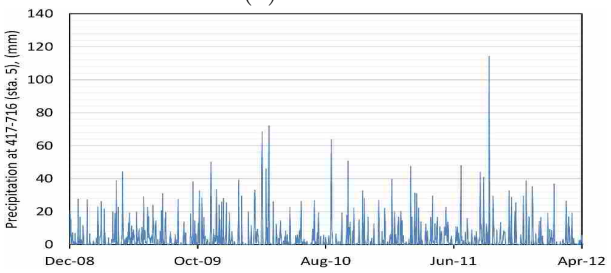

(e) Node 5

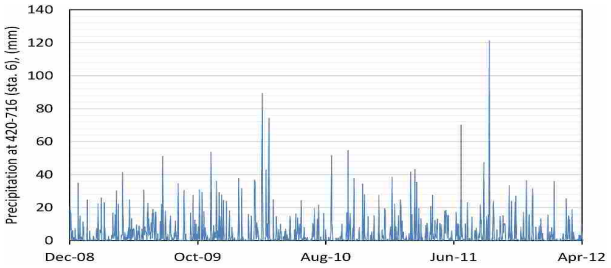

(f) Node 6

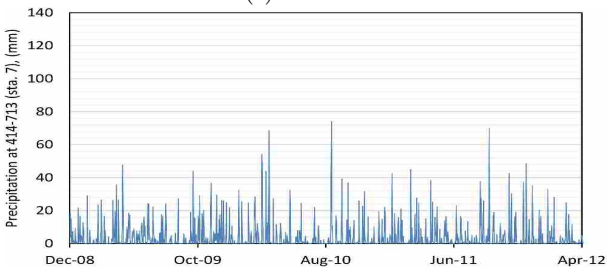

(g) Node 7

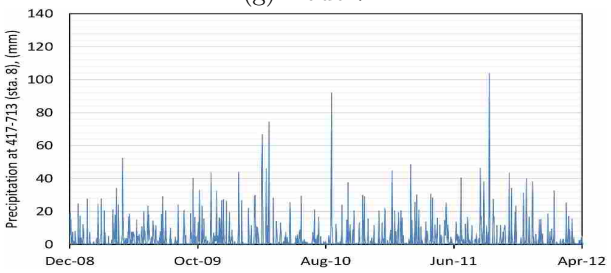

(h) Node 8

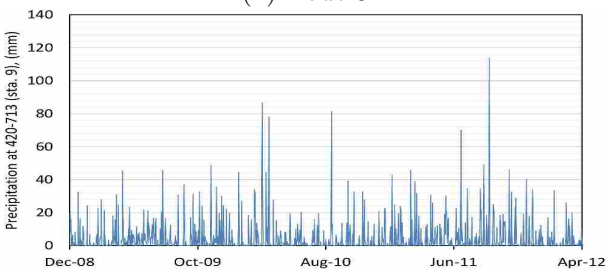

(i) Node 9

Figure 16: Daily precipitation (2008-2012) at CFSR model nodes 1, 2, 3, 4, 5, 6, 7, 8 and 9. See Figure 14 for node locations (1 mm = 0.039 in).

location of the Warwick land-based station, are shown in Figure 14. The names and locations of the nine model nodes are summarized in Table 5.

Figure 16 plots the observed daily precipitation variation from 2008 –2012 at CFSR model nodes 1 to 9. Among these 9 nodes, only node 5 is inside the Pawtuxet River Watershed.

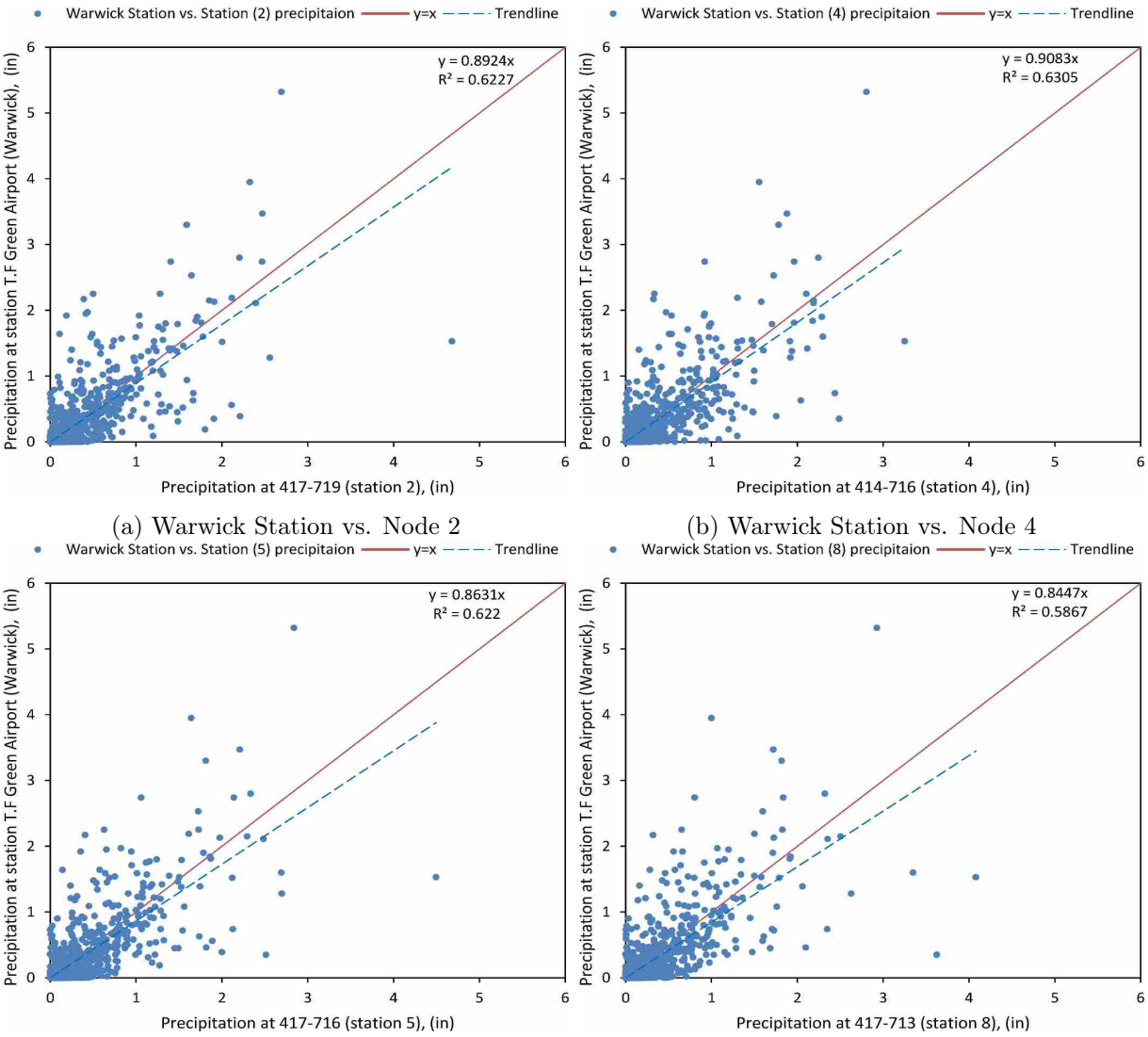

(a) Warwick Station vs. Node 2

(b) Warwick Station vs. Node 4

(c) Warwick Station vs. Node 5

(d) Warwick Station vs. Node 8

Figure 17: Comparison of daily observed precipitation data of Warwick land-based station with daily CFSR model precipitation in nodes 2, 4, 5, and 8.

Figure 17 compares the observed daily precipitation data of the Warwick land based station with the closest CFSR model node 5 (see Figure 14), as well as with nodes 2, 4 and 8. $R^2 \approx 0.6$ in all the reanalysis model nodes. Based on the correlation coefficients, there is a relatively good agreement between the hindcast CFSR and the observed data.

Figure 18 shows four comparisons of spatial distribution of the daily precipitation in

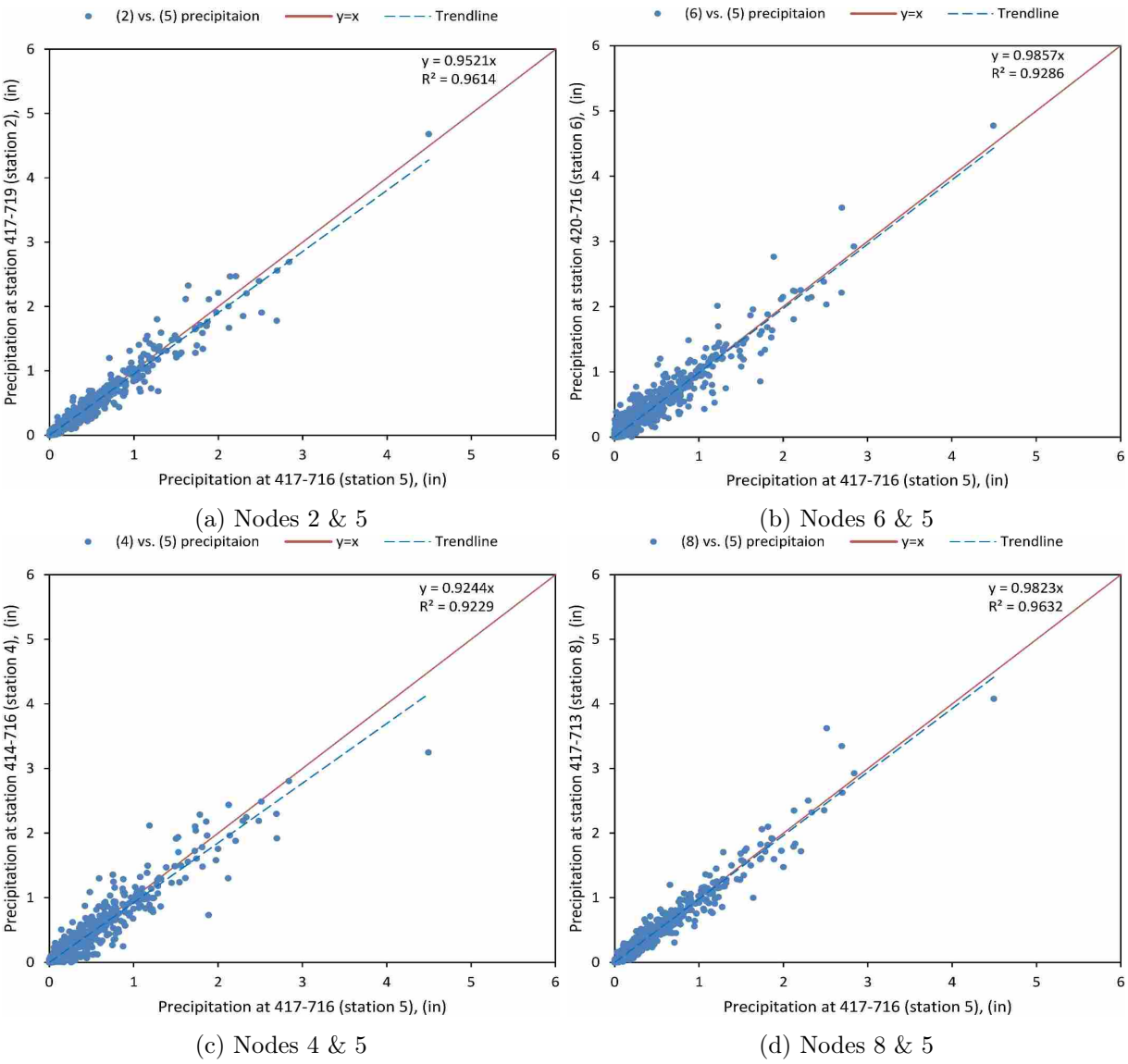

(a) Nodes 2 & 5

(b) Nodes 6 & 5

(c) Nodes 4 & 5

(d) Nodes 8 & 5

Figure 18: Comparison of spatial distribution of daily precipitation at CFSR model nodes a) 2 & 5, b) 4 & 5, c) 6 & 5 and d) 8 & 5.

during 2008–2012 period. Daily precipitation data from nodes 2, 4, 6, and 8 are compared with that from node 5; node 5 is closest in location to the land-based station in Warwick. The spatial distribution of the daily precipitation data over the nodes is approximately uniform with acceptable correlate coefficient of $R^2 > 0.9$. Usually there is a correlation between rainfall and elevation, but the watershed elevation does not vary significantly (Figure 7). As it can be seen, there is no clear trend of rainfall increasing/decreasing over the watershed.

Based on Figure18, it is acceptable to apply the uniform precipitation data to the entire watershed; therefore, we used the hourly precipitation data from the Warwick land-based station as uniformly distributed precipitation over the entire watershed. However, we also

recommend to add more rain gauges in watershed area for more exact runoff calculation at the end of this project. Further, we did an uncertainty analysis to show how rainfall data can affect the flood prediction, as explained in later chapters.

3.3.4 Intensity-Duration-Frequency Curves

An Intensity-Duration-Frequency (IDF) curve represents the probability of a given rainfall intensity for a specified duration. As duration of precipitation increases, the maximum intensity of precipitation decreases. Rainfall intensity, rainfall duration, and rainfall frequency (i.e., probability) are the parameters of IDF curves. IDF curves are created according to

Table 6: Intensity-duration-frequency (in/hr) values for Warwick, RI (Lat:41.7°, Lon:-71.44°).

Duration	IDF (in/hr) in Providence									
	Average recurrence interval (years)									
	1	2	5	10	25	50	100	200	500	1000
5-min:	3.8	4.67	6.1	7.27	8.89	10.2	11.4	13.1	15.4	17.1
10-min:	2.69	3.31	4.31	5.15	6.3	7.19	8.08	9.29	10.9	12.1
15-min:	2.11	2.6	3.38	4.04	4.94	5.64	6.33	7.29	8.55	9.5
30-min:	1.45	1.79	2.35	2.81	3.45	3.94	4.43	5.1	5.99	6.66
60-min:	0.925	1.15	1.51	1.8	2.21	2.53	2.85	3.28	3.85	4.28
2-hr:	0.603	0.755	1	1.21	1.49	1.71	1.93	2.23	2.62	2.92
3-hr:	0.47	0.587	0.78	0.94	1.16	1.33	1.5	1.73	2.03	2.26
6-hr:	0.308	0.379	0.496	0.593	0.727	0.829	0.932	1.07	1.25	1.38
12-hr:	0.197	0.237	0.302	0.357	0.432	0.489	0.547	0.622	0.72	0.794
24-hr:	0.118	0.141	0.178	0.21	0.252	0.286	0.319	0.361	0.417	0.46
2-day:	0.066	0.079	0.101	0.119	0.144	0.164	0.183	0.209	0.242	0.268
3-day:	0.048	0.057	0.072	0.085	0.103	0.117	0.13	0.148	0.172	0.19
4-day:	0.038	0.046	0.058	0.067	0.081	0.092	0.102	0.116	0.134	0.147
7-day:	0.026	0.031	0.038	0.044	0.052	0.058	0.065	0.073	0.083	0.091
10-day:	0.021	0.024	0.03	0.034	0.04	0.045	0.049	0.055	0.061	0.067
20-day:	0.015	0.017	0.02	0.022	0.025	0.028	0.03	0.033	0.036	0.038
30-day:	0.012	0.014	0.016	0.017	0.02	0.022	0.023	0.025	0.026	0.028
45-day:	0.01	0.011	0.013	0.014	0.016	0.017	0.018	0.019	0.02	0.021
60-day:	0.009	0.01	0.011	0.012	0.013	0.014	0.015	0.016	0.017	0.017

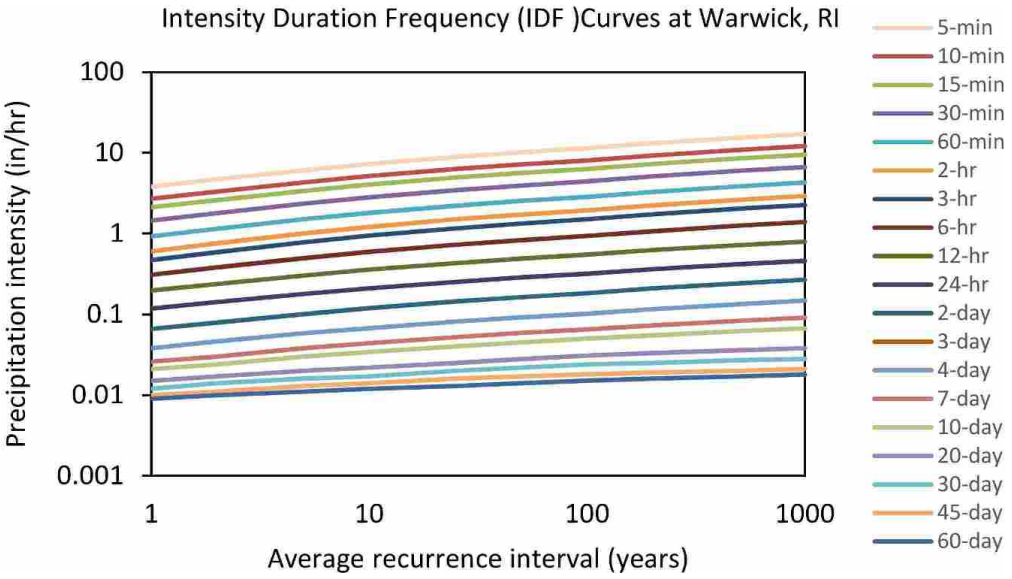

Figure 19: Annual Intensity-Duration-Frequency (IDF) curves at Warwick, RI.

the rainfall data in monitoring stations for long term records, and they are illustrated by statistical rainfall depths for specific return periods and storm durations. The IDF curves for the United States are provided by the U.S. National Weather Service (NWS).[23]

There are nine stations in Rhode Island with available IDF curves: in New Shoreham, South Kingstown, Newport, Glocester, Providence, Warwick, Tiverton, Westerly, and Woonsocket. Comparing IDF table in Warwick with the IDF table in other locations in the watershed shows that they have relatively similar IDF values, another indication that there is nearly uniform precipitation distribution in the area, for extreme events.

Table 6 shows the IDF table for Warwick, RI at 41.7°latitude and -71.44°longitude, and Figure 19 shows IDF curves for average recurrence intervals up to 1000-year return period at Warwick, RI. The rainfall durations range from 5 minutes to 60 days. For instance, in this IDF curve, the return period of 1.5 in/hr precipitation intensity for a duration of 3 hours is 100 years. This intensity will lead to total 4.5 in precipitation in 2 hours. In March 2010, 8.83 inch rainfall occurred in 2-days during 29th and 30th (Figure 15). In the IDF table, the intensity of precipitation for a 100-year event and 48 hr duration is 0.183 in/hr. Multiplying 0.183 by 48 hrs (2 days), equals to 8.8 in of rainfall, which is approximately equal to the March 2010 rainfall in 2 days. For the 500-year return period, the intensity is 0.242 in/hr for 48 hrs duration or 11.6 in (i.e., 0.242×48) of rainfall. This shows that although the return period of flow discharge in March 2010 event is 500 year (will be discussed in Sec. 3.4), the return period of the rainfall is about 100 year. Land cover and land use changes as well as

[23] http://hdsc.nws.noaa.gov

other hydrological factors can lead to these differences.

3.3.5 Climate Change Effects on Precipitation in New England

Climate Solutions New England (CSNE), which was initiated through the University of New Hampshire's Sustainability Institute, has prepared a detailed analysis for climate change that have occurred in the past decades and has forecasted changes to 2100 for New England, by region. The statistical results of climate changes for 182 Global Historical Climate Network (GHCN) stations and for the precipitation of 308 GHCN stations are available to the public from CSNE.[24]

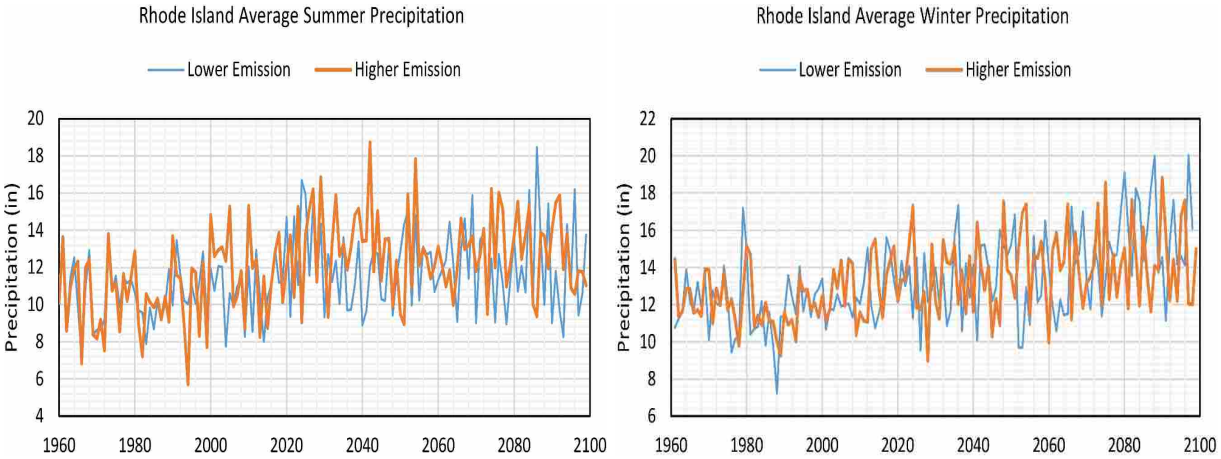

Figure 20: Rhode Island average precipitation from 1960, projected to 2099. Two projections are shown: one based on lower emissions and the other based on the higher emissions scenario; a) summer and b) winter precipitation averages. Source: CSNE

CSNE analysis of past climate data has shown that in the state of Rhode Island, the rate of climate change over the last 40 years has been much higher than in previous years. The major impacts relevant to our study are increased average rainfall and extreme rainfall events. Figure 20 shows the average precipitation variation in summer and winter model predictions for 1960-2099 for two different global greenhouse gas emission scenarios: low and high emission. The annual average precipitation in Rhode Island has increased 6-11% since 1970 and is expected to increase by 18-20% by 2020-2099. Since 1970, the study shows that the frequency and magnitude of extreme precipitation events have increased. Results from this study predict an increase in the number of extreme precipitation events, more frequent flooding, and more severe flooding for the time period 2020-2099. The increase in the number of flood events can be observed in historical data as well (Figure 4).

[24] www.climatesolutionsne.org

Accordingly, more research is necessary to study the impact of climate change in riverine flood risk assessment. The advantage of the present study is that the model can simulate changes in precipitation, and can be used for assessments of flood risks associated with climate change.

3.4 Flow Data

3.4.1 Observed Data

Stream gauge stations provide river stage and streamflow data. The locations of the 13 USGS stream gauge stations inside the Pawtuxet River Watershed are shown in Figure 21. Table 7 shows the historical peak flows recorded at these USGS stream gauges inside the Pawtuxet River Watershed.[25] It was explained before that two stream gauge USGS 01116500 at Cranston in the North Branch and USGS 01116000 at Washington in the South Branch are located in the main river branches, which provide flow data for the validation of the hydrologic model in this study. These two stream gauges are highlighted in Table 7. Zarriello and Bent (2011) reported recent increases in peak flows across 25 stream gauges in Rhode Island and Massachusetts, including the 2 stream gauges highlighted in Table 7. The increase in peak flows from the former peak of USGS record to the record breaker 2010 peaks at each of the RI gauges ranges from 2–275%, with a median increase of 88% .

March 2010 Event Observed Flow

Figure 22 shows the hourly streamflow data at the Main Branch USGS station 01116500 in Cranston and at South Branch USGS station 01116000 in Washington during the time period 2008–2013. In Figure 22a, a threshold of 2,000 cfs is shown in dotted red which will be later used to select extreme events in the watershed model. Two peaks near March 2010 can be seen in the data, one with a peak flow of 14,900 cfs and the other with a peak flow of 5,880 cfs. Even though the rainfall occurred between March 29 – 31, 2010 (see Figure 15), the high discharge of the Pawtuxet River continued onwards past April 4, 2010, with a peak flowrate of 14,900 cfs between March 31 and April 1, 2010. The same two peaks near March 2010 can be seen in Figure 22b for the South Branch, but they are of much smaller magnitude than the corresponding peaks in Cranston due to differences in the drainage areas.

Table 8 shows a comparison of peak discharge and peak gauge height at Pawtuxet River streamflow stations before and after the March 2010 flooding events. The stream gauge records in the Pawtuxet River Watershed indicate that the largest increase in the record peak flow magnitude was at Cranston in the Main Branch of the Pawtuxet River and at

[25] http://waterwatch.usgs.gov

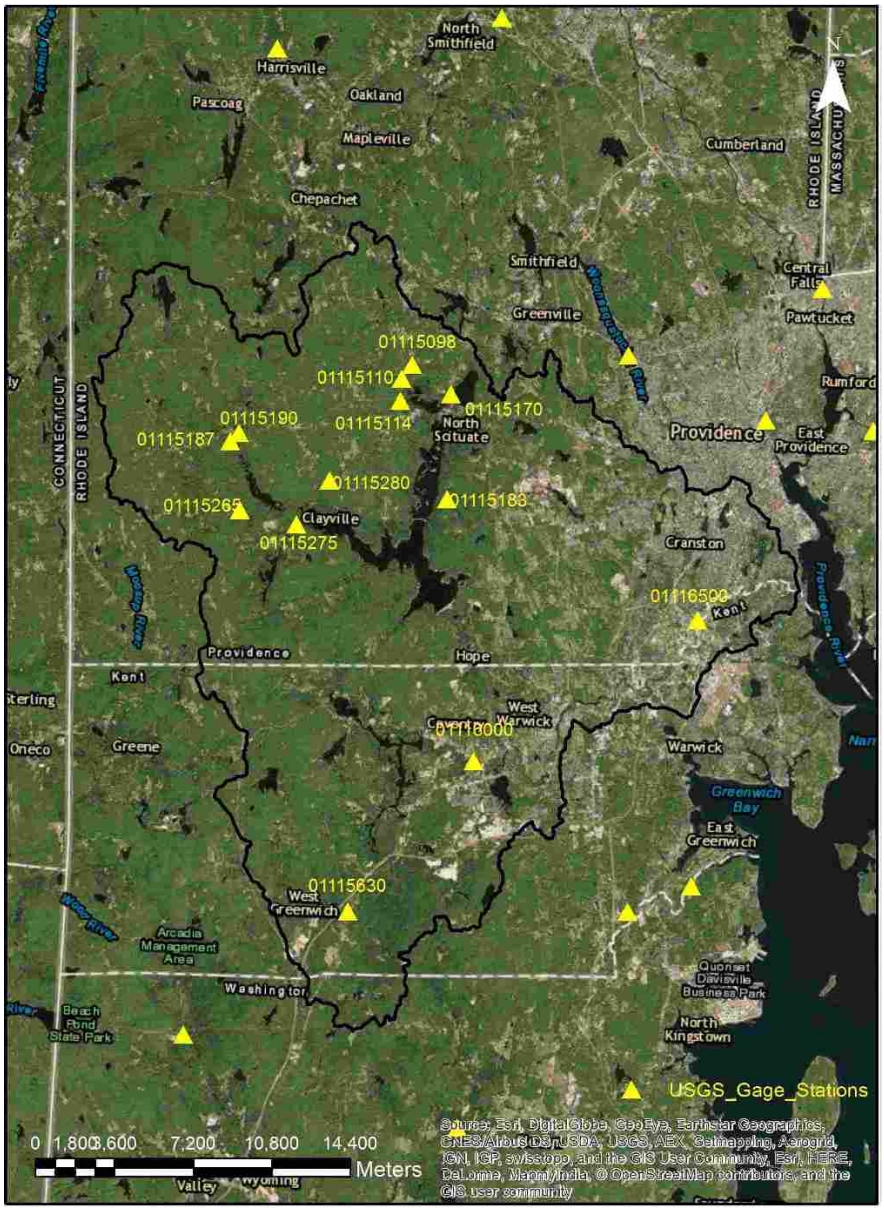

Figure 21: USGS stream gauge stations in the Pawtuxet River Watershed, RI.

Washington in the South Branch of the Pawtuxet River; increasing from 5,440 to 14,900 cfs and from 1,980 to 5,490 cfs, respectively. Apart from the drainage area, a factor contributing to the high peak values at station 01116500 in Cranston is that the land cover in the eastern and central parts of the watershed is in the residential/commercial/industrial category which leads to reduction in the infiltration of the water while increasing the runoff. However, the western and northern regions of the watershed are mainly forest areas that can reduce runoff.

Table 7: Historical peak flows at USGS stream gauges in the Pawtuxet River Watershed, Source: USGS. The stations on river reaches are highlighted.

USGS Station	USGS Station Name	Peak Flow (cfs)	date
01115098	Peetoad Brook at Elmdale Rd Nr North Scituate, RI	404	Mar 30, 2010
01115110	Huntinghouse Bk at Elmdale Rd at N Scituate, RI	782	Mar 30, 2010
01115114	Rush Brook Near Elmdale Rd Near North Scituate, RI	593	Jul 24,2009
01115120	Unnamed Trib To the Scituate Res Nr North Scituate, RI	39	Mar 30, 2010
01115170	Moswansicut Stream Nr North Scituate, RI	194	Mar 30, 2010
01115183	Quonapaug Bk at Rt 116 Nr North Scituate, RI	94	Mar 30, 2010
01115187	Ponaganset River at South Foster, RI	1,330	Mar 30, 2010
01115190	Dolly Cole Bk at Old Danielson Pk at S Foster, RI	369	Mar 30, 2010
01115265	Hemlock Brook at King Rd Nr Foster, RI	1,990	Mar 30, 2010
01115275	Bear Tree Brook Nr Clayville, RI	56	Mar 30, 2010
01115630	Noonseneck River at Nooseneck, RI	1,100	Mar 30, 2010
01116000	**South Branch of the Pawtuxet River at Washington, RI**	**5,490**	**Mar 31, 2010**
01116500	**Pawtuxet River at Cranston, RI**	**14,900**	**Mar 31, 2010**

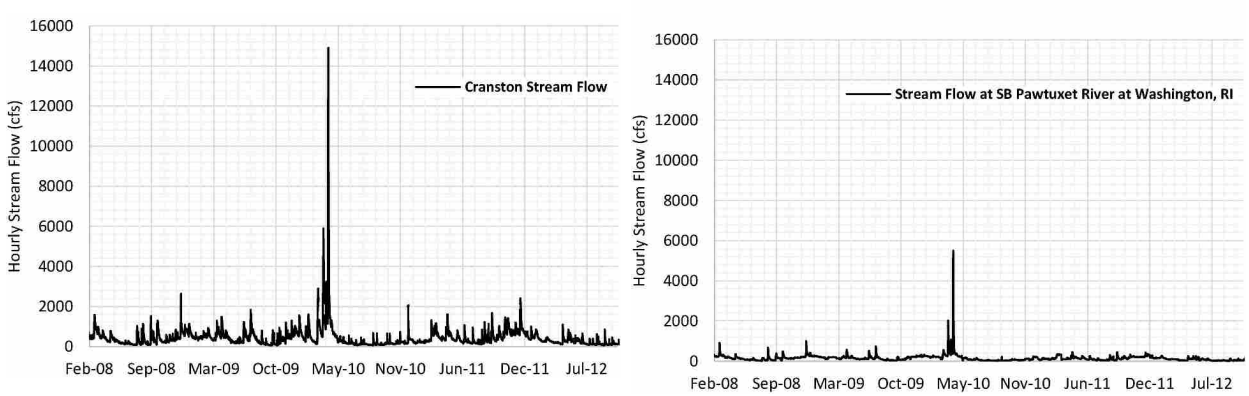

Figure 22: Hourly streamflow 2008–2013 at (a) Cranston, The Main Branch of the Pawtuxet River, RI and (b) Washington in the South Branch of the Pawtuxet River, RI.

3.4.2 Annual Exceedance Probability of Flood Peaks

The annual exceedance probability (AEP) is the expected probability that an annual peak discharge will be exceeded a certain discharge. The annual peak is the maximum instantaneous discharge occurring during the year. The reciprocal of the AEP is the recurrence interval, or return period, in years.

Table 8: Peak flow at selected USGS Gauges before and after March 2010 event (Zarriello and Bent, 2011).

	Before March 2010 event			after March 2010 event		
USGS Station	Date	Gauge Height (ft)	Discharge (cfs)	Date	Gauge Height (ft)	Discharge (cfs)
1116000	Jun 6, 1982	5.30	1980	Mar 31, 2010	9.22	5480
1116500	June 7, 1982	14.50	5440	Mar 31, 2010	20.79	14900

In this study, the return period of the discharges, AEPs, and the peak flow values for various time periods at stream gauges in Cranston and Washington, RI are used from a USGS study by Zarriello et al. (2012). Table 9 lists the AEP, return period, and peak flow for 1940–2010 at Cranston in the Main Branch and at Washington in the South Branch, and in North Branch at its confluence with the South Branch of the Pawtuxet River. Apart from historical events, these peak flow AEP data are used as input in the hydraulic model to generate the flooding maps.

Matching the peak discharges from Figure 22a with the values reported in Table 9, the observed peak flow of 14,900 cfs (March 2010) corresponds to a return period of about 500-year in the Main Branch, and the observed peak discharge of 5480 cfs from Figure 22b, slightly exceeds a 500-year event in the South Branch of the Pawtuxet River.

Table 9: Estimated magnitude of flood flows and Annual Exceedance Probability (AEP) at USGS 01116500 in North Branch, USGS 01116000 in South Branch, and in North Branch at confluence with South Branch of the Pawtuxet River for the period of record through 2010 (Zarriello et al., 2012)

.

AEP(%)	Return period (years)	Estimated peak flow (cfs) @ USGS 01116500	Estimated peak flow (cfs) @ USGS 01116000	Estimated peak flow (cfs) in the North Branch at the confluence with the South Branch
10	10	3840	1470	1960
2	50	6940	2600	3320
1	100	8820	3230	4090
0.2	500	15000	5170	6450

3.4.3 Contributions of the Subbasin Branches of the Pawtuxet River to the Discharge Values

Table 10 shows the drainage area, drainage area ratios (with respect to total watershed area), and flow discharge ratios for 10-, 50-, 100-, and 500-year events in the North and South Branches of the Pawtuxet River(Zarriello et al., 2012), using the data in Table 9. The drainage area and flow discharge are divided by the area and discharge in the Main Branch at the Cranston gauge. This table demonstrates that the drainage area ratio is higher for the North Branch than for the South Branch, and the flow discharge ratio is also higher for the North than the South branch. It is interesting to note that the ratio of flow peaks in the South and North Branches are very close to ratio of drainage area for those branches

Table 10: Drainage area and discharge ratios of the South and North Branches relative to Cranston gauge. See Figure 6.

Pawtuxet River	Outlet Point	Drainage Area (mi^2)	Drainage Area Ratio	Discharge Ratio Return period (years)			
				10	50	100	500
North Branch	Confluence of North and South Branches	108	0.49	0.51	0.48	0.46	0.43
South Branch	USGS Gauge 01116000	62.6	0.29	0.39	0.38	0.36	0.31
Main Branch	USGS Gauge 01116500	220	1.00	1.00	1.00	1.00	1.00

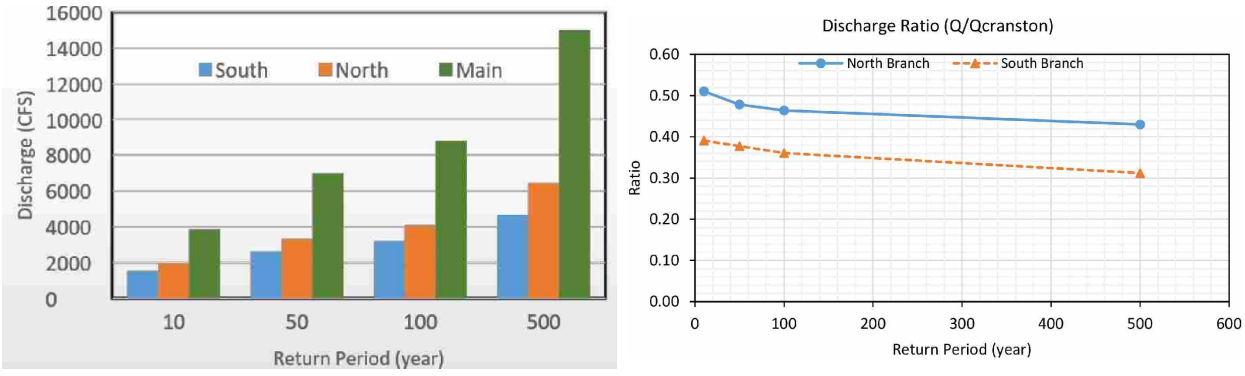

(a) *(b)*

Figure 23: Peak discharge (left) and peak discharge ratios (right) the North Branch, South Branch, and Main Branch of the Pawtuxet River, for 10-, 50-, 100-, and 500-year return period flood events. Discharge ratios are the peak flow discharges of the North Branch and South Branch divided by the observed flow in Cranston along the Main Branch.

(Figure 23); i.e., the contribution of each of North and South Branches in flooding are almost proportional to their drainage area ratios. Also, the ratio of the discharge slightly decreases by increasing the return period. Due to the residential/industrial land use in the downstream parts of the watershed (around Cranston Gauge), the rate of infiltration is less during rainfall compared to the upstream parts (North and South Branches), leading in more runoff. Figure 23 shows the diagram of peak discharge and peak discharge ratios corresponding to Table 10.

Here, we've discussed the data sources we used for the integrated watershed and river model. Next, we discuss the methodology used in the modeling work, including the general process, software, and the calculation theories used.

4 Methodology

In general, models are representations of systems or natural processes. For our project, the model variables (runoff, ground water, soil water flow) are themselves controlled by a variety of physical characteristics of the watershed. In this section, we review the physical processes, models, and theoretical equations that are used in flood simulation.

4.1 Overview

Figure 24 illustrates processes that simulates runoff resulting from precipitation in a watershed (Feldman, 2000). Precipitation on the land surface either evaporates back into the atmosphere, flows off the land surface as runoff, or infiltrates into the soil layers to join the groundwater or the baseflow in river. Figure 25 represents the steps applied in this project for the runoff and flood simulation (Knebl et al., 2005). Spatial distributed data are preprocessed in ArcGIS and HEC-GeoHMS to produce the drainage network model, which acts as an input to the rain-runoff model in HEC-HMS. The rainfall-runoff model in HEC-HMS also takes distributed basin data, meteorological data, and modeling control specifications to compute the time series of discharge. From the HEC-HMS model, time series of flow

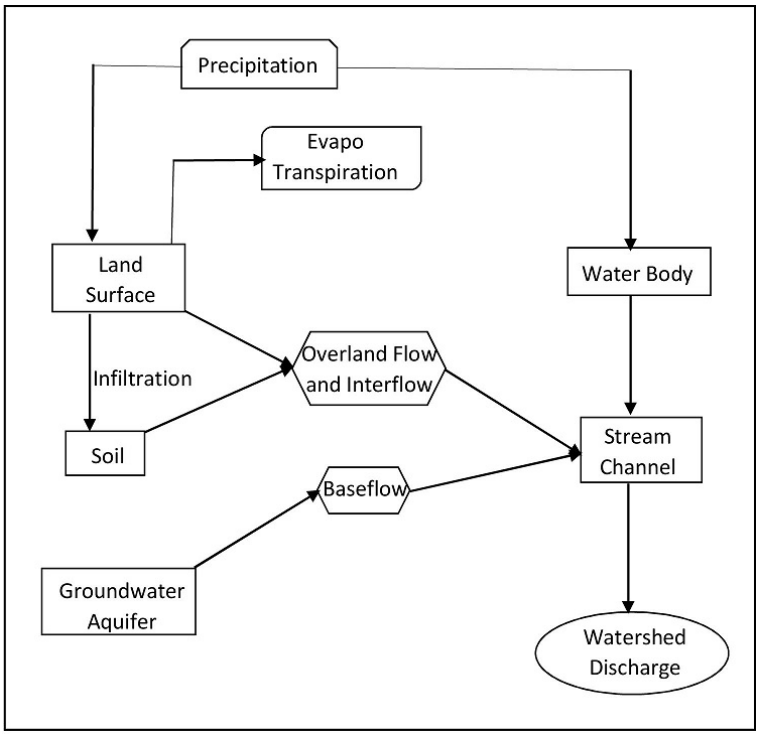

Figure 24: Hydrologic processes from precipitation to discharge in a watershed (Feldman, 2000).

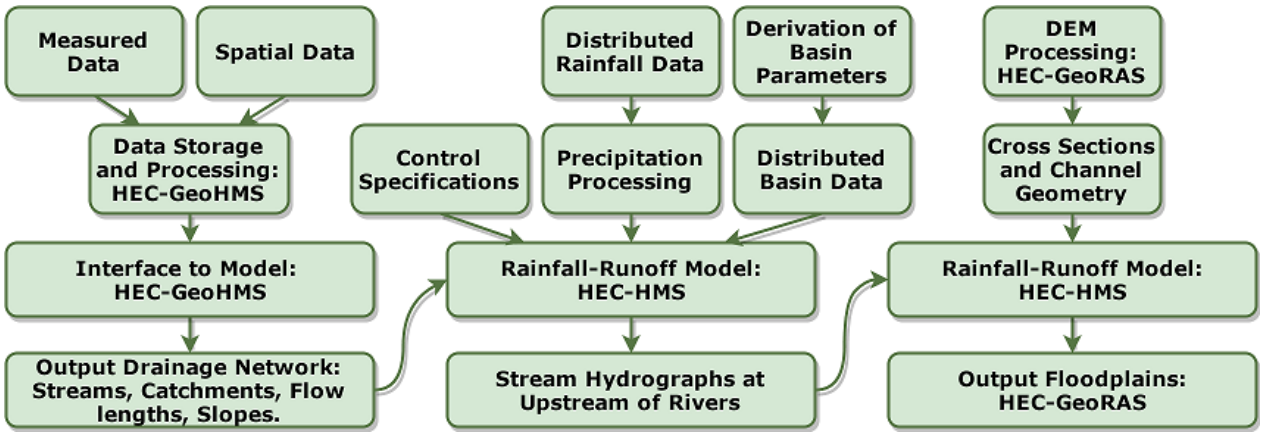

Figure 25: Flowchart of distributed hydrologic and hydraulic modeling of flow in watersheds (Knebl et al., 2005).

at upstream of rivers are used as input into the river hydraulic model (HEC-RAS), along with river cross sections, channel geometry, river structures, and roughness. Finally, in the hydraulic model, water elevations are computed. These elevations are superimposed on DEM to compute flood maps in HEC-GeoRAS.

Distributed model forecasts are required for flood inundation models. Recently, flood modeling has been improved with the advent of Geographic Information Systems (GIS), high resolution digital elevation models (DEMs), and distributed hydrologic models.

4.2 HEC-GeoHMS

The Geospatial Hydrologic Modeling Extension of HEC-HMS hydrology toolkit (HEC-GeoHMS) is developed for engineers and hydrologists who may not have extensive GIS experience in mind. It is designed to pre/postprocess watershed geospatial data for the hydrologic model HEC-HMS. The geo-spatial toolkit has many features, further details and information are explained in Doan et al. (2000). HEC-GeoHMS uses ArcGIS and its Spatial Analyst toolkit to develop the hydrological modeling inputs for the Hydrologic Engineering Center's Hydrologic Modeling System (HEC-HMS); (Scharffenberg and Fleming, 2006). ArcGIS and its Spatial Analyst extension are available via the Environmental Systems Research Institute (ESRI).

HEC-GeoHMS transforms the drainage paths and watershed boundaries into a hydrologic data structure by analyzing terrain data. This transformed structure represents the drainage network. The HEC-GeoHMS program enables the users to visualize spatial information and watershed characteristics, allowing the user to perform spatial analysis and delineation of subbasins and streams in the watershed. HEC-GeoHMS allows the user to create hydrologic inputs for HEC-HMS.

4.3 HEC-HMS

The Hydrologic Modeling System (HEC-HMS) is a program that can simulate precipitation-runoff processes in watersheds. This model is well suited for the modeling of large river basins and flood hydrology, as well as small urban or natural watershed runoff modeling.

HEC-HMS is a generalized modeling system, and can represent many different types of watersheds. Various mathematical models, included in HEC-HMS, are appropriate for modeling watersheds with different conditions. Choosing the appropriate modeling design options requires knowledge of the watershed characteristics, the goals of the hydrologic study, as well as engineering/scientific judgement.

HEC-HMS is a product of the Hydrologic Engineering Center (HEC) within the U.S. Army Corps of Engineers, initially developed in 1992 as a replacement for HEC-1, long considered a standard for hydrologic simulation. The program is now widely used and accepted for many official purposes, such as floodway determinations for the Federal Emergency Management Agency (FEMA) in the United States (Scharffenberg and Fleming, 2006).

A physical watershed is modeled with a basin model in HEC-HMS, with main model components such as subbasins, reaches, reservoirs, junctions, diversions, sources, and sinks. A subbasin is a subset of watershed catchment. Reaches include rivers and streams connecting these subbasins. Reservoirs include dams and lakes. A junction is a confluence of two or more reaches. Diversions include bifurcations or withdrawals. Lastly, model sources represent natural sources such as springs, and model sinks represent natural sinks such as outlets and terminal lakes.

4.3.1 Runoff/Infiltration Formulation

Infiltration or runoff from rainfall can be predicted from the empirical loss rate parameter called the runoff Curve Number (CN), which is based on various soil and land use databases. CN is also known as the Soil Conservation Service (SCS) runoff Curve Number, after the USDA Natural Resources Conservation Service (NRCS, formerly the Soil Conservation Service) developed the CN method.

In the HEC-HMS modeling program, there are a number of methods that may be used to calculate runoff through the watershed model. These methods include the initial constant, SCS Curve Number, exponential loss, Green Ampt, and Smith Parlange methods; one-layer, three-layer, and gridded methods are also available, with options for canopy and surface components for more complex modeling. For our modeling, we chose the runoff method based on the SCS Curve Number method. It should be noted that each method can be potentially calibrated to produce more accurate results (Scharffenberg and Fleming, 2006).

Physical characteristics and purpose of modeling (i.e., event or continuous simulation) should be considered in selection of a method.

CN is based on the area soil type, land use, hydrologic condition, and depth of the high water table. USDA (1986) indicates CN based on characteristic of land cover descriptions and hydrologic soil groups. The runoff equation is:

$$P_e = \begin{cases} 0 & \text{for } P \leq I_a \\ \frac{(P-I_a)^2}{P-I_a+S} & \text{for } P > I_a \end{cases} \tag{1}$$

where P_e is the runoff (excess rainfall) in inches/mm, P is the rainfall in inches/mm, and S is the potential maximum soil moisture retention in inches/mm. I_a is the initial abstraction, or the amount of water intercepted by ground vegetation before runoff occur. I_a is generally taken to be in the range of $0.2S - 0.5S$ (Lim et al., 2006).

Here, $I_a = 0.2S$ so that once the initial abstraction has been replaced, the runoff equation becomes:

$$P_e = \frac{(P - 0.2S)^2}{P + 0.8S}, \tag{2}$$

where the potential maximum soil moisture retention is related to CN by in US Customary Units:

$$S = \frac{1000 - 10CN}{CN}. \tag{3}$$

$30 \leq CN \leq 100$, where low values reflect better infiltration in areas such as forests, and higher values reflect poorer infiltration and more runoff in areas such as urbanized zones. CN of 100 means zero infiltration in the above formulation. After runoff is calculated at each rainfall time step (e.g. hour), a unit hydrograph (e.g. Snyder, SCS) will route the runoff and compute the flow discharge.

4.3.2 Calibration Process

Model calibration is a critical step to development of an accurate model. Figure 26 shows a generalized flowchart of the calibration process. A starting estimate of the model parameters is selected, and runoff is calculated. The parameters utilized in watershed modeling such as CN, time lag, initial abstraction, and base flow are used in calibration to obtain a best fit of model to the observed data. The model parameters are adjusted until the computed runoff matches corresponding observed data with minimum error. In the calibration process, the optimal parameter values are required to minimize the objective function (i.e. error) within the HEC-HMS methods. In the precipitation-runoff models, this function measures

the degree of variation between computed and observed hydrographs (Scharffenberg and Fleming, 2006).

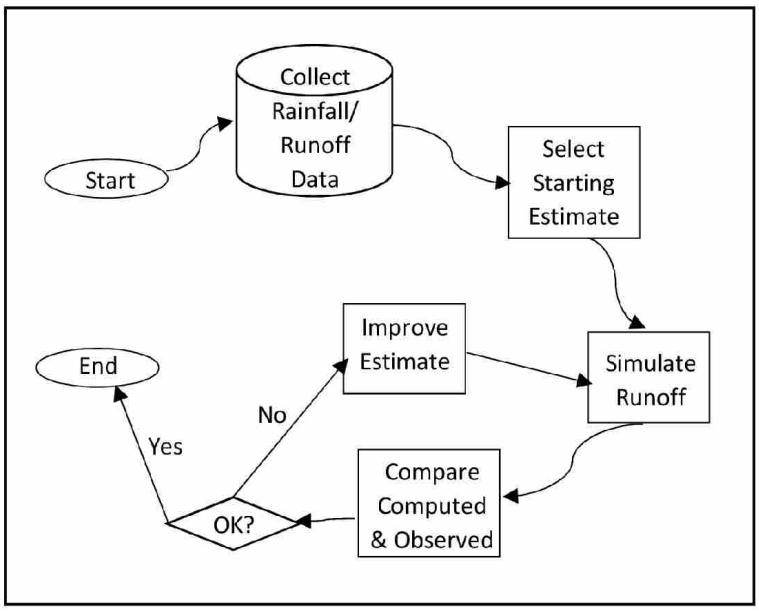

Figure 26: Calibration process in a hydrological model (Feldman, 2000).

4.3.3 Uncertainty Analysis

We will also perform an uncertainty analysis for the HEC-HMS discharge results in Section 6.1.3, with four different sources of precipitation input to measure the 90% and 80% confidence intervals for the discharges computed by HEC-HMS. Since we will use a small sample size of precipitation data sources, we use Student's t-distribution probability density function to find the confidence interval for precipitation and discharge.

To find the confidence interval where the population mean μ is located, we use:

$$\bar{X} - t_{\frac{\alpha}{2}} \left(\frac{s}{\sqrt{n}} \right) < \mu < \bar{X} + t_{\frac{\alpha}{2}} \left(\frac{s}{\sqrt{n}} \right), \tag{4}$$

where $\bar{X}$ is the sample mean, s is the sample standard deviation, n is the sample size, the value for $t_{\frac{\alpha}{2}}$ is tabulated for the t-distribution dependent on the degree of freedom and percentage of error, where the degree of freedom is $n - 1$.

A Matlab code was also developed to produce the precipitation confidence interval. Two confidence intervals of 90% and 80% were considered for the precipitation. It is also recommended to use a logarithmic scale log-normal distributed to avoid negative numbers.

4.3.4 Hydrologic Reservoir Routing

Reservoirs route (i.e. reduce) the flood discharge in addition to store the water. Figure 27 shows typical hydrographs for inflow and outflow of a reservoir. In the figure, the shaded area is the volume of the water stored in the reservoir above the crest elevation of the spillway which is released gradually from the spillway.

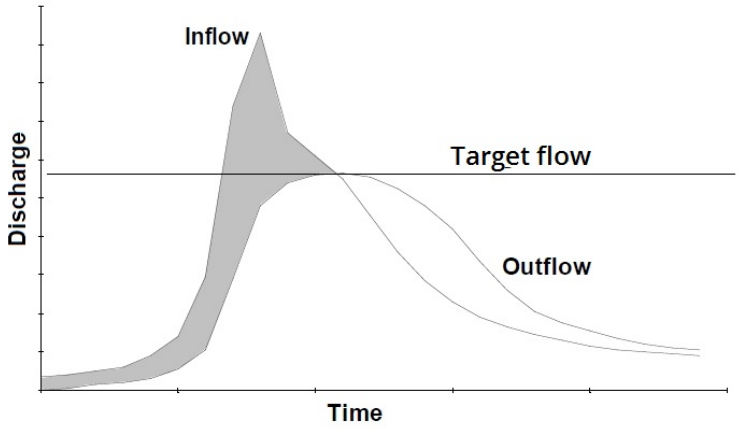

Figure 27: Inflow and outflow hydrograph from a reservoir spillway crest.

The outflow from the spillway is computed with the spillway equation depending on the type of spillway. The calculation is based on the continuity equation in which the inflow to the reservoir minus the outflow of the reservoir should be equal to the rate of change of the storage in the reservoir:

$$Q_{\text{in}}{}^{(\text{t})} - Q_{\text{out}}{}^{(\text{t})} = \frac{dS(h)}{dt}, \tag{5}$$

where Q_{in} is the inflow to the reservoir, Q_{out} is the outflow from the spillway, and $S(h)$ is the Reservoir storage which is a function of reservoir elevation h.

For ogee spillways, the outflow of the spillway is calculated according to the spillway formula (Chen, 2015):

$$Q = CLH^{\frac{3}{2}} = CL(h - h_{\text{crest}})^{\frac{3}{2}}, \tag{6}$$

where Q is the flow rate in cfs, C is the discharge coefficient generally ranging between 3–4, L is the spillway crest length in ft, H is the difference in elevation between the reservoir's water surface elevation h and the spillway crest elevation (h_{crest}: total hydraulic head), where $h > h_{\text{crest}}$.

Using Equations 5 and 6, the calculation is performed for recursive time intervals in the following equation:

$$Q_{\text{in}}{}^{\text{k}} - CL(h^{\text{k}} - h_{\text{crest}})^{\frac{3}{2}} = \frac{S(h^{\text{k+1}}) - S(h^{\text{k}})}{\Delta t}. \tag{7}$$

where $Q_{\text{in}}{}^{\text{k}}$ is average inflow to the reservoir at k^{th} time step, h^{k} is reservoir water elevation at k_{th} time step, $S(h^{\text{k+1}})$ and $S(h^{\text{k}})$ are reservoir storage at $(k+1)^{\text{th}}$ and k^{th} time steps, and Δt is the time interval. After $\text{S}(\text{h}^{\text{k+1}})$ is computed, the $\text{h}^{\text{k+1}}$ will be determined using storage elevation curve of the reservoir, and this will be continued for routing (Feldman, 2000). HEC-HMS has the ability to perform these calculations. We also did our own analysis in MATLAB and compared with HEC-HMS. If the water elevation in the reservoir is below the spillway crest, the total runoff will be stored in the reservoir, during the simulation.

4.4 HEC-GeoRAS

HEC-GeoRAS is one of the extensions of ArcGIS which provides geospatial geometry for HEC-RAS, and also postprocessing of the model results. Using a DEM file in HEC-GeoRAS, the user can extract cross sections along the river and add storage area, different structures and levees to the model. The user can then export the geospatial file to HEC-RAS for further simulations. HEC-GeoRAS is also powerful in post-processing of the results from HEC-RAS to map the inundation and boundaries along the river. The outputs of HEC-GeoRAS are flooding maps for several return periods which can be used to communicate the risk of flooding.

Figure 28 illustrates the relations of the HEC-RAS and Hec-GeoRAS softwares; each step of the process including preprocessing, modeling, and postprocessing are presented in detail.

4.5 HEC-RAS

HEC-RAS stands for Hydrologic Engineering Centers River Analysis System and is a software for modeling river hydraulics, both 1D and 2D. The model can be run in steady or unsteady models. It includes a graphical user interface that helps the user easily access the capabilities of the model, such as data storage, graphics, geometry and report results (Ackerman, 2009).

HEC-RAS performs a steady flow computation to calculate water surface elevation of the river. It can also simulate 2D unsteady flow and floodplains. Sediment transport simulation is another module of this model. All of the mentioned simulations use a common model geometry.

The geometry in a HEC-RAS model is defined by cross sections along the river. The number of required cross-sections depends on the rate of change in the river sections; a more

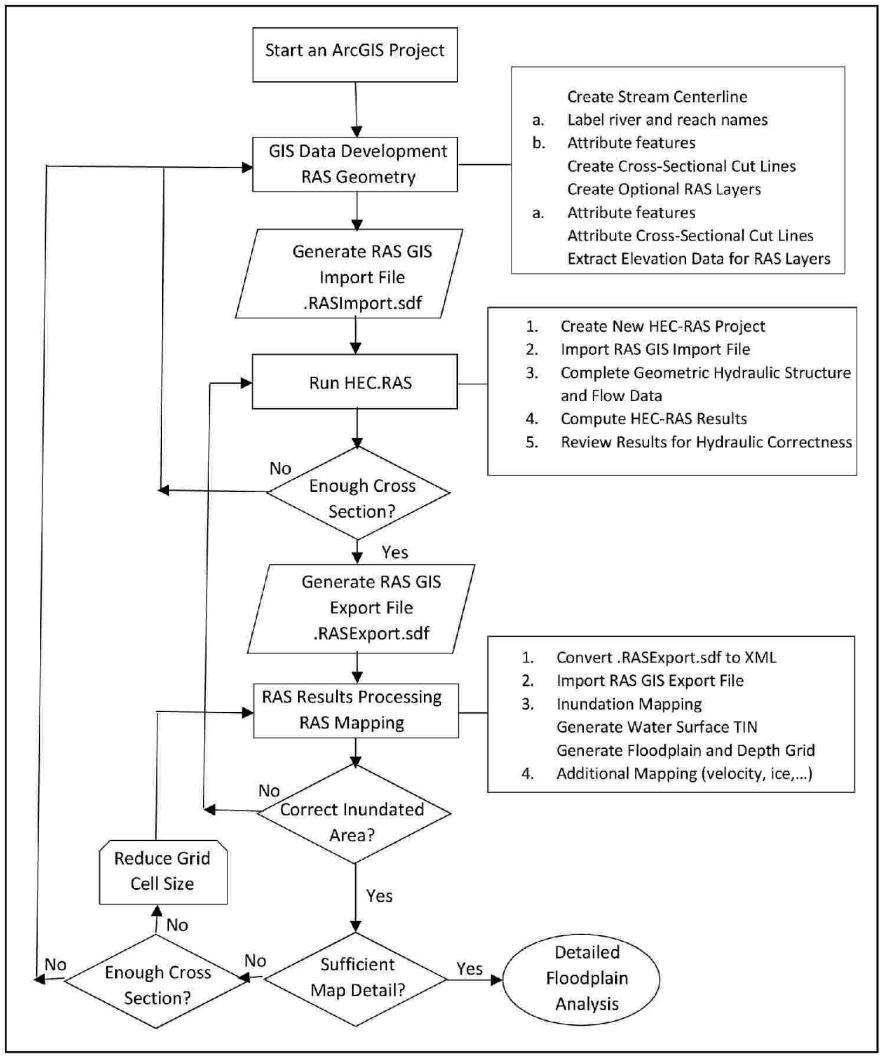

Figure 28: Flowchart of HEC-RAS and HEC-GeoRAS for flood simulation (Ackerman, 2009).

rapidly changing river profile requires more cross sections for sufficient spatial resolution. The length of the cross sections, called the cutline in the software, should be chosen so that the entire floodplain would be located inside the boundaries of the cross sections. In the geometry section of HEC-RAS, model elements such as bridges, culverts, inline structures, dams, lateral structures, and storage areas can be specified and defined.

Flow data (as upstream boundary condition) are the the next critical part of the model definition to complete the setup for simulation. Several flow scenarios can be applied in each location along the river. Finally, boundary conditions for the river must be applied. Known water surface, critical depth, normal depth and rating curves are examples of different kinds of boundary conditions in the river model that can be specified at the downstream of a river.

After the river geometry and boundary conditions have been specified, HEC-RAS can

run the simulation to calculate steady flow, unsteady flow, or sediment transport along the modeled river. HEC-RAS applies the energy equation for 1D steady flow, and mass and momentum conservation for the 1D and 2D unsteady flow calculation. The type of boundary conditions depends on subcritical (controlled at the downstream with Froude Number [Fr] less than 1), supercritical (Fr>1), and mixed flow regimes. In majority of cases the flow is subcritical. After spillways and dams, flow is supercritical which is followed by a hydraulic jump.

4.5.1 Steady State Flow Simulation

HEC-RAS applied only 1D simulation for the steady flow analysis. It uses the conservation of energy equation as follows,

$$Z_2 + Y_2 + \frac{a_2(V_2)^2}{2g} = Z_1 + Y_1 + \frac{a_1(V_1)^2}{2g} + h_e, \tag{8}$$

where Z_1 and Z_2 are elevation, Y_1 and Y_2 water depth, V_1 and V_2 cross sectional averaged velocities, a_1 and a_2 are velocity coefficients, and g and h_e are gravitational acceleration and energy head loss, respectively, where 1 and 2 refer to adjacent river cross sections. Equation 8 is used to calculate the water surface level for the gradually varied river flow in each of the cross sections. Calculations continue through neighboring cross sections. Figure 29 shows various parameters of the energy equation (Equation 8) in the model for two neighboring cross sections.

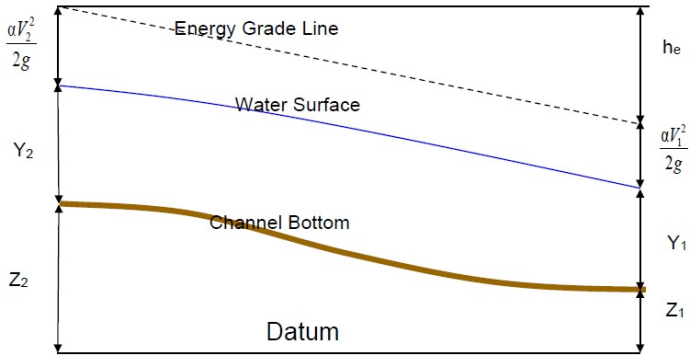

Figure 29: Energy equation terms (Brunner, 2016).

Energy head loss h_e can be calculated by the Equation 9:

$$h_e = L\bar{S}_f + C|\frac{a_2(V_2)^2}{2g} - \frac{a_1(V_1)^2}{2g}|, \tag{9}$$

where L is the discharge weighted length, S_f is the friction slope, and C is the expansion/contraction loss coefficient.

Figure 30 shows the cross section divisions in the model. Cross sections in the model are divided into left and right overbanks, in addition to the main channel. In the figure, the left overbank is represented by divisions n_1 and n_2, the right overbank by n_3, and the main channel by n_{ch}, each division with its area A and perimeters P. Each of the overbank sections are subdivided into units to determine the total conveyance K and uniform distribution of the velocity. The main channel section is not subdivided unless the roughness coefficient changes. The total amount of discharge is the sum of the left, right and main channel flows.

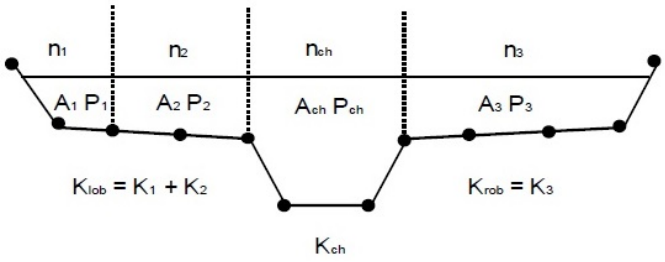

Figure 30: Cross section divisions in HEC-RAS model (Brunner, 2016).

4.5.2 Unsteady Flow Formulation

1D and 2D unsteady simulation models are available in the HEC-RAS software. 1D equations are explained here, HEC-RAS uses the mass and momentum conservation laws in unsteady simulations (Brunner, 2016). The continuity equation in unsteady flow indicates that the rate of flow into the control volume is equal to rate of change in the fluid inside the control volume, expressed in Equation 10,

$$\frac{\partial A}{\partial t} + \frac{\partial Q}{\partial x} - q_1 = 0, \tag{10}$$

where A is the channel cross sectional area, t is time, x is the horizontal coordinate, Q is the flow discharge, and q_1 is the lateral inflow per unit length. A control volume sketch illustrates these quantities used to describe mass and momentum conservation in Figure 31.

Based on the Newton's second law, the momentum equation indicates that the sum of momentum flux and external forces to the control volume is equal to the rate of change of momentum in control volume. Equation (11) shows the final form of the momentum equation used in HEC-RAS:

$$\frac{\partial Q}{\partial t} + \frac{\partial (QV)}{\partial x} + gA(\frac{dz}{dx} + S_f) = 0, \tag{11}$$

where V is the cross section average velocity and z is the local channel elevation.

For numerical calculations, HEC-RAS uses the implicit finite difference scheme for 1D unsteady flow equations. For 2D unsteady, it applies the hybrid discretization scheme combining finite differences and finite volumes for the flow equations.

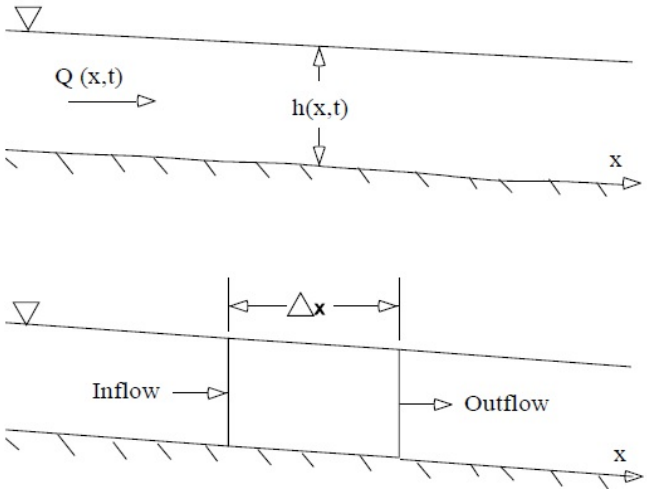

Figure 31: Control volume for mass and momentum conservation (Brunner, 2016).

4.5.3 Simulation of Dams in HEC-RAS

HEC-RAS uses Equation 12 for uncontrolled overflow computation used to simulate dams (Chen, 2015):

$$Q = CLH^{\frac{3}{2}}, \tag{12}$$

where C is the weir flow coefficient, L is the length of the spillway crest, and H is the upstream energy head above the spillway crest. Typically, $2.6 \leq C \leq 4.0$ $[\sqrt{ft}]$, depending on the shape of the spillway. A broad crested, ogee shaped, and sharp crested are the three shapes of spillways that can be applied in the HEC-RAS model. The weir coefficient is an important parameter in this equation that should be considered carefully.

For ogee crested weirs, the program allows for fluctuations in the discharge coefficient to account for upstream energy heads that are either higher or lower than the design head. Figure 32 plots the discharge coefficient relative to the coefficient for the design head as a function of the ratio of head on the crest to the design head.

For weir flow, in which the sharp crested spillway crest shape is selected, the user has the option of using the standard weir equation, the Rehbock equation, or the Kindsvater and Carter equation. If the standard weir equation is selected, the user must enter a weir coefficient. If either the Rehbock or the Kindsvater and Carter equation are selected, then the weir coefficient will automatically be calculated. Table 11 is a list of typical weir coefficients for various shapes of weir crests. For the three branches of the Pawtuxet River, almost all the dams are broad crested weirs with a weir coefficient of $C = 2.6[\sqrt{ft}]$. Some of the dams have a few gates, which are considered in the model.

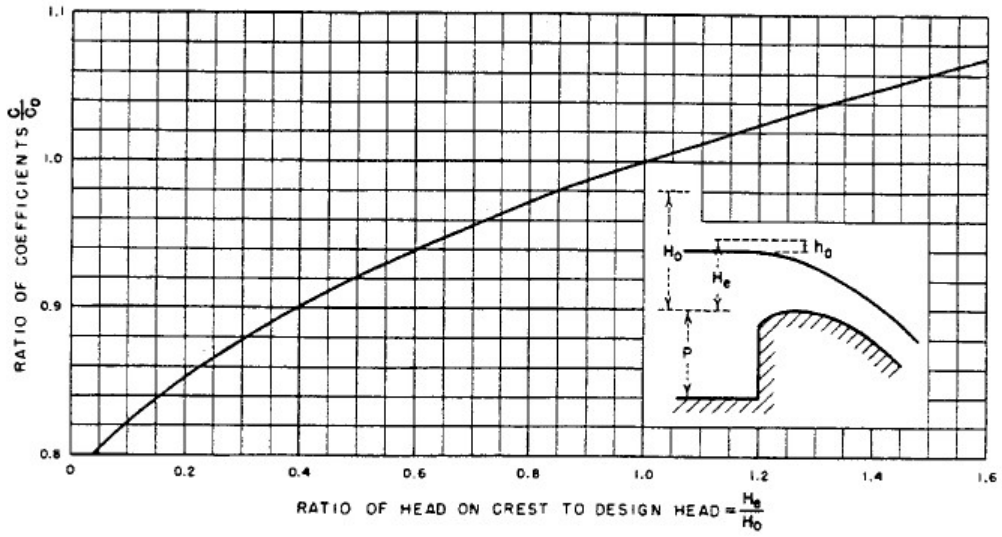

Figure 32: Discharge coefficient of an ogee spillway as a function of energy head, H_e. C is the coefficient of discharge for an arbitrary energy head (i.e., H_e), C_0 is the coefficient of discharge at the design head H_o (corresponding to the design discharge, e.g., 200-year) (USBR, 1977).

Table 11: Typical Overflow Weir Coefficients (Brunner, 2016).

Weir Crest Shape	Typical Coefficient Range ($\sqrt{ft}$)
Broad Crested	2.6 - 3.1
Ogee Crested	3.2 - 4.1
Sharp Crested	3.1 - 3.3

We have described in this section the models, and theory of our modeling methodology. Next, we discuss the integrated watershed and river model, along with the model parameters and methods chosen.

5 Development of Hydrologic/Hydraulic models

This section describes how we prepared the integrated model of the Pawtuxet River and watershed. We used HEC-HMS to calculate the flood discharge to the river reaches, and those discharges were used in HEC-RAS to estimate water elevation and extent of flooding.

5.1 Watershed Model

Two different watershed models were developed, one model with a 24 subbasin delineation and the other model with a 9 subbasin delineation. The hydrological model parameters for the watershed model with 24 subbasin are close to those for the model with 9 subbasins. The model with 24 subbasins is recommended for studies requiring finer detail upstream of the Scituate and Flat River Reservoirs, but for our studies we chose the model with 9 subbasins in order to decrease the model nonlinearity and for simplicity in calibration (i.e., less number of subbasins requires less parameters to calibrate).

5.1.1 Terrain Processing

Terrain pre-processing includes a series of steps to derive the drainage network by applying the terrain data as model input. The process consists of computing the flow direction, flow accumulation, stream definition, and watershed delineation. The computed datasets are then utilized in subsequent steps in computing subbasin and stream delineation.

Figure 33 shows the preliminary steps in preparing data for terrain processing. Preparation includes characterizing fill sink, flow direction, stream definition, flow accumulation, stream segmentation and slope-grid to determine the watershed slope. All these steps are required for subbasin delineation in the watershed modeling. More information about each tool utilized to obtain Figure 33 is available in Doan et al. (2000).

It is important that accurate and high resolution DEM be used for hydrological modeling. If the DEM is not accurate enough, the simulated rivers may follow very different paths from their actual path; inaccuracy in the DEM could result in incorrect watershed delineation. In general, the DEMs contain elevation averages at regular intervals which may not accurately represent stream locations and watershed boundaries. Therefore, it is important to manually check that the watershed and stream delineation in the terrain processing steps is done correctly. The available tools in the basin processing menu in HEC-GeoHMS give the capability to delineate and edit basins to be in agreement with the physical configuration of the river and watershed.

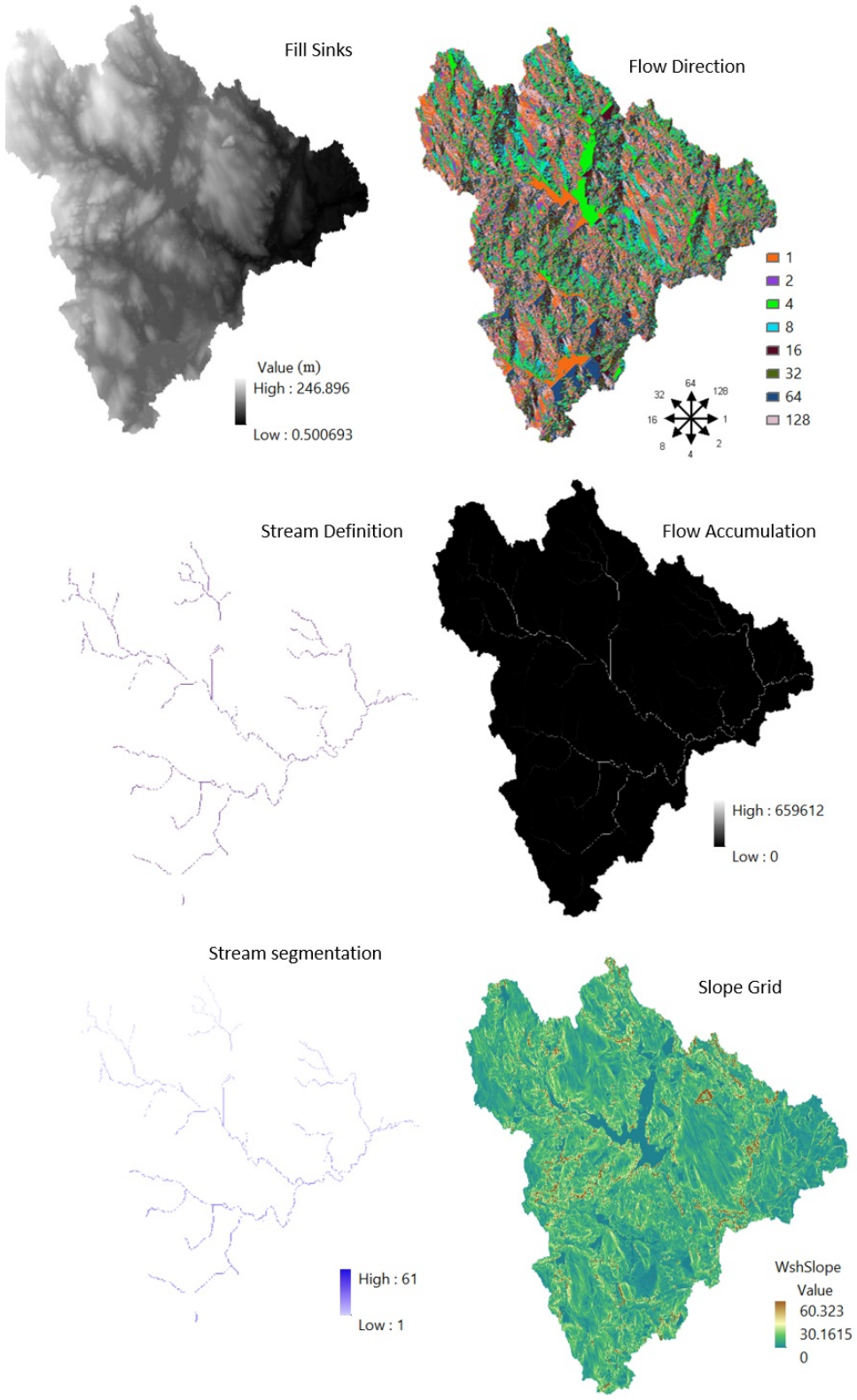

Figure 33: Preliminary steps in preparing data for the terrain analysis, prior to subbasin delineation in HEC-GeoHMS (1 m = 3.28 ft).

5.1.2 Subbasin Delineation

As mentioned, we generated two Pawtuxet River watershed models, one finer model for studies involving upstream of the reservoirs, divided into 24 subbasins, and one coarser model suitable for the flooding studies downstream of reservoirs investigated here, divided into 9 subbasins. These divisions are all performed in HEC-GeoHMS, and the outputs are exported to HEC-HMS. All the units in HEC-GeoHMS were SI units and were subsequently converted to US customary units to be used in the HEC-HMS model.

A variety of tools in HEC-GeoHMS are utilized to create subbasins in the model. It is possible to see the delineation results, evaluate outcomes, and accept or reject the delineation results. During the interactive basin processing, the results can be confirmed and during the batch mode, outlet locations can be supplied and the program will delineate subbasins at those locations.

The area-threshold method was utilized in the Pawtuxet River watershed modeling. In this method, water in each grid cell can flow to one of the eight neighbor cells with the most

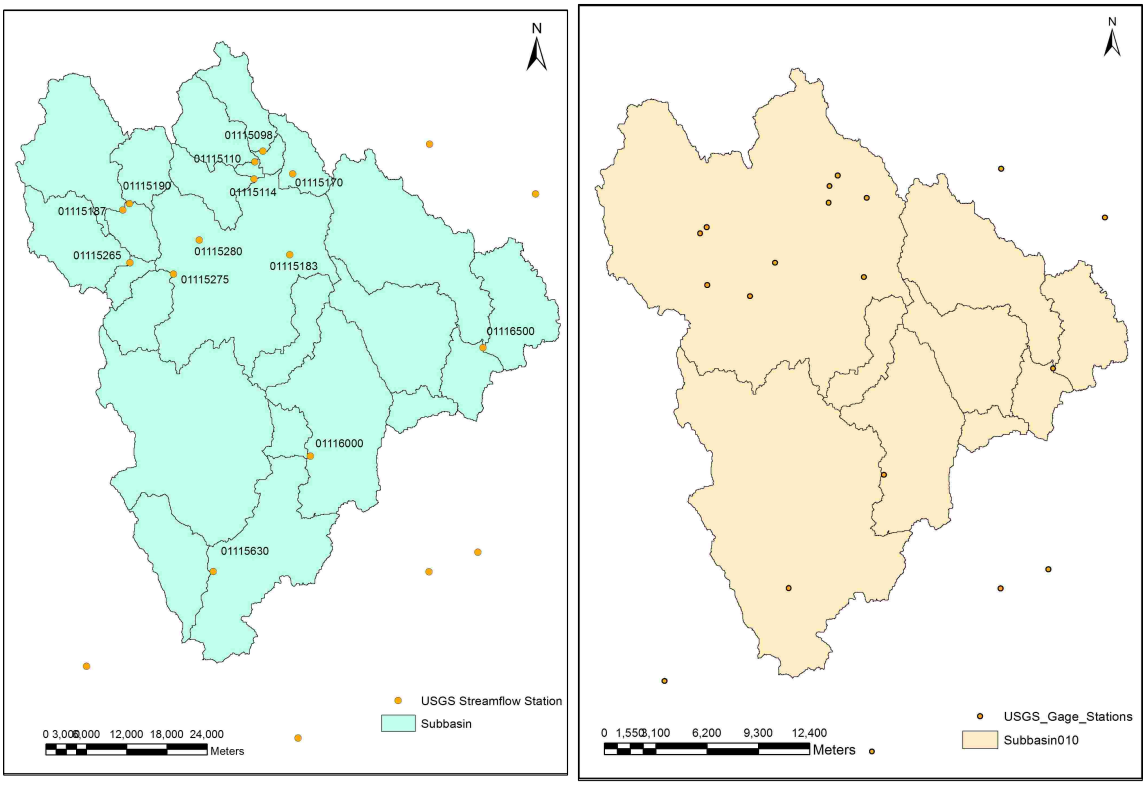

(a) Pawtuxet River watershed model with 24 subbasins.

(b) Pawtuxet River watershed model with 9 subbasins.

Figure 34: Subbasin delineation for watershed model with 24 and 9 subbasins. Locations of USGS stream gauges are shown in yellow circles.

slope in the surrounding. Then each cell is assigned a value according to the number of cells that flow into a particular cell in that location. Each cell that exceeds the pre-defined threshold value becomes part of the stream network.

Depending on the method set for the HMS process, each subbasin must be characterized with parameters such as CN and the initial loss constant (Doan et al., 2000). After preparing all the necessary terrain processing data shown in Figure 33 in GeoHMS, the subbasin delineation was utilized for the Pawtuxet River watershed model.

Figure 34a shows the 24 subbasin model that we would recommend to use in studies involving areas upstream of either of the Scituate or Flat River Reservoirs. For the 9 subbasin model that we have implemented in the flooding study downstream of reservoirs, we ensured that the subbasin delineation retained important physically-meaningful boundaries. Figure 34b shows the map of the watershed defined with 9 subbasins. The 9 subbasin model is designed to cover the North and South Branches of the Pawtuxet River within two independent subbasins. Furthermore, the largest northern subbasin includes the Scituate Reservoir, and the outflows at the subbasin outlet is largely affected by the Scituate Reservoir structure and its routing. The second largest subbasin is located on the South Branch and encompasses the Flat River Reservoir; it is most directly affected by the Flat River Reservoir structure and its routing. The USGS stream gauge 01116000 is located about 2.5 miles downstream of the Flat River spillway.

The summary of terrain processing results for the Pawtuxet River watershed model are presented in Table 12 for nine subbasins model. The CN calculation will be described later. Figure 35 depicts the two models of the Pawtuxet River watershed project with 24 and 9 subbasins in HEC-HMS.

Table 12: Subbasin parameters for the Pawtuxet River watershed model with nine subbasins.

Subbasin ID	Area (mi^2)	CN	Subbasin Lag (min)
W520	90.8	65.6	460
W740	5.2	63.9	165
W650	62.6	60.0	614
W780	20.0	69.4	260
W540	13.3	71.4	243
W570	2.5	73.7	105
W840	4.3	77.9	136
W430	20.8	72.1	293
W530	9.3	74.6	248

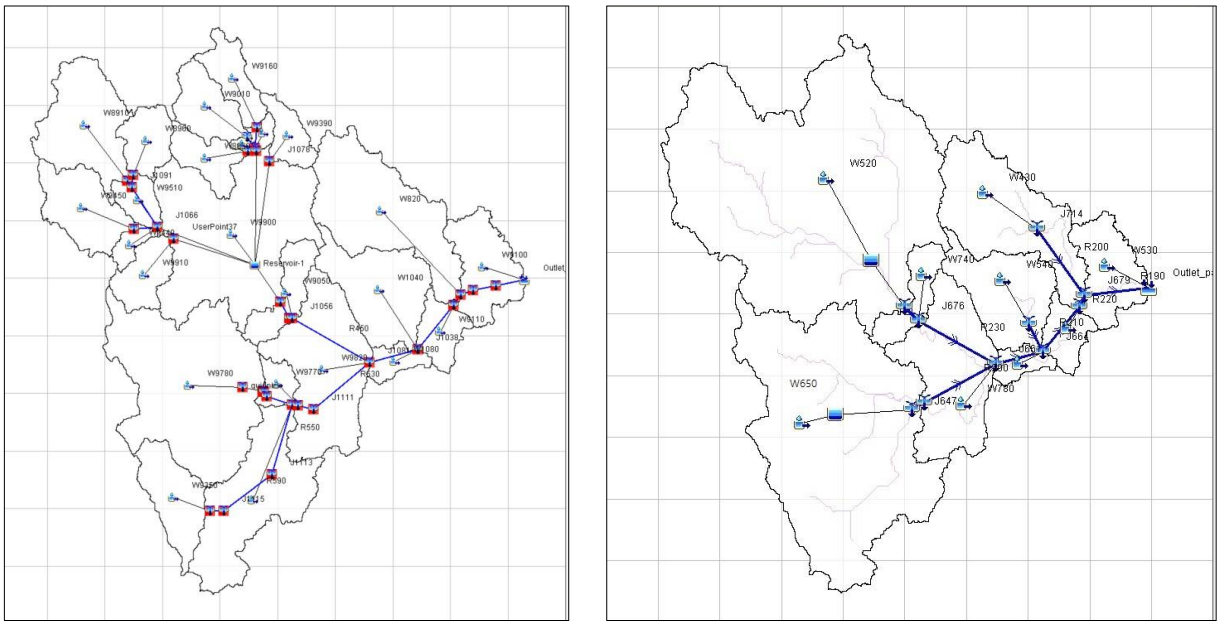

(a) HEC-HMS model with 24 subbasins. *(b) HEC-HMS model with 9 subbasins.*

Figure 35: Modeling of the Pawtuxet River watershed with 24 and 9 subbasins in HEC-HMS.

5.1.3 Infiltration Map

The land use and soil type data are required to be merged in a polygon layer to create CN grids using the CN Grid tool; a lookup table which relates land use and hydrologic soil groups to a CN was produced in Table 13 (Doan et al., 2000). Soil type data should contain the percentage of each hydrologic soil groups (HSG: A, B, C and D) in the soil layer polygons. We used the soil database available from the Natural Resources Conservation Service, as described in Section 3.2.4. Using the Union tool in HEC-GeoHMS, the land use and soil type layers are merged. The union tool includes attributes from both layers in the merged dataset. In order to merge LULC and HSG, the LULC is re-classified into 13 categories and then merged with soil groups via ArcView tools. The 13 re-classified LULC categories are listed in Table 13.

The resulting CN map of the Pawtuxet River watershed is shown in Figure 36. The CN map shows that the east parts of the watershed have larger CN values, which indicates that these areas are more urbanized. The minimum and the maximum CN values in this project are CN = 30 for forest coverage with HSG A and CN = 100 for water bodies such as reservoirs, ponds, lakes, and rivers. Note that the CN grid values are only available in the grid points, and it is possible to calculate an averaged CN in each subbasin. Therefore, the CN grid values for the watershed with 9 or 24 subbasins are the same at each grid, but the averaged CN values for each subbasin are different and depend on the area of each defined

Table 13: CN look-up table for re-classified land cover data.

No.	CN Look-Up Table	A	B	C	D
1	Water	100	100	100	100
2	Highly Developed	77	85	90	92
3	Medium high Developed	61	75	83	87
4	Medium Developed	57	72	81	86
5	Medium low Developed	51	68	79	84
6	Low Developed	46	65	77	82
7	Industrial	81	88	91	93
8	Road	98	98	98	98
9	Barren	63	77	85	88
10	Agricultural	30	58	71	78
11	Herbaceous	68	79	86	89
12	Forest	30	55	70	77
13	Wetland	48	67	77	83

subbasin. The averaged CN values for each subbasin were presented in Table 12.

5.1.4 Rainfall-Runoff Modeling

The general rainfall-runoff modeling process was shown in Figure 25. The methods that we used in the rainfall-runoff calculations in HEC-HMS were SCS for surface runoff method, monthly constant method for the baseflow calculation method, and lag time method for reach routing calculations. Selections are mostly based on the similarity to the former projects with similar studies in United States and other countries. As mentioned other choices may lead to similar results by proper calibration.

For routing of the subbasin surface runoff (i.e., converting the runoff volume to the time series of discharge), Unit Hydrograph method (UH) is a popular method. UH method options in HEC-HMS include Clark, SCS, S-graph, Snyder, and user-specified. Options for channel routing are the kinematic wave and the ModClark distributed method. In this project, the SCS method was selected. The reach routing can be simulated by kinematic wave, lag, modified pulse, Muskingum, Muskingum-Cunge, and Straddle stagger methods. The lag method was selected as the routing method in HEC-HMS computations for our Pawtuxet River watershed model. More importantly, we adjusted lag times by using the HEC-RAS model as it accurately computes lag times in the Main Branches. In order to consider

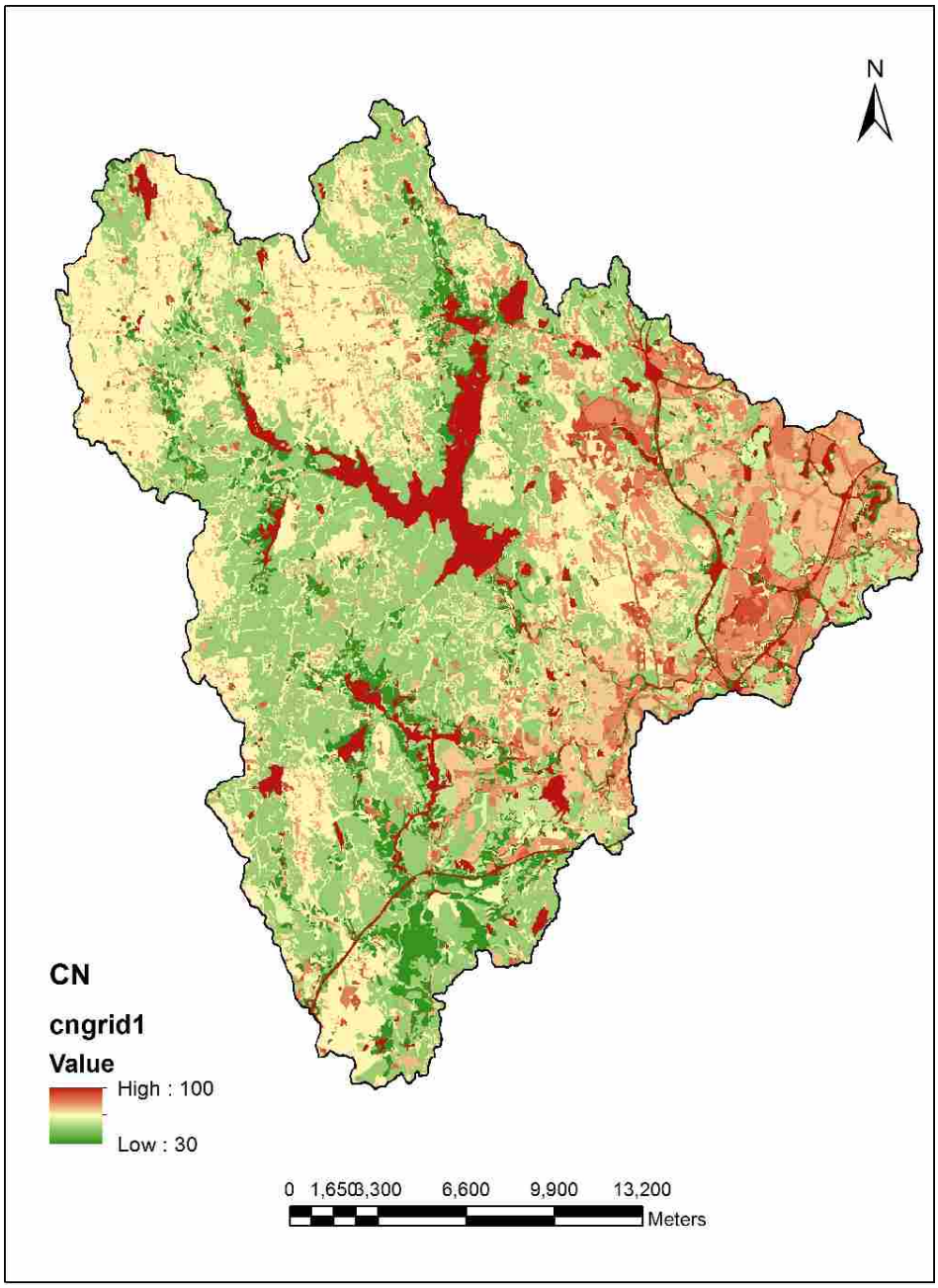

Figure 36: Curve Number (CN) map of the Pawtuxet River Watershed.

the subbasin baseflow, the monthly constant method is selected among several methods available (i.e., bounded recession, linear reservoir, monthly constant, nonlinear Boussinesq, and recession).

5.2 River Model

The river model was developed in HEC-RAS for each of the Main, North and, South Branches of the Pawtuxet River. As discussed in Section 4.5, setup of the river model includes specification of the river geometry, including structures and cross sections of the river, boundary conditions, and flood event profiles.

The river model is based on a previous USGS HEC-RAS model[26], with several updates in this study to include changes to structures along the river in recent years, elongation of the cross section cutlines, and other changes in the cross sections. The updated USGS HEC-RAS model is developed to be compatible with the latest HEC-RAS version (5.0.0) and is a 1D hydraulic model. The updated HEC-RAS model we are presenting is based on the data that we extracted from the USGS model. Further, the developed model includes unsteady simulations unlike the previous USGS model.

5.2.1 River Structures

The Pawtuxet River includes three branches in its basin, with many structures such as dams and bridges in each of the branches. The North Branch originates at the Scituate Reservoir in Scituate and connects to the South Branch at West Warwick. The South Branch originates from the Flat River Reservoir in Coventry. The Main Branch of the Pawtuxet River starts at the confluence of the South and North Branches and drains to the Providence River next to Narragansett Bay in Warwick. Structures along all branches are modeled in the HEC-RAS model of the river. Table 14 shows the number of structures and dams as well as the cross section information used in the HEC-RAS model.

Table 14: Summary of structures, dams, and river cross sections.

	Main Branch	North Branch	South Branch
Length (mi)	11.2	6.6	9.1
Cross Sections (mi^2)	205	87	188
Bridges	17	7	11
Dams	4	7	11
Manning Coefficient	0.03-0.10	0.03-0.10	0.03-0.10

During our site visits, two major changes were observed in the river. The first major change was partial removal of the Pawtuxet Falls Dam at Pawtuxet Village in Fall 2011.

[26] Gardner Brent 2016, New England Water Science Center, USGS; personal communication.

This change was performed to improve the river ecosystems and water quality, mitigate flooding, and respect community concerns. Photographs of the Pawtuxet Falls Dam before and after the 2011 partial removal are shown in Figure 37. The second change in the areas around river was the newly constructed levee around the Wastewater Treatment Facilities in Warwick. During the March 2010 floods, these facilities were inundated.

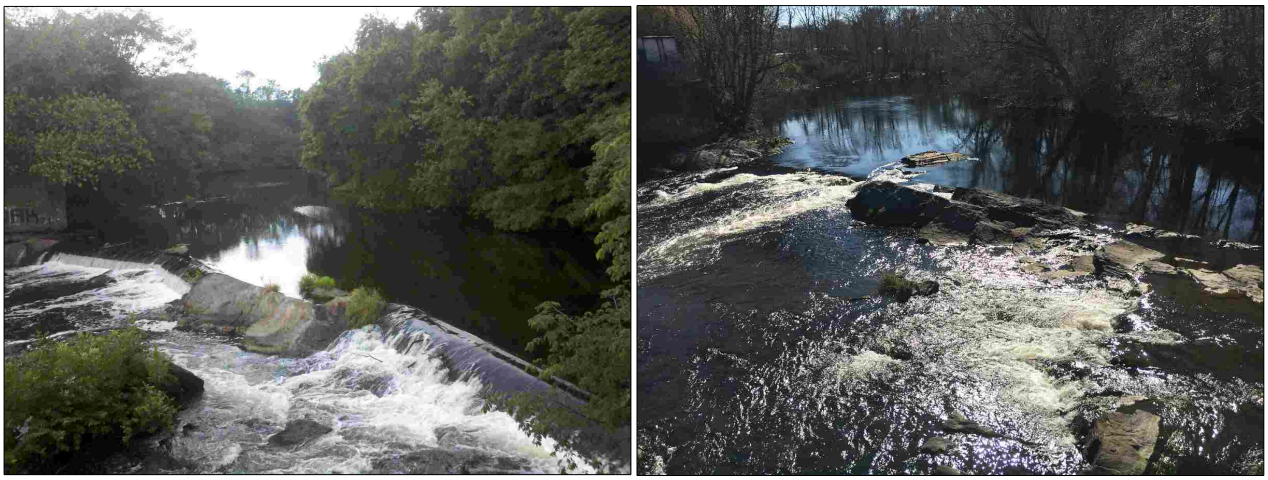

(a) Pawtuxet Falls Dam, before partial removal. (b) Pawtuxet Falls Dam, after partial removal.

Figure 37: Pawtuxet Falls Dam partial removal, Fall 2011, Source: NBEP.

Figure 38 shows a photograph of the flooded Wastewater Treatment Facilities during the March 2010 flood events. We updated the river model to include the partial removal of the Pawtuxet Falls dam and the new levee structures in Warwick. Figure 39 compares some of the HEC-RAS modeled structures with their corresponding physical structures.

5.2.2 River Geometry

Cross sections in this study are obtained from the USGS hydraulic model and checked with the available land surface elevation data (LiDAR DEM) for the floodplains. Above the water surface, LiDAR elevations were also used to check the USGS model cross section geometry. Below the water surface, there is no LiDAR data available, because LiDAR cannot penetrate the water surface, and the USGS survey data are used for the bathymetry of the river. But, some of the cross sections did not contain surveyed information. In these cases, a constant depth was added to the LiDAR depth values, just for the river channel (i.e., instead of exact bathymetry, a constant averaged depth was used).

Figure 40 compares the bathymetry extracted from the USGS HEC-RAS model and the LiDAR DEM. The elevation remains constant between 100–200 ft in the x-axis, reflecting the inability of LiDAR to penetrate the river surface, and the fact that this cross section is

Figure 38: Warwick Waste Water Treatment flooded during spring 2010.

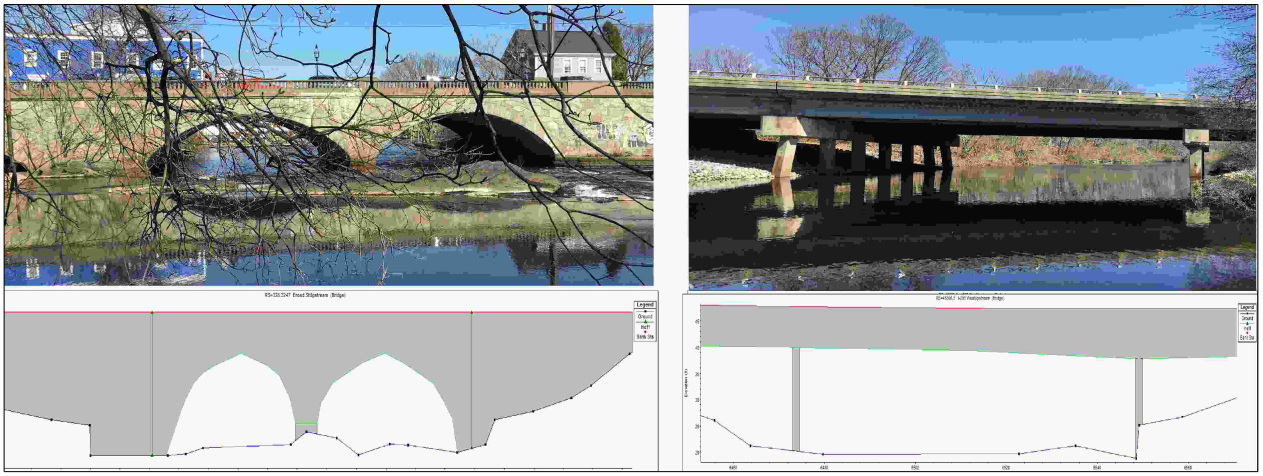

Figure 39: Examples of bridge structures models. The Pawtuxet Village Bridge (left), and I-295 West Ramp Bridge (right).

not surveyed. The HEC-RAS cross sections were modified (by adding a constant depth) for these cross sections at the main channel. Above the water surface, the topography from the two datasets match reasonably well.

Figure 41 compares the bathymetry extracted from the USGS HEC-RAS model and from the LiDAR DEM, for a section of the channel that is surveyed. It can be seen that the USGS surveyed bathymetry gives a more accurate description of the main channel geometry, as expected compared with DEM.

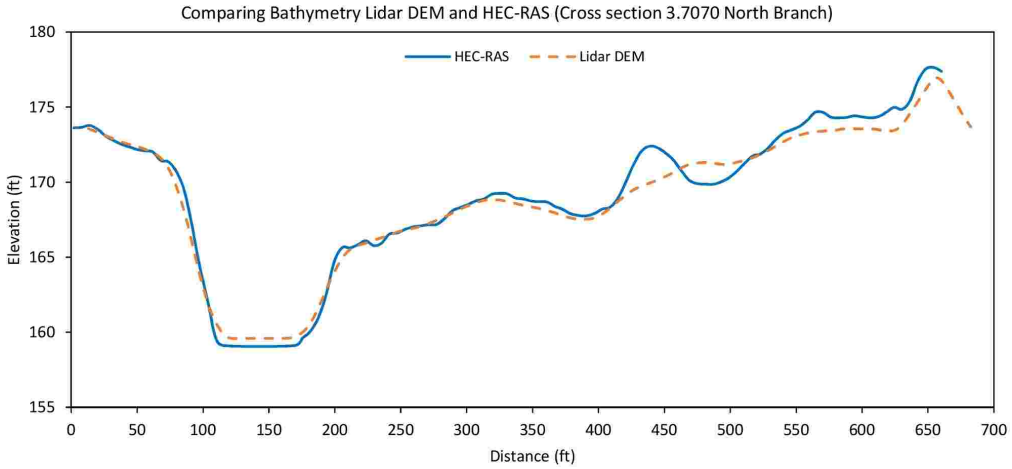

Figure 40: Comparing topography and bathymetry data from HEC-RAS and LiDAR DEM for a non-surveyed channel on the North Branch, as an example.

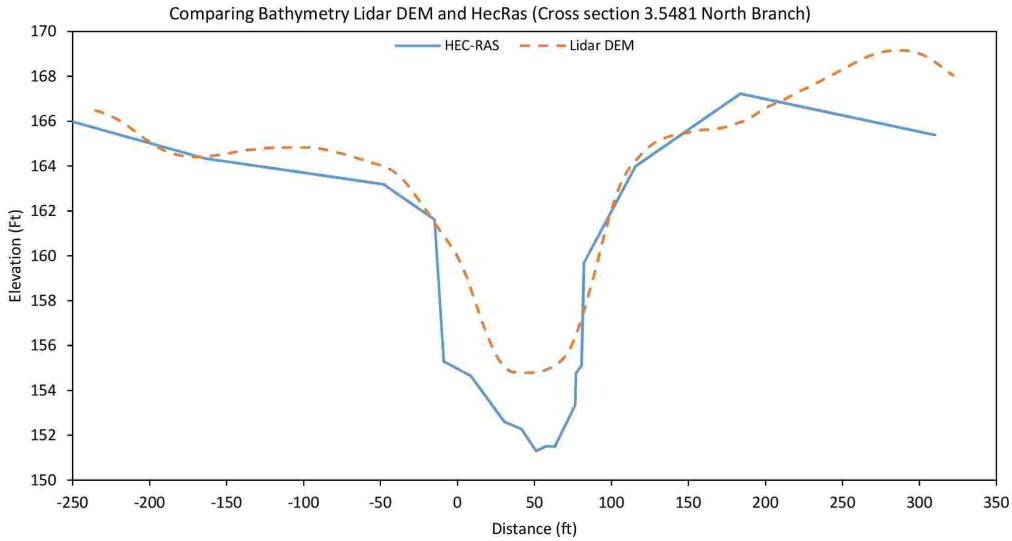

Figure 41: Comparing topography and bathymetry data from HEC-RAS and LiDAR DEM for a surveyed channel on the North Branch, as an example.

5.2.3 Updating River Cross Sections

Cross sections in the river should be defined so that they contain the whole area of the flooding extent. Many cross sections in the updated USGS HEC-RAS model were edited and extended in order to cover the entire flooding area, using the most recent LiDAR data.

In the Main Branch model, cross sections were appropriate in the original USGS model. The Main Branch of the Pawtuxet River is located in an urban area, where the most flooding damage happens. As it is necessary to have a precise flooding maps in this high-density section of the river, the number of cross sections available of the Main Branch of the Pawtuxet

River is considerably greater than that of the North and South Branches. In addition, the available cross section cutlines are long enough to capture all the inundated areas in HEC-GeoRAS model without further editing.

On the other hand, many cross sections in the North and South Branches of the Pawtuxet River needed to be updated. Around the North and South Branches, population density and urban coverage is less than those of the Main Branch; perhaps because of this reason, a fewer number of cross sections were surveyed along these branches. Many cross sections in the North and South Branches were not long enough to contain the flooding extent of the river.

The flood maps are created in HEC-GeoRAS by combining the DEM and simulated elevations in HEC-RAS. Especially, in curved sections of the Pawtuxet River, if the cross sections were not extended enough, the entire sections of the floodplain will be missed by HEC-GeoRAS. Therefore, to ensure that all the floodplain areas are included, cross sections were elongated. An example a problem in flood mapping when cross sections are not properly elongated is shown in Figure 42. The top plot shows the flooding map with short cross sections in the hydraulic model. When compared to the bottom plot with elongated cross sections, the top plot is missing inundation areas. Accordingly, cross sections in the North and South Branches were revised, in order to properly capture the entire flooding plain in transferring the results from HEC-RAS to HEC-GeoRAS. To update the cross sections in the model, the USGS HEC-RAS model was transferred to HEC-GeoRAS in ArcGIS. In ArcGIS, the DEM with 1 m resolution was used to generate the flooding maps. In the cross sections that needed to be extended, the elevations of both ends of the cross sections were set to be higher than a 500-year event water elevation.

The original USGS and updated USGS HEC-RAS model for the North Branch and South Branch of the Pawtuxet River are illustrated in Figure 43 and 44.

5.2.4 Steady Flow Simulation

Boundary conditions needs to be specified for model simulations. Usually, water level at a downstream boundary and discharge rate at an upstream boundary are applied. For the downstream of the Main Branch, known water elevations at the Narragansett Bay were assumed. Various sea level scenarios when assessing the impact of SLR on flooding were implemented at this boundary. Since upstream of the Main Branch is downstream of the North and South Branches, the downstream boundary condition for the North and South Branches is chosen a known water surface. The value of this known water surface is extracted from the water level in the upstream cross section of the Main Branch of the Pawtuxet River, so that the water surfaces are constrained to be equal elevations at the confluence of the branches. The computed discharge from HEC-HMS for real events or estimated flow rate

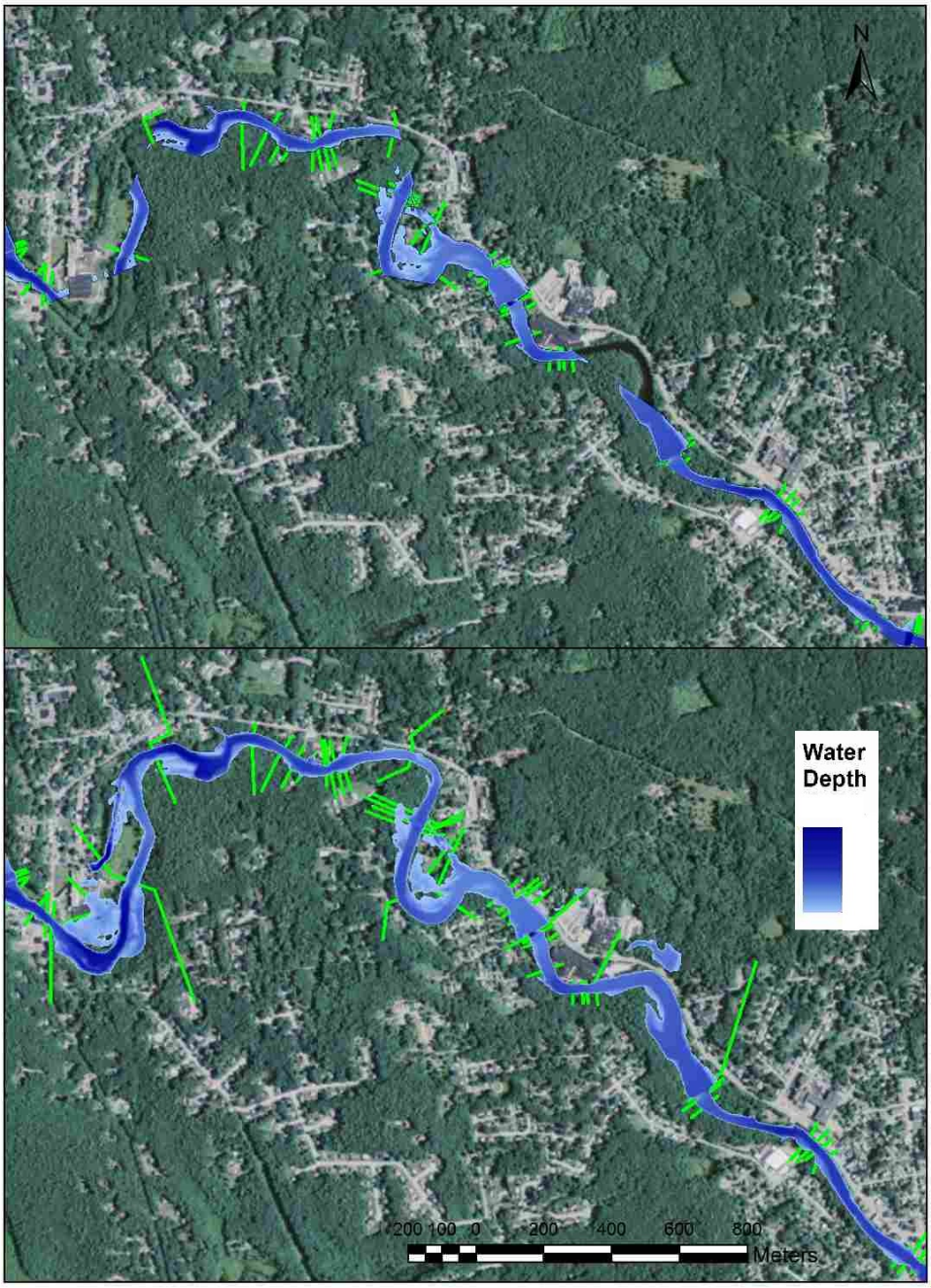

Figure 42: Missed inundation areas caused by short cross sections in HEC-RAS model (original USGS) in North Branch of the Pawtuxet River (top) and the revised model (this study) including elongated cross sections (bottom).

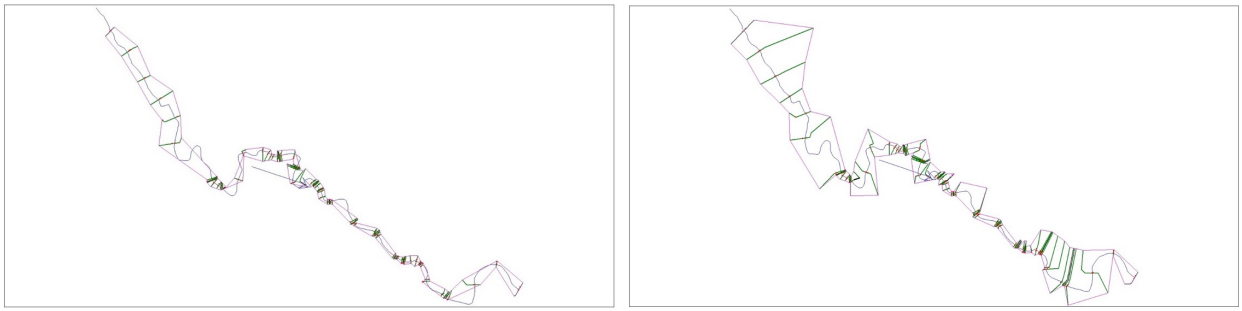

(a) *(b)*

Figure 43: Updating cross sections in the North Branch of the Pawtuxet River: before (left), and after (right) lengthening of cross section cutlines.

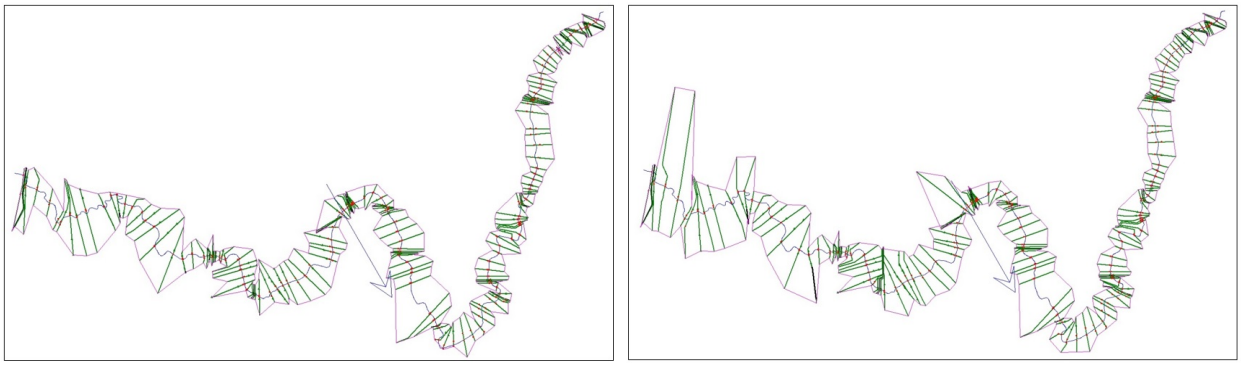

(a) *(b)*

Figure 44: Updating cross sections in the South Branch of the Pawtuxet River: before (left), and after (right) lengthening of cross section cutlines.

with specified return periods were applied at upstream boundaries of the North and South Branches. The upstream boundary condition of the Main Branch is the summation of flow discharge at the South and North Branches.

5.2.5 Event Profiles

In the steady simulations that have been carried out in this project, a number of events were defined for the model. Each event was distinguished with a profile; several profiles can be specified in the model. The peak flow of each event is used as input (upstream boundary condition) for the river model, based on observed or simulated flow rates.

Table 15 lists the cross section and annual exceedance probability of flood flow values that we specified for each of the reaches (Main, North, and South Branches) in the Pawtuxet River hydraulic model. The AEP flood flow magnitudes for 10-, 50-, 100-, and 500-year events in the Pawtuxet River, corresponding to AEP of 10%, 2%, 1% and 0.2% respectively,

Table 15: AEP flood flows (cfs) specified for the Pawtuxet River hydraulic model (Zarriello et al., 2012).

Cross section ID	Flow (cfs)			
	Return period (years)			
	10	50	100	500
Main Branch of the Pawtuxet River				
59306.51	3570	6450	8200	13940
48953.66	3840	6940	8820	15000
23621.69	3860	6970	8850	15060
5.720315	4300	7760	9860	16780
North Branch of the Pawtuxet River				
6.6515	1960	3320	4090	6450
South Branch of the Pawtuxet River				
48413.96	1330	2360	2880	4290
35496.46	1500	2620	3180	4680
21342.66	1620	2800	3380	4930
17890.34	1750	2980	3590	5190

are reported by Zarriello et al. (2012). The observed flow of 14,900 cfs at station 1116500 in the Main Branch of the Pawtuxet River, Cranston corresponds to the predicted 500-year event flow of 15,000 cfs at cross section 48953.66 in the Main Branch of the Pawtuxet River (Table 15). The observed flow of 5,490 cfs at station 1116000 in the South Branch of the Pawtuxet River, Washington can be compared with the predicted 500-year event flow of 4,680 cfs at cross section 35496.46 in the South Branch of the Pawtuxet River (Table 15).

5.2.6 Unsteady Flow Simulation Settings

An unsteady HEC-RAS model was developed and applied to the flooding of March 28 – April 4, 2010 event. Along the river, the cross sections were interpolated every 500 ft. The time step to run the model was 30 seconds.

For the boundary conditions, flow hydrograph was applied as the upstream boundary

condition for each of the three reaches of the Pawtuxet River. These hydrographs were produced by the rainfall-runoff HEC-HMS model. The downstream boundary condition for the Main Branch was the stage hydrograph. This hydrograph was accessed from NOAA's online database: https://tidesandcurrents.noaa.gov . The time series of the water level at Providence Station during March 28 – April 4, 2010 was extrcted. The downstream boundary condition for both South and North Branches is the rating curve. The rating curve was extracted from the HEC-RAS unsteady results for the Main Branch; the resulting rating curve for the Main Branch is the downstream boundary condition at the South and North Branches.

In this section, we described the parameters chosen for the watershed and river models. The results of the modeling study are presented and discussed next.

6 Results and Discussion

The results presented here are discussed in two main sections, the watershed modeling results from the HEC-HMS, and the river modeling results from the HEC-RAS. The HEC-HMS model is calibrated, validated, and an uncertainty analysis was also performed for this model. We will also discuss the watershed modeling results, including the effects of the Scituate and Flat River Reservoirs on flooding. For the HEC-RAS model, we discuss the online flood maps. We also present the results from the unsteady flow river model. The river results discussed in the section include the effect of dams, levees, debris, and sea level rise on flooding.

6.1 HEC-HMS Model Results

The watershed model was calibrated and validated using observed data. An uncertainty analysis was also performed to show that a large uncertainty lies within the input rainfall data; an ensemble approach for rainfall is recommended to address the model uncertainty in the future. Further results include assessment of the impact of the Scituate and Flat River Reservoirs on flooding.

6.1.1 HEC-HMS Model Calibration

To calibrate the watershed model, we selected two events from March 2010 which have hourly data from the land-based station at the T.F. Green Airport in Warwick, RI. The two selected events are listed in Table 16. Event #1 starts at March 28, 2010 at 22:00 (EDT) and ends at April 4, 2010 at 00:00 (EDT), a duration of 145 hours, or a little over 6 days. The total rainfall for Event #1 was 8.83 inches, with a peak flow recorded at Cranston of 14,900 cfs. Event #2 starts March 11 of 2010 at 1:00, ending at March 21, 2010 a 23:00. The total rainfall for this event was 5.5 inches, with a peak flow at Cranston of 5,880 cfs. Our data comes from USGS station 01116500 in Cranston. Hourly streamflow data availability is listed in Table 26 in Appendix A. This station is located in the eastern part of the watershed in the Main Branch of the Pawtuxet River, as can be seen in Figure 21.

Table 16: Selected hourly flooding events.

Event	Start Date (EDT)	End Date (EDT)	Rainfall Duration (hr)	Rainfall Depth (in)	Peak Flow @ Cranston (cfs)
1	Mar 28, 2010 22:00	Apr 04, 2010 00:00	145	8.83	14900
2	Mar 11, 2010 01:00	Mar 21, 2010 23:00	262	5.5	5880

Looking back to Figure 22, these two events are plotted. In the hourly streamflow data at Cranston, RI from 2008–2013, one can see that the two peaks of 14,900 cfs of Event #1 and 5,880 cfs of Event #2 from Table 16 are the largest two peaks during this time period. As a reminder, from the values reported in Table 8, we see that hourly Event #1 with an observed peak flow of 14,900 cfs corresponds to a return period of about 500-year, and hourly Event #2 with observed peak of 5,880 cfs corresponds to a return period of between 25 to 50 years at this gauge.

Parameters such as time lag, base flow, and CN can be adjusted to calibrate the model. Although the calculated runoff was reasonable based on the original CN, the peak flow needed calibration. We found that adjustment of the time lag has the most influence on the peak flow. Modifying the reach and basin time lag improved the timing of the streamflow peaks; for instance the calibrated parameter for subbasin W650 (See Figure. 35b) Calibrated to 714 minutes compared to original time lag of 614 minutes. The volume of runoff was estimated very close to observations using the computed CN.

Figures 45 and 46 plot the hydrographs for the original watershed model, observed data, and calibrated watershed model for Events #1 and #2 at the USGS stations 01116500 in Cranston, and 01116000 at the Washington Station in the South Branch. The calibrated results for the hydrological model show a reasonable agreement between model results and observations at the chosen USGS stream gauge locations, matching the general form of the observed hydrographs and with similar peak times. In calibration process, the most important peak flow to match was in Cranston for Event #1, as it experienced the highest flood peak during the 2010 floods. The hydrograph from the original model overestimated the peak streamflow for Event #1 in both the Cranston and Washington, South Branch locations. The peak streamflow value for Event #2 underestimated the observed peak in Cranston but matched the observed data in the South Branch station. After the calibration, for Event #1 the model peak matches closely to the observed peak at Cranston and did not overestimate the peak as much at the South Branch station. The calibrated model peaks for Event #2 were similar to the original model peak in Cranston and slightly less than the original model peak in the South Branch. As reported in Knebl et al. (2005), during severe events such as the March 2010 events, gauge capacity can be exceeded in some cases, and gauge data should be extrapolated in these cases.

6.1.2 Validation

Table 17 lists some extreme events since 1978, with daily precipitation and discharge data available from T.F. Green Airport meteorological observation gauge and Cranston stream gauge station, respectively. The criteria for selecting these events were discharge of more

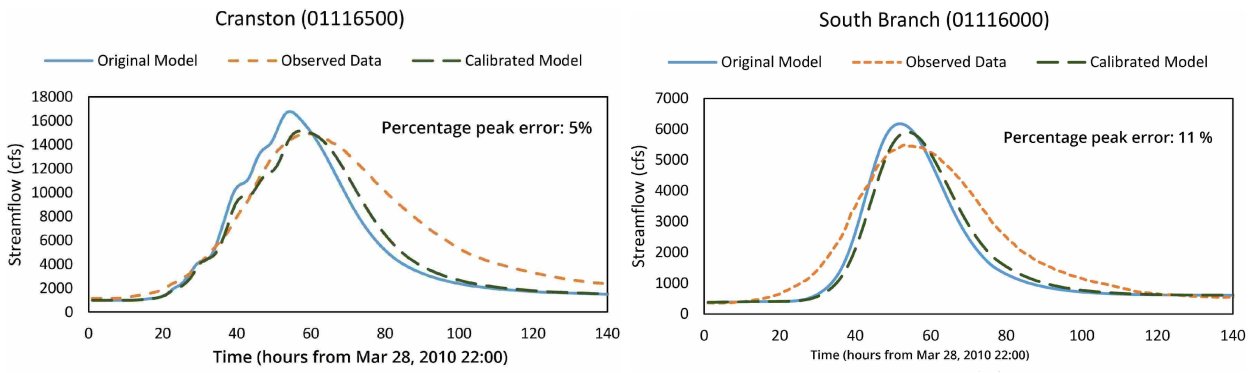

Figure 45: Hydrographs for the original model, observed data, and calibrated model for Event #1 at USGS stations 01116500 in Cranston and 01116000 in the South Branch.

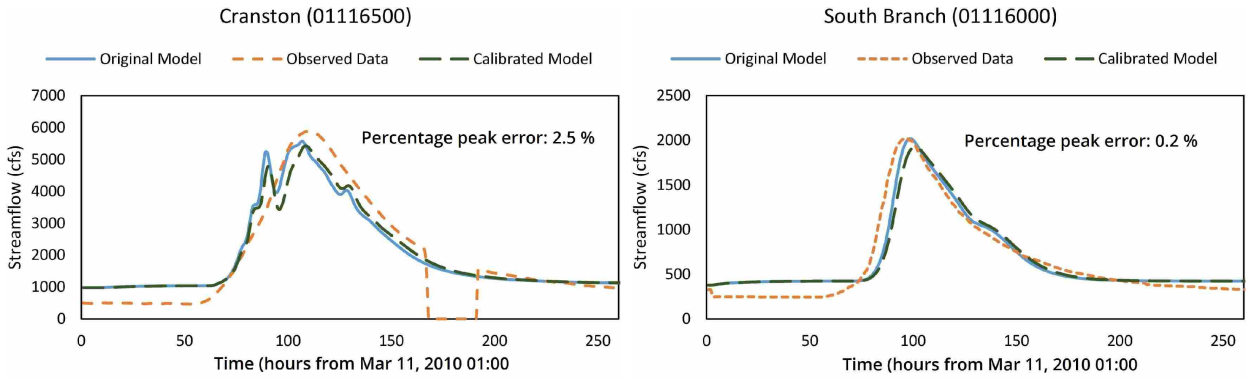

Figure 46: Hydrographs for the original model, observed data, and calibrated model for Event #2 at USGS stations 01116500 in Cranston and 01116000 in the South Branch.

than 2000 cfs, the 5-year return period event. Each event is listed with its start and end date, rainfall duration, rainfall depth, and peak flow measurement at Cranston.

We validated the watershed model against events C and H from Table 17, with daily precipitation data from the Cranston stream gauge data. Fo validation, model parameters were not changed. Figure 47 shows model validation using the calibrated watershed model for daily data events in June 1982 and June 2006 at Cranston station 01116500. The calibrated model hydrographs for these two events match relatively well in the general form, number of peaks, and peak values. Several sources of uncertainty affect model results. The most important parameter is precipitation which is discussed in the next section.

Table 17: Some extreme flooding events since 1978 based on daily data available from Cranston stream gauge station.

Event	Start Date	End Date	Rainfall Duration (day)	Rainfall Depth (in)	Peak Flow @ Cranston (cfs)
A	Jan 1, 1978	Jan 31, 1978	30	9.01	2590
B	Jan 15, 1979	Feb 15, 1979	31	5.92	3650
C	Jun 1, 1982	Jun 30, 1982	30	11.08	5170
D	Apr 5, 1983	Apr 30, 1983	26	11.89	4190
E	Dec 1, 1986	Dec 15, 1986	15	4.62	2110
F	May 1, 1998	May 31, 1998	31	6.05	2510
G	Apr 1, 2000	Apr 30, 2000	30	5.06	2160
H	Jun 1, 2006	Jun 15, 2006	15	5.56	3370
I	Mar 1, 2010	Apr 15, 2010	47	16.68	14000

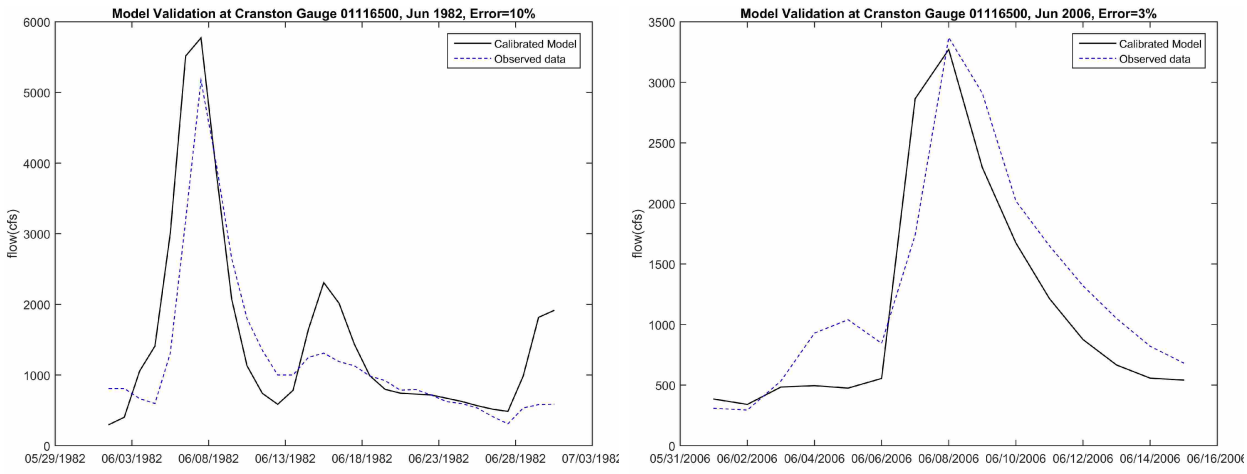

(a) June 1982 *(b) Jun 2006*

Figure 47: Validation of the calibrated watershed model using events in Jun 1982 and Jun 2006 at Cranston station 01116500. Errors are calculated based on the observed and modeled peak flow in each event : $Er = \left(|Q_p^{Obs} - Q_p^{Mod}|\right)/Q_p^{Obs}$. The precipitation data were daily for these simulations.

6.1.3 Uncertainty Analysis

We performed an uncertainty analysis to quantify the effect of errors in the precipitation data on the computed discharges. Lack of observed hourly/daily precipitation data in many events in past/future can lead to large uncertainties.

In the HEC-HMS model, hourly data were available from one observation gauge in the

Pawtuxet River watershed, located at the T.F. Green Airport in Warwick. Other supplementary data to fill the gaps are the CFSR and ECMWF datasets, discussed in Section 3.3.2, as well as with NWS subbasin averaged precipitation data, discussed in Section 3.3.1. Figure 48 shows the daily precipitation data from each of these sources, showing the uncertainty in the precipitation data. The daily precipitation data from the CFSR, ECMWF, and NWS datasets are selected at locations closest to Warwick station.

Using the confidence interval expression in Section 4.3.3, we used the four precipitation data sources to find the confidence interval for the precipitation, and used the upper and lower values of the interval to run the HEC-HMS model and determine the confidence interval for the discharge.

Figure 49a shows the 90% confidence intervals for the daily precipitation data, and Figure 49b shows the precipitation data for each of the observed, ECMWF, CFSR, and NWS sources as well as the upper 90% limit and lower 90% limit. The data is for mid-March through early April 2010. Figures 50a and 50b show the same analysis for the 80% confidence interval.

Once we found the upper and lower precipitations for the 90% and 80% confidence intervals, we ran the HEC-HMS watershed model to find the corresponding discharge time series for the confidence intervals of 90% and 80%. Figure 51a shows the HEC-HMS discharge results for the precipitation at 90% confidence interval. The observed discharge at Cranston is also plotted in this figure. Figure 51b shows the HEC-HMS computed discharges when forced with each of the precipitation data sources (observed at Warwick, ECMWF, CFSR, and NWS), the upper 90% limit, and the lower 90% limit precipitation. The observed discharge at Cranston is also shown. Figure 52a and 52b shows the analogous HEC-HMS results for

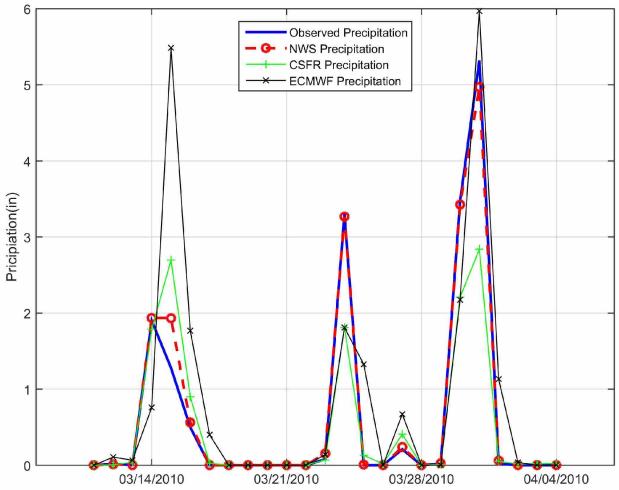

Figure 48: Daily precipitation data for mid-March through early April, 2010 from Warwick meteorological station as well as NWS, CSFR, and ECMWF hindcasts.

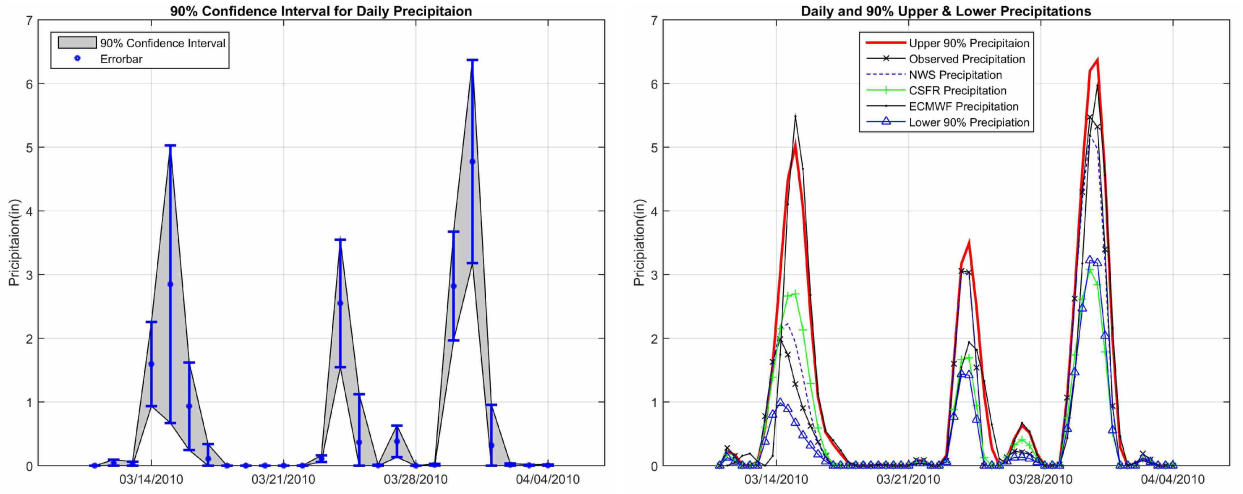

(a) *(b)*

Figure 49: (a) 90% confidence intervals for the daily precipitation data and (b) precipitation from observed, ECMWF, CFSR, and NWS sources, along with upper and lower 90% confidence limits, mid-March through early April 2010.

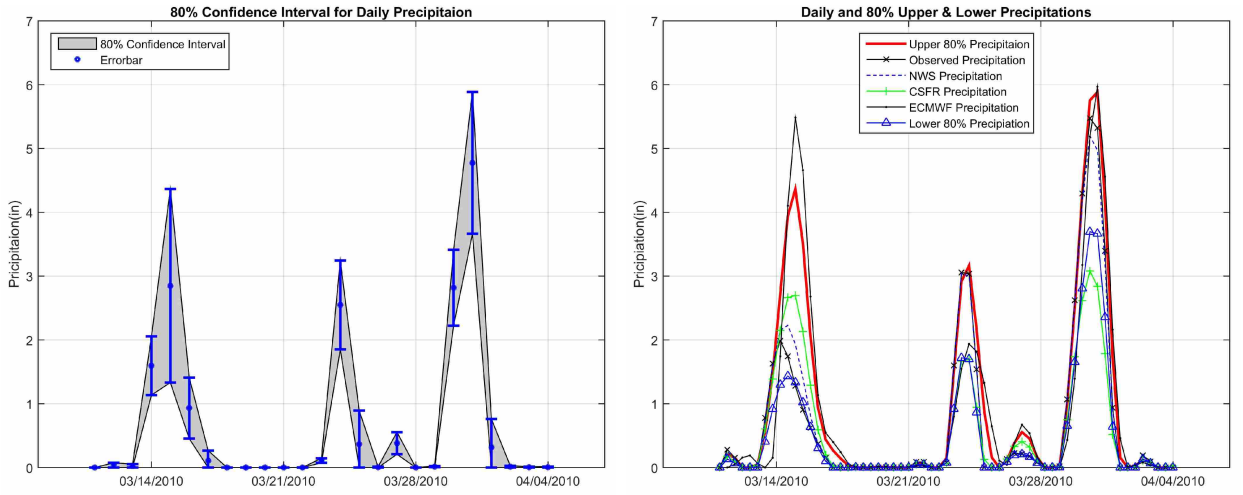

(a) *(b)*

Figure 50: (a) 80% confidence intervals for the daily precipitation data and (b) precipitation from observed, ECMWF, CFSR, and NWS sources, along with upper and lower 80% confidence limits, during mid-March through early April 2010.

the 80% confidence interval. Note that model prediction based on observed rainfall is within these uncertainty limits. Therefore, if several sources of precipitation is used, the upper and lower limits are reliable estimate of discharge.

One could spend much time to adjust the model parameters in the calibration process, but

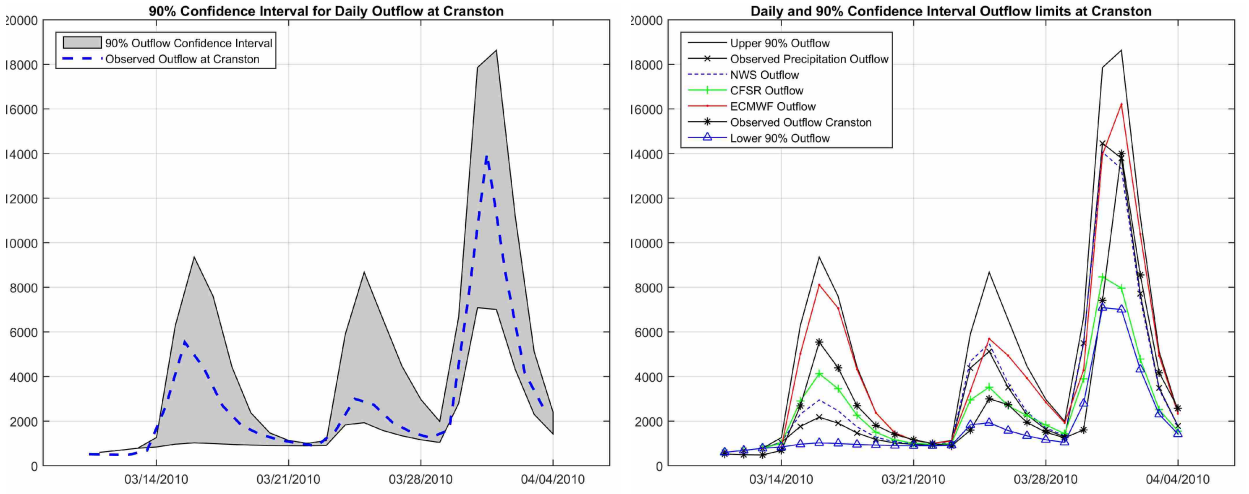

(a) *(b)*

Figure 51: (a) HEC-HMS outflow results for the precipitation at 90% confidence interval and (b) outflow results when forced with observed, ECMWF, CFSR, NWS, upper 90% limit, and lower 90% limit. Observed outflow at Cranston are also plotted for comparison.

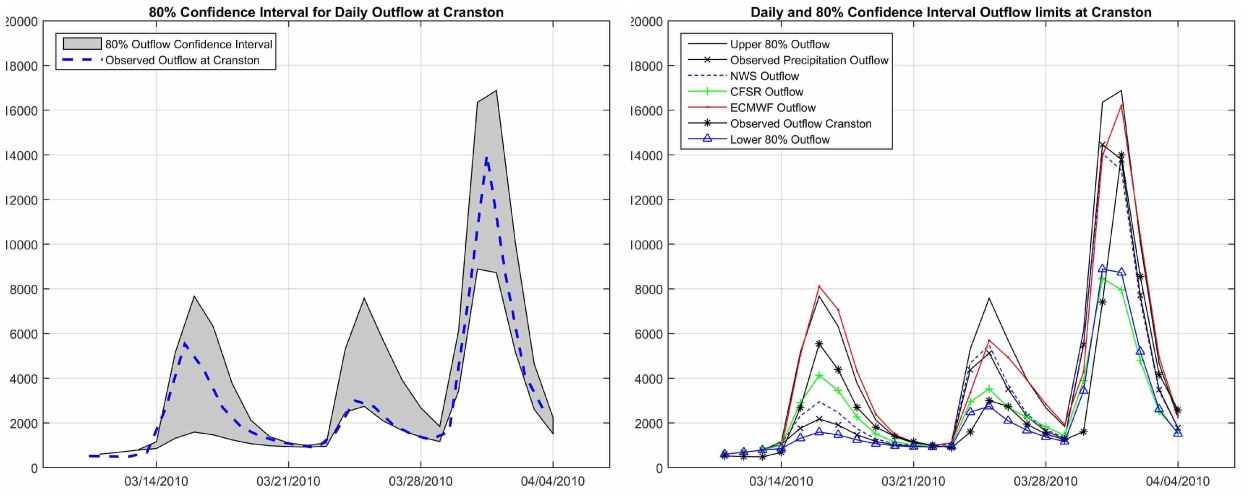

(a) *(b)*

Figure 52: (a) HEC-HMS outflow results for the precipitation at 80% confidence interval and (b) outflow results when forced with observed, ECMWF, CFSR, NWS, upper 80% limit, and lower 80% limit. Observed outflow at the Cranston gauge are also plotted for comparison.

a large uncertainty is present in the input precipitation data. This uncertainty can be reduced by adding more precipitation gauges in the watershed. It is recommended, particularly for forecasting, to use an ensemble of rainfall data and compute a confidence interval for flooding (Demeritt et al., 2007).

6.1.4 Effect of the Scituate Reservoir on Flooding

There are two large reservoirs in the watershed: the Scituate Reservoir, and the Flat River Reservoir. The flood discharge in the North Branch of the Pawtuxet River is affected by the Scituate Reservoir, while the South Branch of the Pawtuxet River streamflow is affected by the Flat River Reservoir. Both affect the flooding in the Main Branch. The Scituate Reservoir has the potential to retain runoff during high flow periods.

Figure 53 shows the amount of runoff generated by precipitation upstream of the Scituate Reservoir. This figure also shows the corresponding elevation of water below the spillway crest that provides the required storage capacity to retain all runoff in the Scituate Reservoir. As runoff volume depends on the CN, these graphs are generated assuming several CN's. If the reservoir water level is at 284 ft (MHW) at the spillway crest, it can not retain any water. As the water elevation decreases, the reservoir can retain a significant volume of runoff. A more

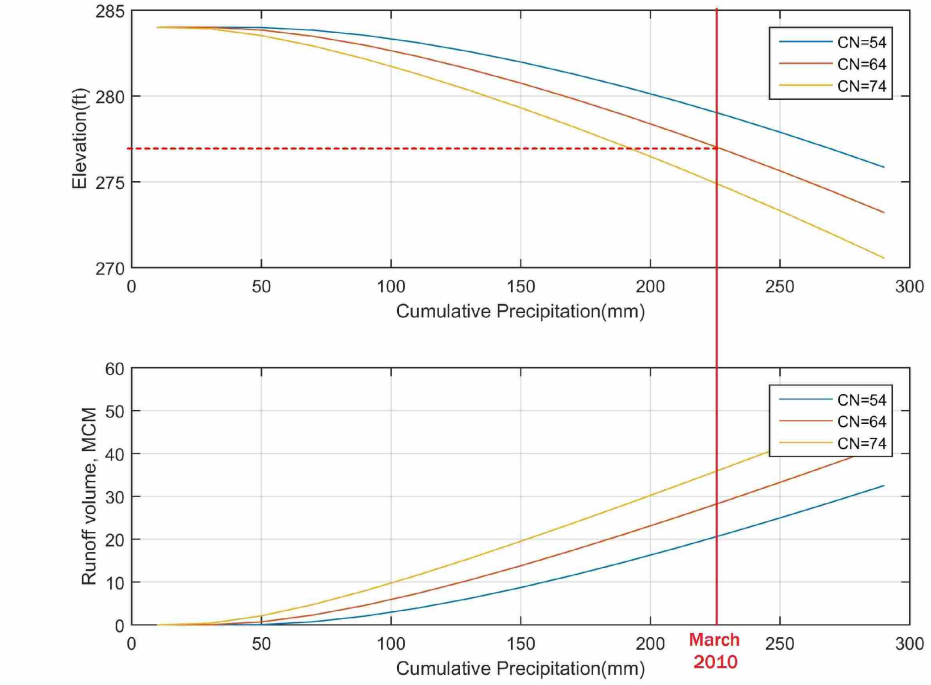

Figure 53: Volume of runoff generated upstream of the Scituate Reservoir versus cumulative precipitation is shown in the bottom plot. The maximum water elevation that is required to trap the runoff (below the spillway crest) in the reservoir is shown on the top plot. The flood capacity is provided by the difference of the spillway crest elevation (284 ft) and water elevation. Datum is MHW. Reservoir drainage area is 91 mi^2 and the surface area of the reservoir is 5.3 mi^2. Note that at 284.0 ft (MHW) the volume is zero (MHW=NAVD88-2.12 at this location).

detailed analysis will be presented later, but this figure shows that a few feet of capacity can trap the entire runoff volume in the reservoir. For instance, for March 2010 event which is highlighted by red in graphs, the total rainfall is 225 mm (8.83 in); assuming CN=64, if the elevation of water at the spillway was about 277 ft, entire runoff volume could be trapped within the created capacity of 7 ft (284-277) in the reservoir.

Figure 54: Photo of flashboards in the Scituate Reservoir spillway. Red arrows show the flashboards.

In order to simulate the effect of the Scituate Reservoir on flooding, a more detailed analysis was carried out by modeling the Gainer[27] Dam Spillway. Two flashboards can be installed on the Scituate Reservoir spillway crest. Figure 54 shows the location of the flashboards on the Scituate Reservoir spillway. There are three possible scenarios to compute the relationship of water elevation and flow discharge. First, flashboards are considered removed. Second, one of the two flashboards are placed. Third, both of the flashboards are put in place. The spillway flow as a function of the water elevation for each of the three scenarios is plotted in Figure 55. The flow rate over the spillway is greater when there is no flashboard, and as expected, the flow rate over the spillway is minimum when there are two flashboards. In other words, flashboards can increase the capacity of reservoirs, but we also note that in large flow rates during flooding events flashboards can be easily broken. Therefore, as a conservative assumption, in the Scituate Reservoir simulations in flooding events, we simulated the reservoir without any flashboards in place.

The spillway discharge with no flashboard is calculated with three different methods and

[27]Gainer is the name of Scituate Reservoir Dam

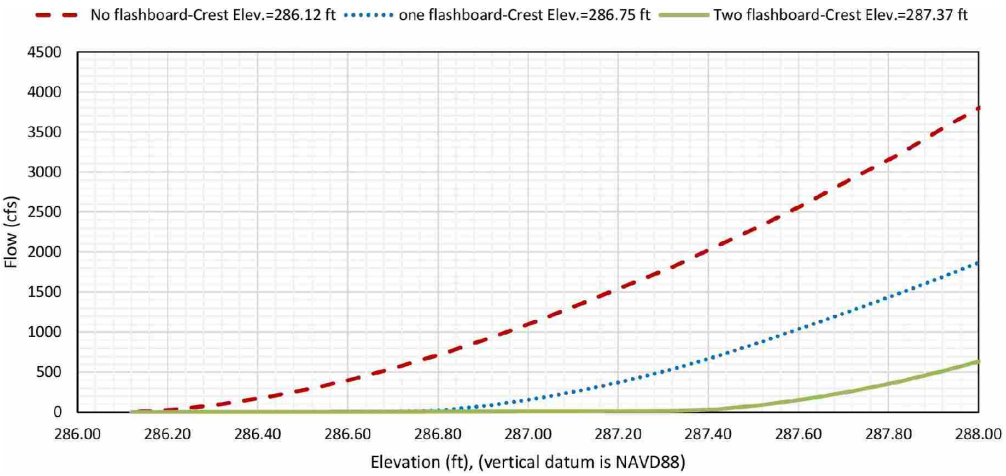

Figure 55: Comparison of flow over Gainer Dam Spillway versus water elevation in the reservoir for three scenarios: without flashboard, one flashboard, and two flashboards. Source of data: Providence Water Supply.

are compared in Figure 56. First, the flow rate is calculated according to the ogee spillways flow rate, Equation 6 [$Q = CL(H - 286.12)^{\frac{3}{2}}$], where $C = 3.35\frac{ft^{\frac{1}{2}}}{s}$, in US customary units for the Gainer Dam Spillway, $L = 416$ ft (net length), and H is the water elevation in NAVD88. Second, the flow rates are computed by the HEC-HMS model and lastly, the flow rate and elevation values determined based on to data sheet given by Providence Water Supply. As it can be seen, all methods lead to similar results.

Figures 57 and 58 plot the modeled inflow and outflow in the Scituate Reservoir when the reservoir is at full capacity and when the reservoir water elevation is 4 ft below crest elevation, respectively. The crest elevation is 286.12 ft (NAVD 88), and in the subbasin of the Scituate Reservoir CN is 65.6. The inflow data was produced from hourly data for Event

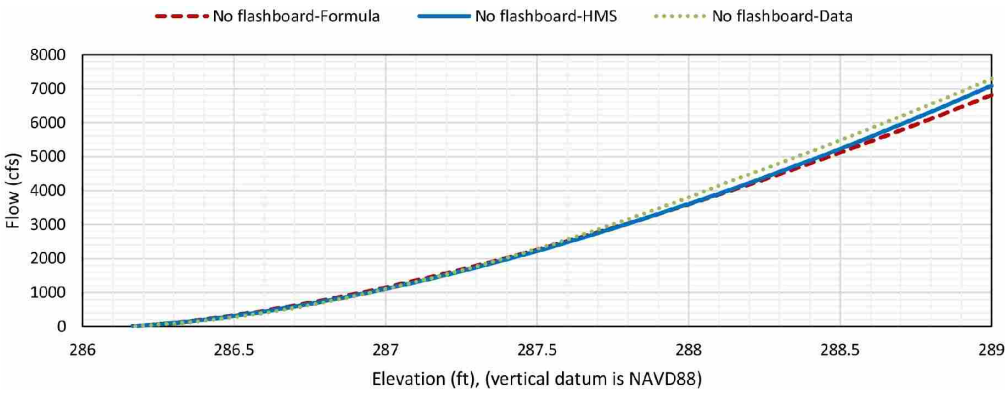

Figure 56: Comparison of Gainer Dam spillway outflow using HEC-HMS, data provided by the dam authorities, and ogee spillway formula. The spillway crest elevation is 286.12 ft (NAVD88).

#1 (March 28 – April 4, 2010) from Table 16. Comparing Figures 57 and 58 shows that with an initial water elevation reduction of 4 ft, the Scituate Reservoir outflow peak could be significantly reduced. With the Scituate Reservoir at full capacity, the peak outflow from the reservoir is predicted to be about 7,000 cfs. However, when the elevation of the water at reservoir is 4 ft below the spillway crest elevation, the peak outflow reduces more than 4,000 cfs.

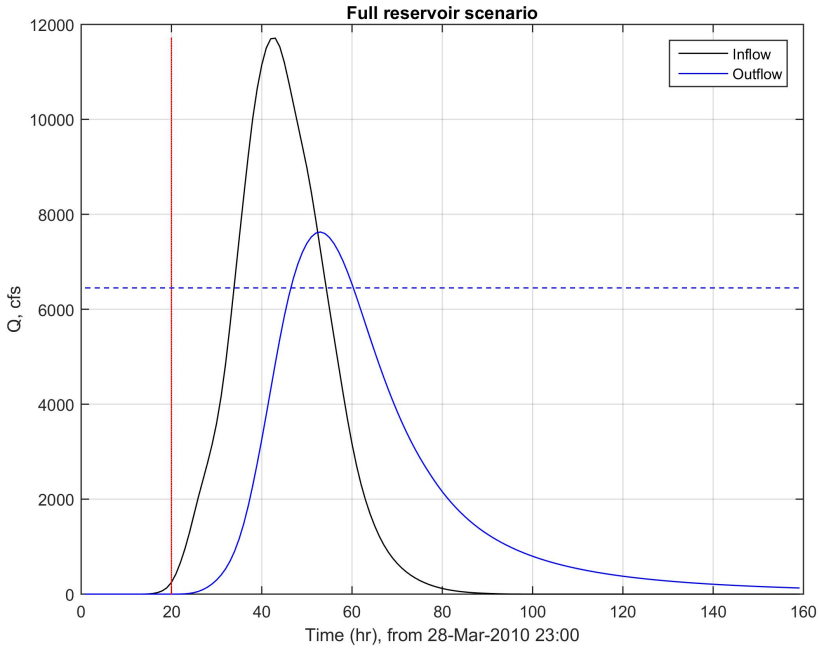

Figure 57: Inflow and outflow of the ogee spillway in the Scituate Reservoir when the reservoir is assumed at the full capacity. Inflow is based on hourly data of Event #1, March 28 – April 4, 2010 from Table 16. Inflow and outflow modeled by HEC-HMS. The red line shows the start of runoff, and blue dashed line shows the estimated 500-yr peak flow.

Control of the water elevation in the Scituate Reservoir would have a large impact on runoff for future flood management. In the March 2010 event, there was about 28 MCM (7400 MGallons) of runoff upstream of the Scituate Reservoir. This volume of runoff could have been contained by the Scituate Reservoir with an additional 6 ft of capacity, with the reservoir's surface area of 5.3 mi^2.[28] With even half of that capacity (i.e. 3 ft), peak outflow from the Scituate Reservoir could have been dramatically mitigated.

[28]For March 2010, the cumulative rainfall was 225 mm (8.8 in). Considering CN=65.6, and replacing CN into Equations 2 and 3, the excess rainfall will be 118 mm (4.6 in). If we multiply 118 mm by the Scituate Reservoir drainage area of 91 mi^2 (236 km^2), the runoff volume approximately equals 28 MCM (6700 M Gallons). Further, if we divide this runoff volume by the Scituate Reservoir surface area of 5.3 mi^2 (13.7 km^2), it results in 2.1 m (6.7 ft) which is the required reservoir capacity.

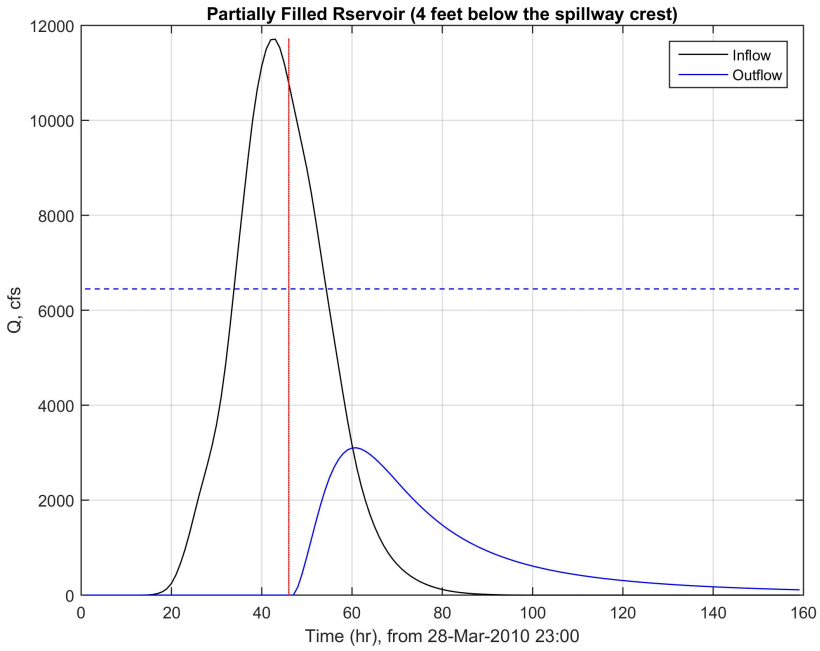

Figure 58: Inflow and outflow over the ogee spillway in the Scituate Reservoir when the initial water level at the reservoir is 4 ft below the spillway crest. Inflow is based on hourly data of Event #1, March 28 – April 4, 2010 from Table 16. The red line shows the start of runoff, and blue dashed line shows the estimated 500-yr peak flow..

Therefore, it is possible to control the downstream flooding by regulating the water elevation in the reservoir. For a given forecast, our model can predict the maximum required water elevation which can control the peak discharge to a specific value. For instance, during the March 28 – April 4, 2010 event, if the initial water elevation of reservoir was 4 ft below the crest elevation, the peak outflow from the Scituate Reservoir would have reduced about 60%. Flood control could be implemented by either keeping the reservoir water level at a specified level before a heavy rainstorm, or installing gated spillways. Gated spillways help control the flooding without reducing the reservoir capacity (Sordo-Ward et al., 2013). This recommendation needs further study to assess the impacts on the structure of dam and also backwater effects around the reservoir. More importantly, since the dam is designed for drinking water supply and not flood control, the regulation of water should make sure that water supply demand is met.

6.1.5 Effect of the Flat River Reservoir

The South Branch of the Pawtuxet River is directly affected by the Flat River Reservoir. There are not much publicly available data for this Reservoir. Its dam is of the gravity type

with length of 700 feet. The area of the reservoir is 0.27 mi^2 (171 acres). As discussed before, since there is not enough data for the Flat Reservoir spillway, some measurements were carried out in a site visit. To approximately model the reservoir and spillway, the area of the reservoir was used to generate an approximate elevation volume relationship. This can be done by assuming a prismatic shape for the reservoir around the crest elevation.

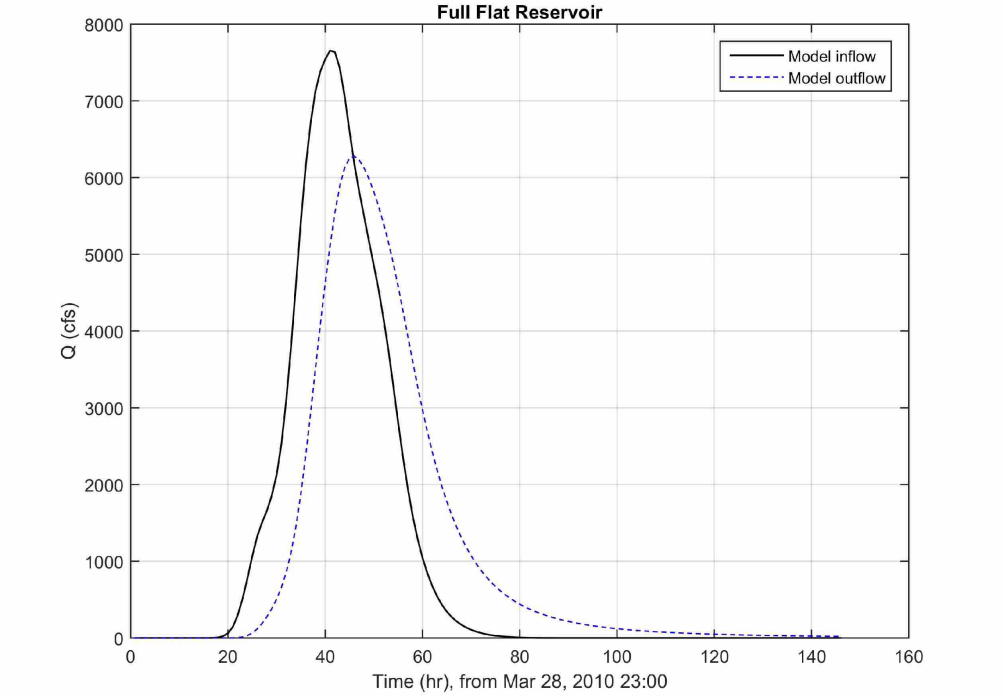

Figure 59: Simulated inflow and outflow to the Flat River when the reservoir is full in Event #1. The spillway crest elevation was approximately considered 237 ft (NAVD88).

Figure 59 depicts the inflow and outflow to the spillway of the Flat River Reservoir dam. For the subbasin of the Flat River Reservoir, $CN = 60$, and the crest elevation was considered 237 ft (NAVD 88). Like the Scituate Reservoir analysis, the inflow data was taken from hourly data for Event #1 (March 28 – April 4, 2010) from Table 16. The initial water elevation of the Flat River Reservoir is taken to be at the crest level. The outflow is calculated in the HEC-HMS, using the flow-elevation curve similar to the one for the Scituate Reservoir. Looking at this figure, the discharge attenuation is much less than that of the Scituate Reservoir as the area of this reservoir is much smaller (1.2 mi^2 compared to 5.3 mi^2).

We should also mention that the *relative* elevation of water to the spillway crest is important in simulation of a spillway in the HEC-HMS model. No benchmark was used to check the absolute value of the crest elevation (in NAVD88 datum) for this reservoir, and the

provided analysis is based on relative values measured at the site.

6.2 River Modeling Results

The purpose of the HEC-RAS hydraulic modeling is to determine the water elevation and floodplain extent along the Pawtuxet River during flooding events. In addition to steady flow results, the unsteady flow model results are also produced. In order to see the effects of historical dams on the flooding extent, the dams were removed from the HEC-RAS river model. Dams were removed individually and collectively to investigate the changes in water level for different return periods. We also estimated a reasonable amount of debris, and added to each bridge pier to compute the impacts on flooding. Finally, the effect of sea level rise and storm surge were assessed during inland flooding events.

6.2.1 Comparison with the FEMA Maps

The HEC-RAS modeled water elevation along the river during the flooding events are computed and compared with the FEMA FIRMs. The computed water elevations are transferred to HEC-GeoRAS to generate the flooding maps for the river. The HEC-RAS model was run for different return periods.

Figure 60 shows the inundation maps from our model results for the Main Branch of the Pawtuxet River, qualitatively compared to the FEMA flooding maps for the entire area. The FEMA map displays flooding areas for the 100-year event flood for all the rivers in the area while our model just shows the Pawtuxet River. Comparing our updated HEC-RAS model flood map and FEMA map shows the floodplain for the Main Branch of the Pawtuxet River. Figure 61 shows the inundation maps from FIRMs and our HEC-RAS model, zoomed in to the area surrounding the Warwick Mall, which was heavily flooded during the March 2010 flooding events. We can see that the results are similar in the two products. Nevertheless, FEMA maps do not show the effect of dams, structures, debris, and sea level rise on flooding that are discussed here.

6.2.2 HEC-RAS Unsteady Flow Results

The steady HEC-RAS model was further developed for the unsteady case. The March 28 – April 4, 2010 flood event was simulated and compared with observed data.

To validate the unsteady results, the outflow hydrographs at two cross sections are compared with the observed data as well as with the HEC-HMS watershed model. One of the cross sections of HEC-RAS is located in the Main Branch, where the Cranston stream gauge

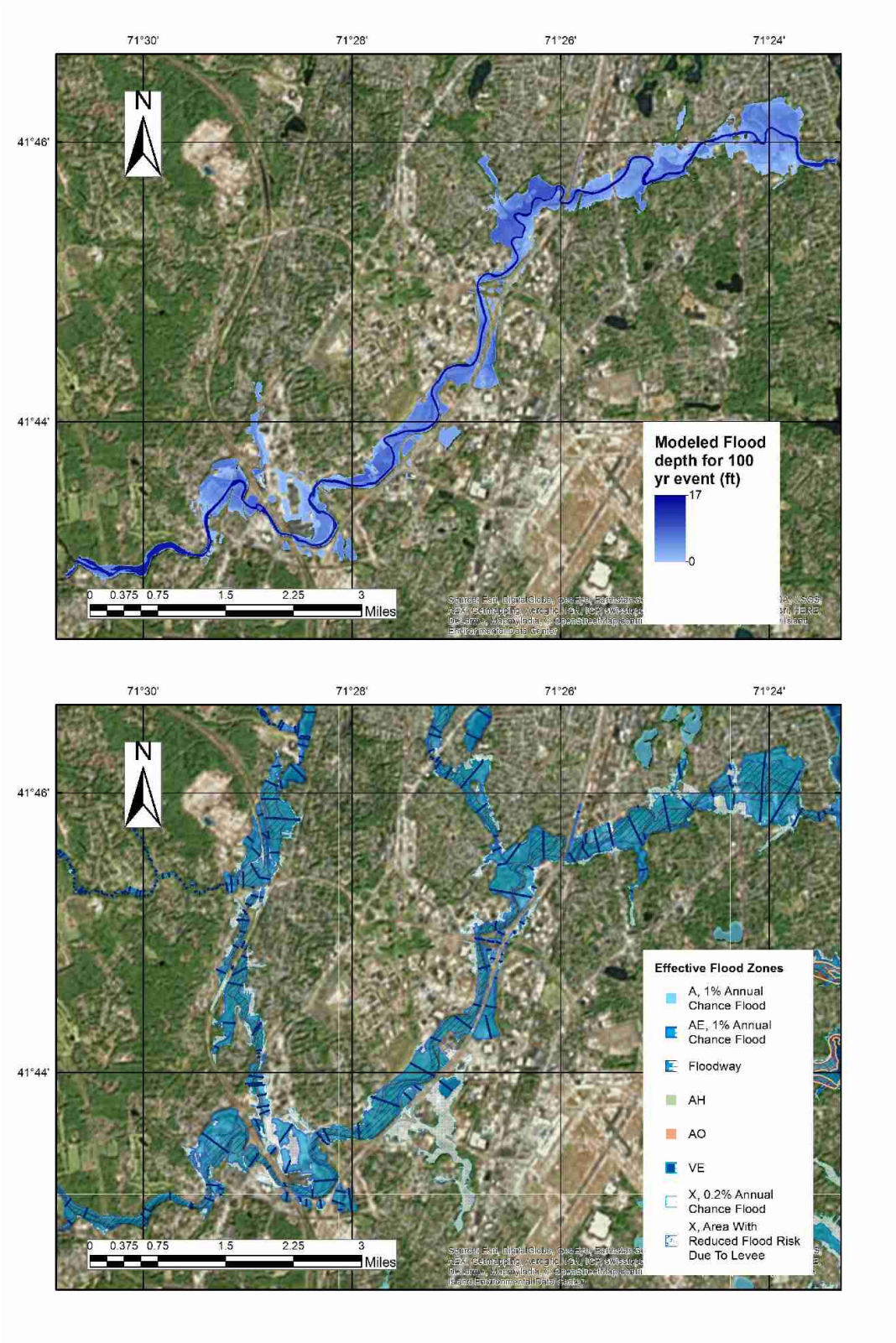

Figure 60: Comparison of the FEMA FIRMs (bottom) and our HEC-RAS model flood map (top) in the Main Branch of the Pawtuxet River for a 100-year return period flood event. Note that the HEC-RAS generated map only includes the Pawtuxet River, whereas FIRMs includes other rivers in addition to the Pawtuxet River.

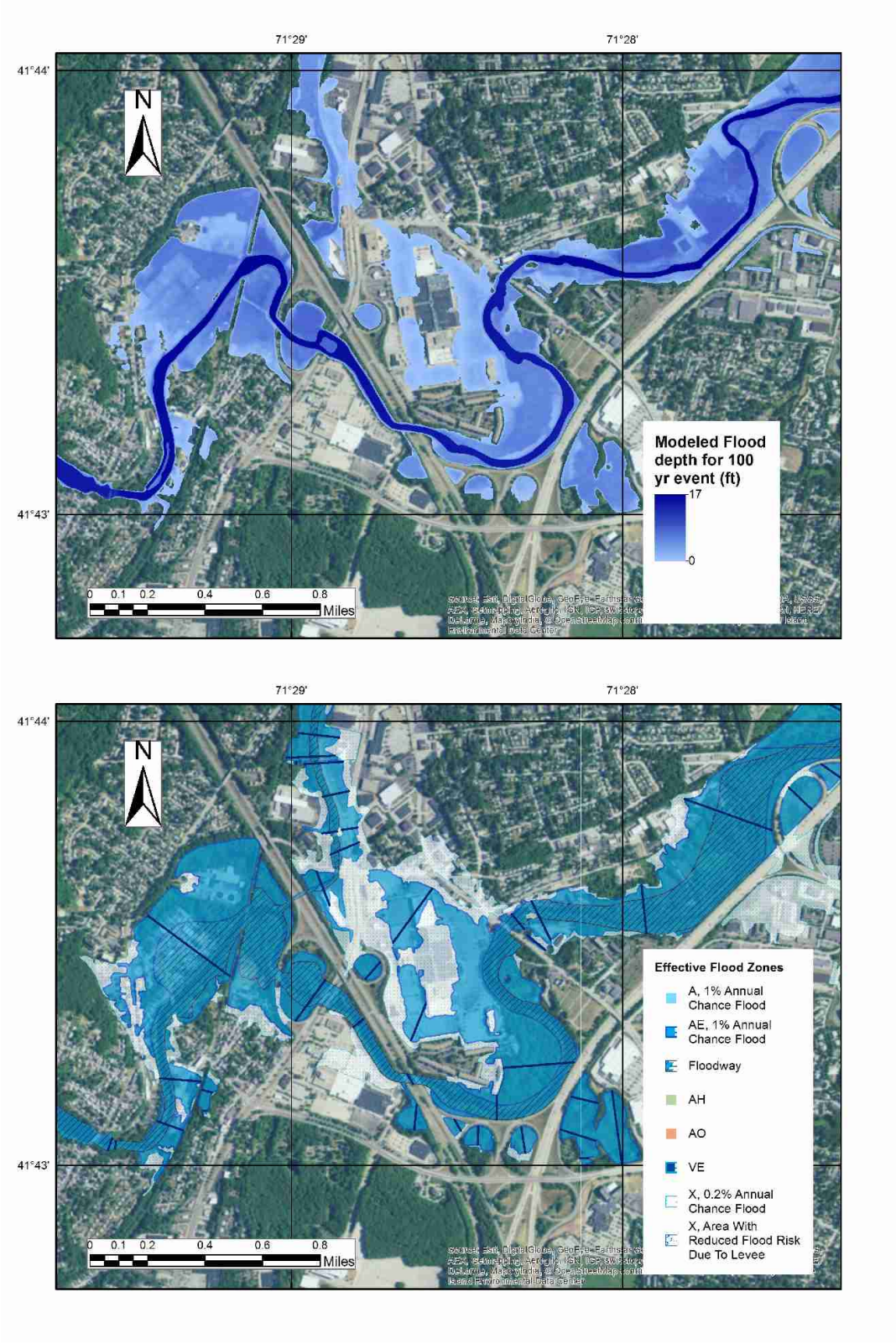

Figure 61: Comparison of the FEMA FIRMs (bottom) and our updated HEC-RAS model flood map (top) for a 100-year event around Warwick Mall.

is located. The other cross section is located in the South Branch, where the Washington stream gauge is located.

Figure 62 shows the computed unsteady flow results by HEC-RAS compared with the observed data and HEC-HMS results. In Figure 62a, the results for the Cranston Gauge location can be seen. The unsteady flow hydrograph matches generally well with the HEC-HMS peak timing and curve shape. The peak timing of the unsteady flow matches relatively well with that of the observed data, and the unsteady hydrograph agrees that of the observed closely from the last 2 days of March, 2010 until the peak about mid-day March 31, 2010. For the comparison at the Washington Gauge (South Branch), Figure 62b shows that the unsteady flow results match closely with the HEC-HMS results, and that both match the general shape and timing of the observed peak data well. It should be noted that HEC-HMS unlike HEC-RAS does not compute water elevation which is necessary for flood mapping.

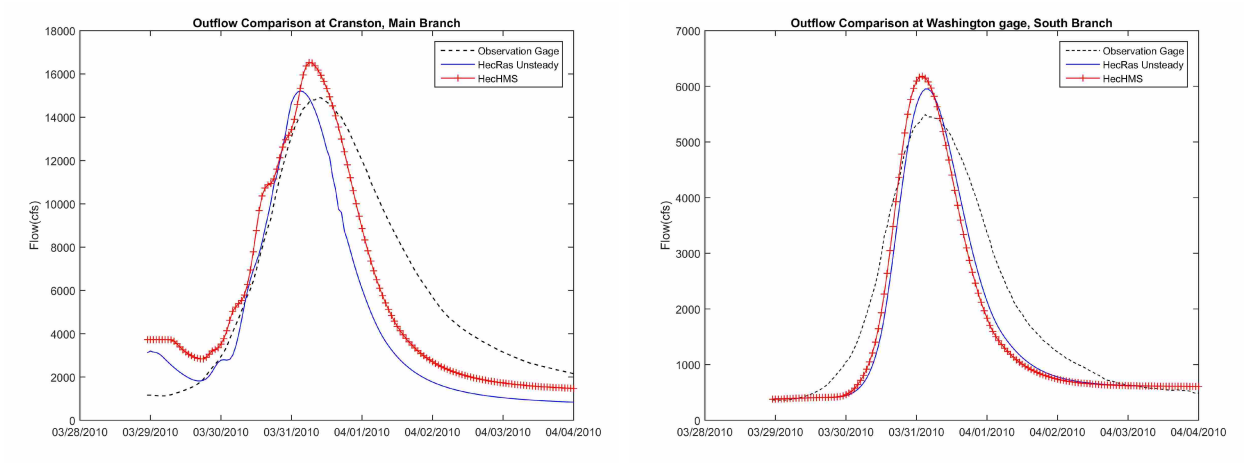

(a) *(b)*

Figure 62: Comparison of the HEC-RAS unsteady flow results, observed data, and HEC-HMS results at (a) Cranston in the Main Branch, and (b) Washington in the South Branch.

Using the validated unsteady HEC-RAS model, the flow and stage hydrograph can be computed for a particular event; however, the steady model can map the maximum inundation. Also, HEC-HMS unlike HEC-RAS unsteady cannot be used to generate realistic unsteady inundation maps. This capability is the main advantage of HEC-RAS unsteady.

6.2.3 Integration of floodmaps to STORMTOOLS

STORMTOOLS is a comprehensive mapping tool for Rhode Island; it provides the ability for homeowners and municipalities to understand the risk of their properties encountering floods and storms. It addresses the effect of sea level rise on coastal flood inundation. The

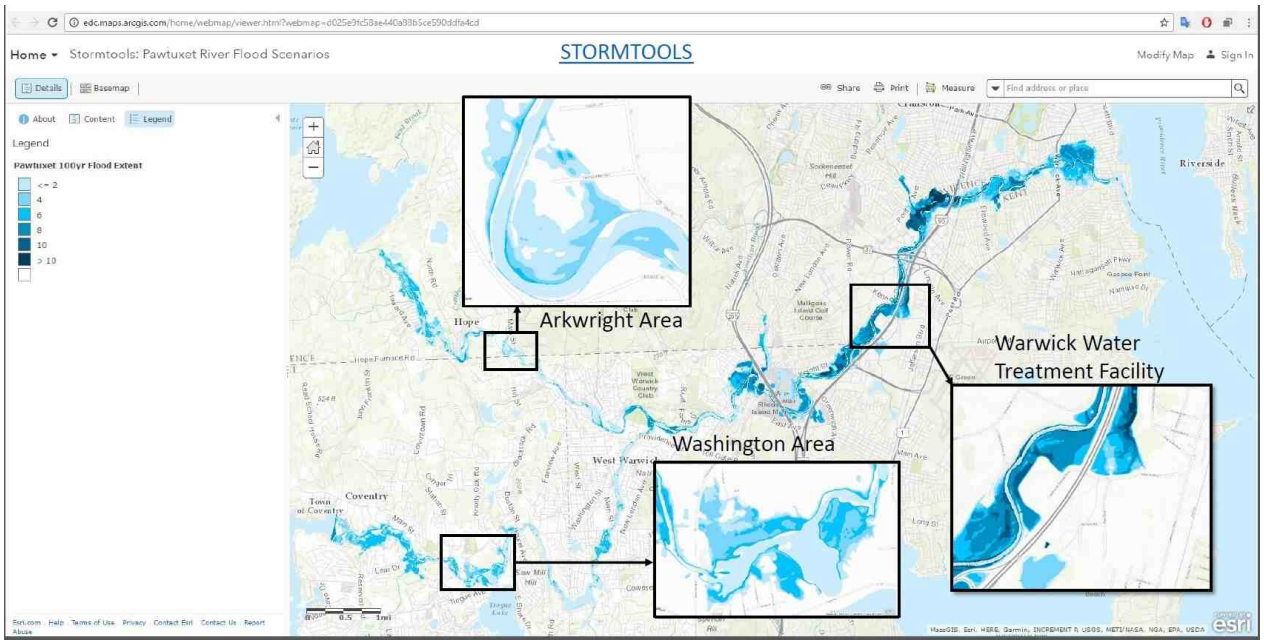

(a)

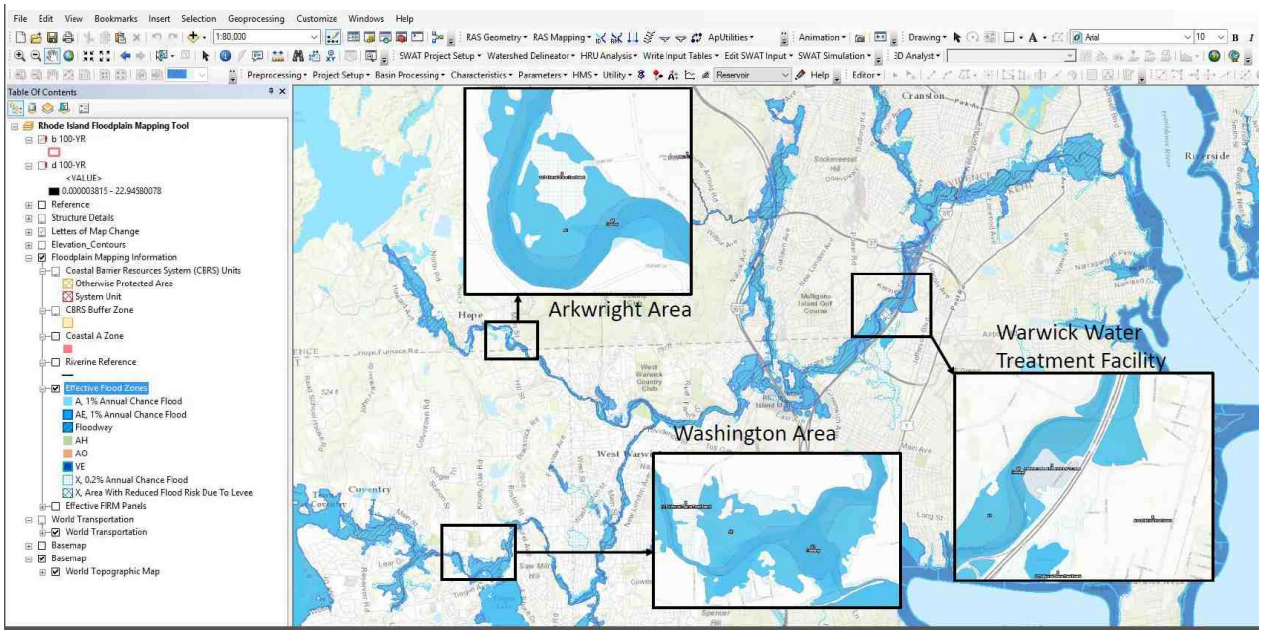

(b)

Figure 63: Pawtuxet River online inundation map integrated into STORMTOOLS (a) compared with FEMA FIRMs (b).

general public has open access to STORMTOOLS and can view different flood scenarios for coastal areas in Rhode Island. The coastal flooding maps in STORMTOOLS are provided by a collaborative efforts of the Rhode Island Coastal Resources Management Council, the University of Rhode Island's Coastal Resources Center, and Rhode Island Sea Grant (Spaulding

et al., 2016). One of the main objectives of this project was to extend these online maps to inland flooding.

The integration of the Pawtuxet River flooding maps in STORMTOOLS was an outcome of and one of the contributions of this project. The Pawtuxet River flooding maps have now been integrated into the STORMTOOLS website and are available to the public.[29] The 10-, 50-, 100- and 500-year flood scenarios are available on the website. The user is able to zoom in and out to see various flooding areas, at high resolution. It is also possible to view the water depth for each flood scenario in the vicinity of the river.

Figure 63a illustrates the online view of STORMTOOLS, for a 100-year flood event in the Pawtuxet River floodplain. The Arkwright area, Washington area, and Warwick Wastewater Treatment Facility have been magnified in the STORMTOOLS view as examples. As a comparison, Figure 63b shows the same view in the FEMA FIRMs. In general, the STORMTOOLS flood map of the Pawtuxet River matches the overall predictions of the FEMA FIRMs, it can also include more scenarios such as increase in flood discharge, effect of debris, dam removals, and impact of sea level rise.

6.2.4 Effect of Historical Dams on Flooding

6.2.4.1 Analysis of Dam Removals in the Main Branch

All of dams in the Main Branch were removed (individually and together) to see their effects on flooding. During the 2010 flooding events a portion of the highways and the Warwick Mall was inundated; we investigate the effect of removing a dam downstream of this critical area. In this section, we focus on the results for removal of two dams individually in the river, as well as for removing all dams in the Main Branch.

Figure 64 shows the location of the four dams in the Main Branch of the Pawtuxet River: the Natick Pond Dam, the Pontiac Dam, the dam downstream of the Pontiac Dam, and the Pawtuxet Falls Dam. The Pawtuxet River intersects two major highways, I-95 and I-295, linking southern and northern Rhode Island. The river traverses through the I-95 highway, the Warwick Mall, and I-295 within a few miles of the Pontiac Dam. Figure 65 shows photos of the four dams in the Main Branch of the Pawtuxet River, taken during site visits. The dams are all located in residential areas, and potentially can affect the highways and other residential areas.

Effect of Pontiac Dam Removal on Flooding

The Pontiac Dam is an important dam to analyze because it is located at the downstream of

[29] http://edc.maps.arcgis.com/home/webmap

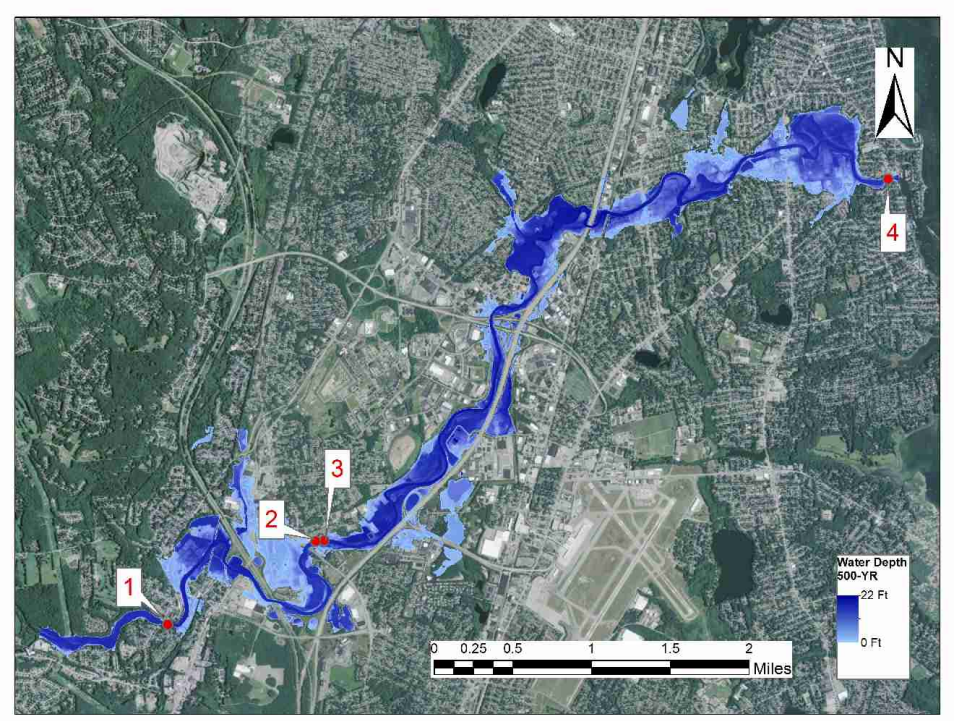

Figure 64: Location of the dams in the Main Branch of the Pawtuxet River. 1-Natick Pond Dam, 2-Pontiac Dam, 3-Pontiac Downstream Dam, 4- Pawtuxet Falls Dam.

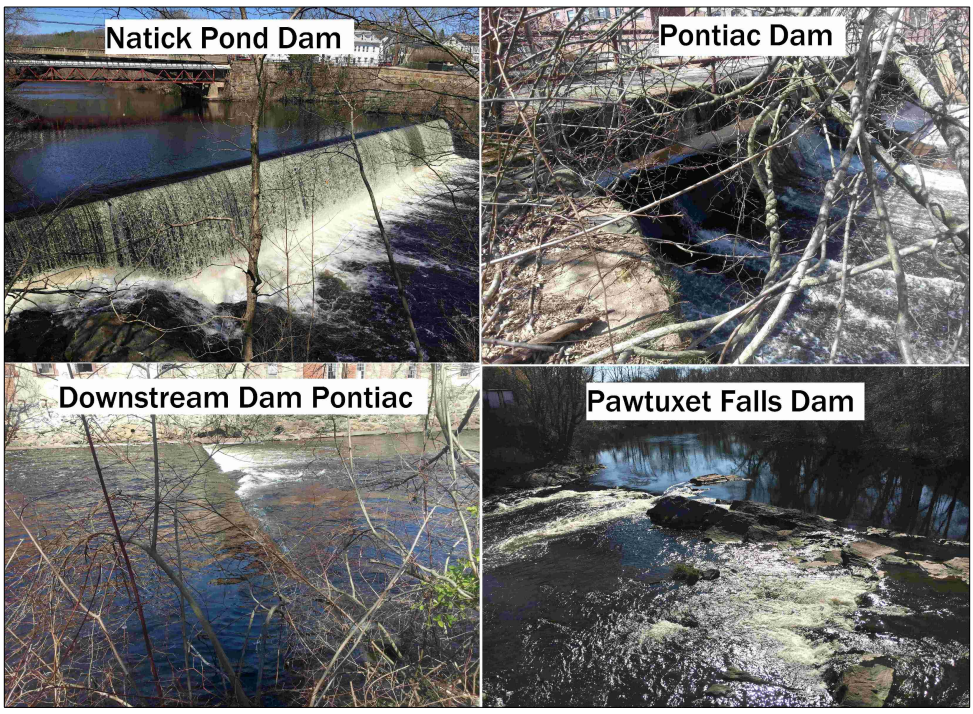

Figure 65: Photos of the dams in the Main Branch of the Pawtuxet River.

the Warwick Mall, neighboring an historic mill. Figure 64 shows the location of the Pontiac Dam. The width of the dam is around 100 ft with a height of around 8 ft. Figure 66 shows the Pontiac dam during a flood event. It seems that the Pontiac Dam has a large influence on the flooding around the Warwick Mall, which was flooded during the March 2010 events.

Figure 66: Pontiac Dam in the Main Branch of the Pawtuxet River during March 2010 flood, Source: Alisa Richardson (RIDEM), 2016, personal communication.

To better investigate the effect of change in elevation due to dam removal, we look at the flooding maps. The results of the HEC-RAS with dam removal were exported to HEC-GeoRAS for 50-, 100- and 500-year flood events. Figure 67 shows that,, the reduced flooded area is much more for 50- and 100-year events than the 500-year event. A 500-year flood event, such as the March 2010 event, is very extreme, and the Pontiac Dam does not have much effect on flood for such a large event. But, it affects smaller scale events.

Figure 68 illustrates the water surface profile during a 100-year event before and after removing the Pontiac dam. The dotted red line shows the location of the Pontiac Dam along the river length. The water level in feet is plotted with and without the dam.

Figure 69 shows the change in the water elevation after removing the Pontiac Dam from the river model. The dotted red line shows the location of the Pontiac Dam along the x-axis. The maximum reduction in elevation of the river is around 4 feet near the dam, for a 50-year or 100-year flood. For a 500-year event, the maximum reduction in water elevation is only about 1.5 ft near the dam.

Removal of Pawtuxet Falls Dam

The partial removal of Pawtuxet Falls Dam was discussed in Section 5.2.1, where Figure

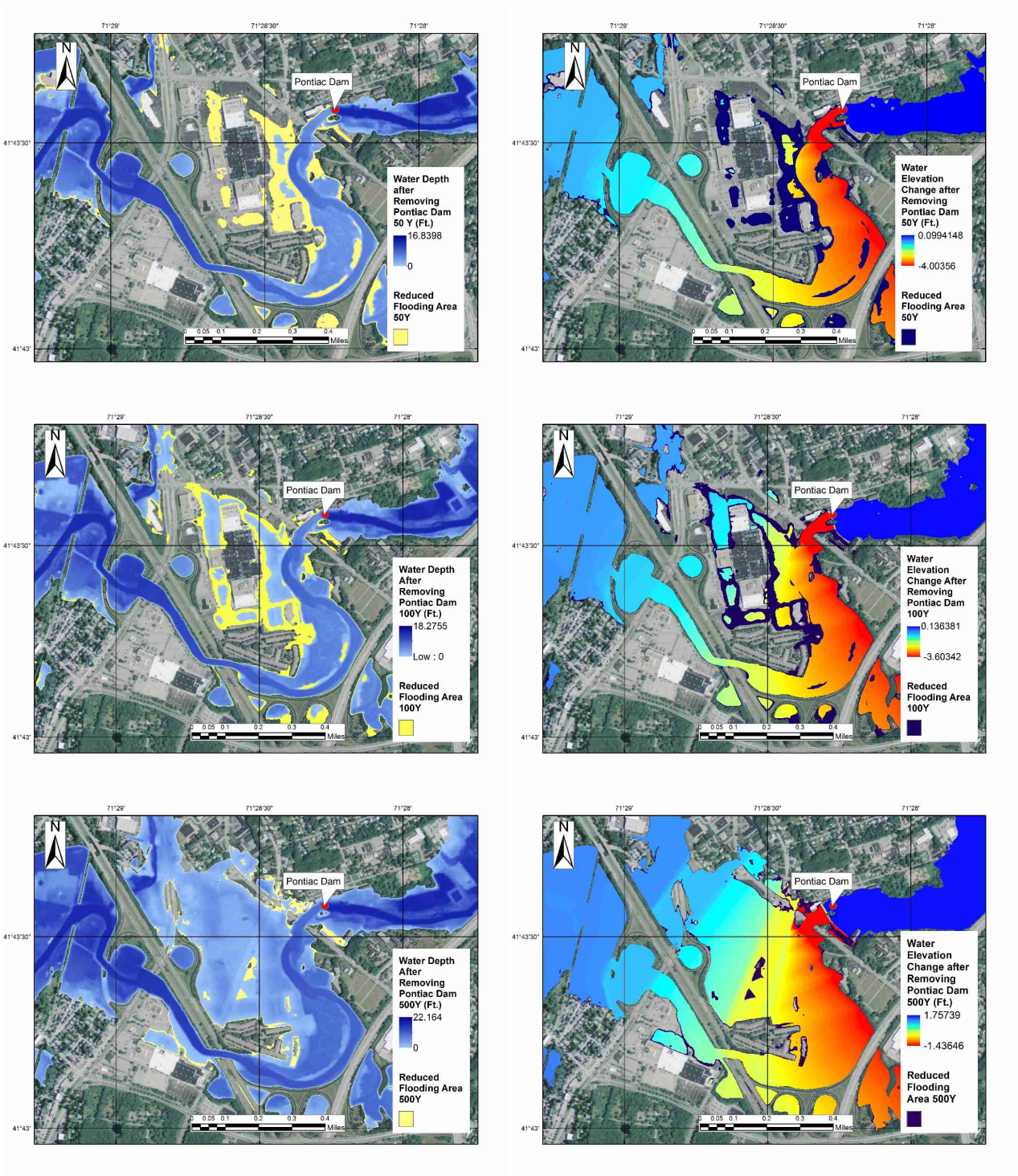

Figure 67: Removal of Pontiac Dam on the Main Branch. Left column: flood water depth in blue contour (after removal) and reduced flooding areas due to dam removal in yellow. Right column shows the flood water elevation change (i.e., water elevation before removal minus water elevation after removal). The reduced flooding area due to removal is shown in dark purple in the right column. The top row shows results for a 50-year event, the middle row for a 100-year event, and the bottom row for a 500-year event.

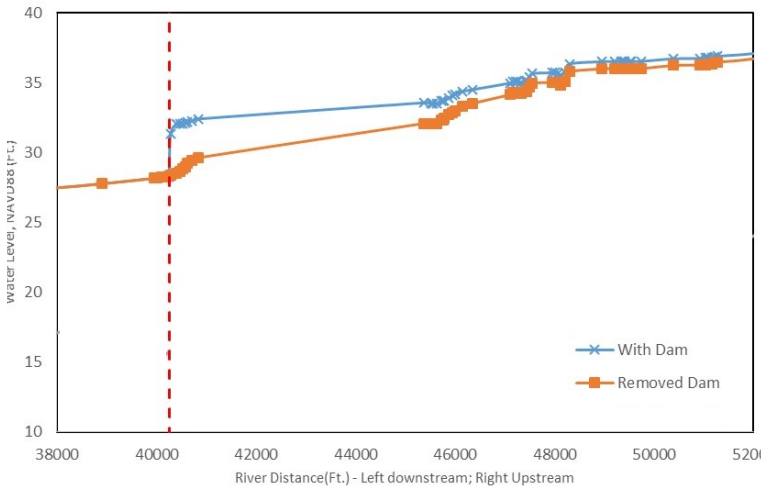

Figure 68: Effect of removing Pontiac Dam on the water surface profile in the Main Branch for a 100-year event. Water levels with and without dam are shown using blue line with x markers, and in orange line with square markers, respectively. Vertical dotted red line shows the location of Pontiac Dam along river length.

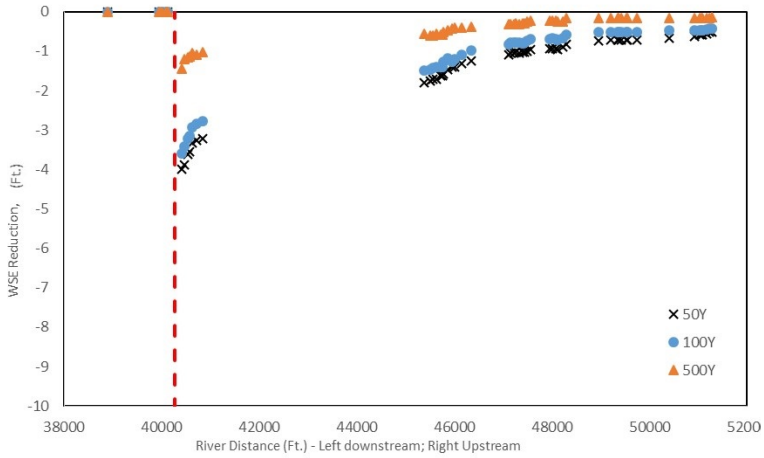

Figure 69: Water surface elevation (WSE) reduction after removing the Pontiac Dam from the HEC-RAS model for a 50, 100, and 500-year event. Vertical dotted red line is at location of Pontiac Dam along river length.

37 displays the dam before and after partial removal. In our HEC-RAS hydraulic model, we have the dam information before partial removal, and we modeled the entire removal of Pawtuxet Falls Dam from the river model to see the effects of removing this dam. Figure 64 shows the location of this dam on the map. The Pawtuxet Falls Dam is the last dam and downstream of the Main Branch of the Pawtuxet River before joining to the Providence River.

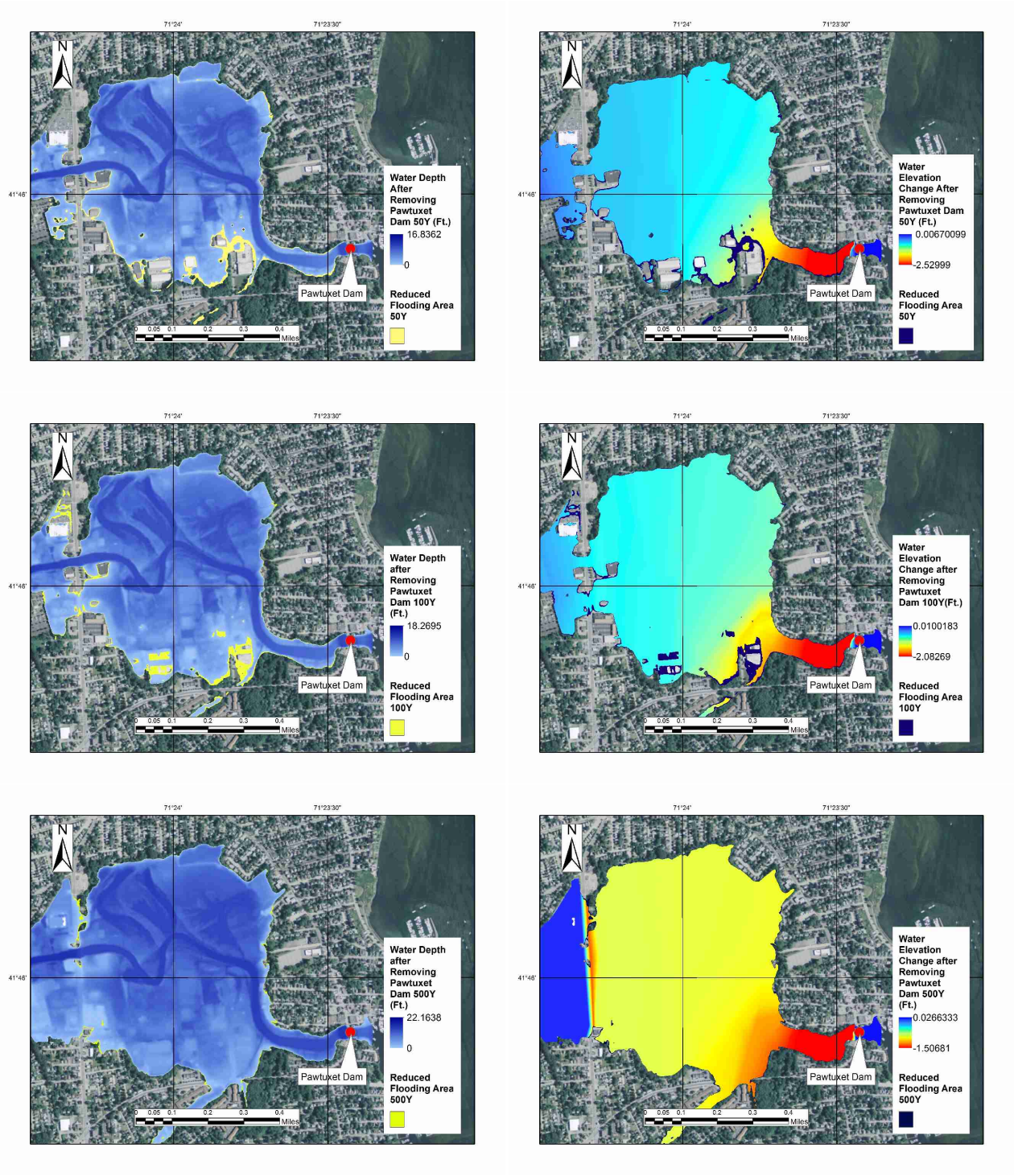

Figure 70: Removal of Pawtuxet Falls Dam at Pawtuxet Village. Left column: flood water depth in blue contour (after removal) and reduced flooding areas due to dam removal in yellow. Right column shows the flood water elevation change (i.e., water elevation before removal minus water elevation after removal). The reduced flooding area due to removal is shown in dark purple in the right column. The top row shows results for a 50-year event, the middle row for a 100-year event, and the bottom row for a 500-year event.

Figure 70 shows the floodplain map for 50-, 100- and 500-year events after removing the Pawtuxet Falls Dam from the Pawtuxet River HEC-RAS model. The removal of the Pawtuxet Falls Dam does not have a large impact on the flooding areas, although as mentioned before, this dam had been partially removed to better support the river ecosystems, improve water quality, and respect community concerns.

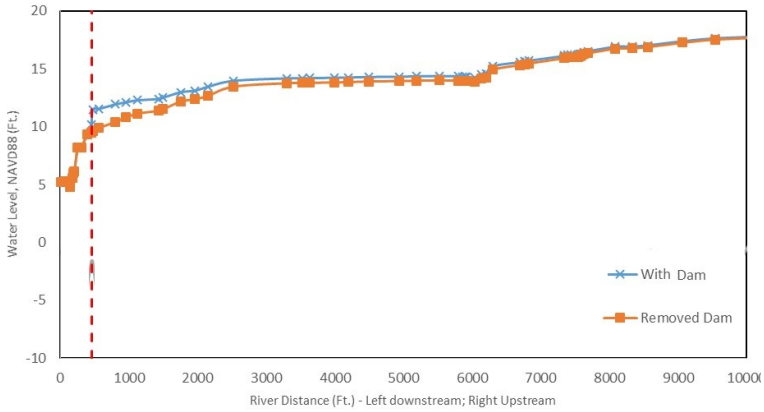

Figure 71: Effect of removing Pawtuxet Falls Dam on the Main Branch of the Pawtuxet River profile for a 100-year event. Water levels with and without dam are shown using blue line with x markers, and in orange line with square markers, respectively. Vertical dotted red line shows the location of the dam along river length.

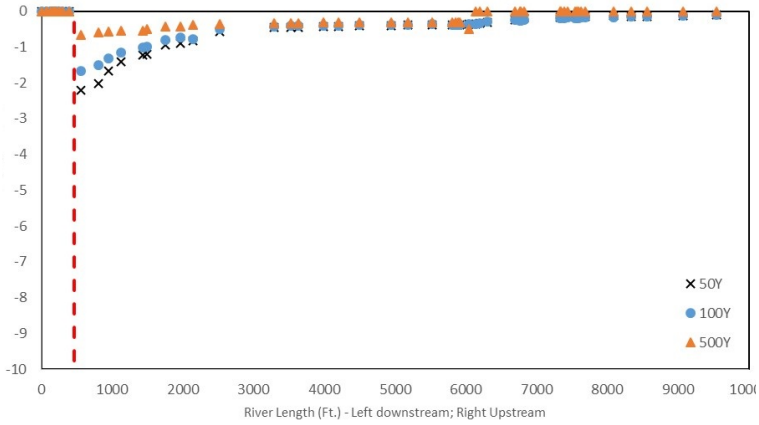

Figure 72: Water surface elevation reduction after removal of the Pawtuxet Falls Dam for 50-, 100-, and 500-year events. Vertical dotted red line shows the location of the Pawtuxet Falls Dam.

Figure 71 illustrates the water surface profile during a 100-year event before and after removing the Pawtuxet Falls Dam. Figure 72 shows the water surface elevation reduction after removing the Pawtuxet Falls Dam based on the river model. The dotted red line shows

the location of the Pawtuxet Falls Dam along the river length. The water surface elevation reduction is shown for the three scenarios of a 50-year, 100-year, and 500-year event. For a 50-year event, the maximum reduction in elevation of the river is around 2.5 ft near the dam. For a 100-year event and 500-year event, the maximum reduction is also near the dam and less than 2 ft and 1 ft, respectively. The elevation reduction magnitude decreases in the as we move upstream.

Removal of all Dams in the Main Branch

We also performed simulations where all dams were removed on the Main Branch to investigate whether the removal has a general impact on flooding. Figure 73 shows the water elevation changes and the changes in the floodplain after removing all dams in the Main Branch of the Pawtuxet River, for 50-, 100-, and 500-year events. The results show that the effects of removing dams are usually restricted to local effects, and that individual dams do not impact each other significantly.

Table 18 lists the maximum water elevation change in the vicinity of each dam of the Main Branch of the Pawtuxet River, along with the river distance from the downstream origin (i.e., confluence with the Providence River). Comparing this table and Figure 73 indicates that a large change in elevation does not necessarily mean large change in inundation (e.g. Natick Pond Dam) as topography controls the flooding extent.

Table 18: Maximum elevation reduction by removing all dams in the Main Branch of the Pawtuxet River.

Main Branch Dams	River Distance from	Max Elevation change (ft)		
	Downstream Origin*(ft)	50-year	100-year	500-year
Natick Pond Dam	53736	-7.38	-7.37	-7.04
Pontiac Dam	40261	-4	-3.6	-1.44
Pontiac Downstream Dam	40117	-0.05	-0.02	-0.02
Pawtuxet Falls Dam	462	-2.22	-1.66	-0.67

* Downstream origin is the confluence of the Pawtuxet and the Providence Rivers.

6.2.4.2 Analysis of the Removal of the Dams in the North Branch

The North Branch of the Pawtuxet River includes 7 dams. The most upstream dam in this branch is the Scituate Reservoir Dam (Gainer Dam), which controls the Scituate Reservoir. This dam has a considerable impact on the flooding of river downstream, which was discussed in Section 6.1.4. The other six dams are local dams which had been mainly used for textile

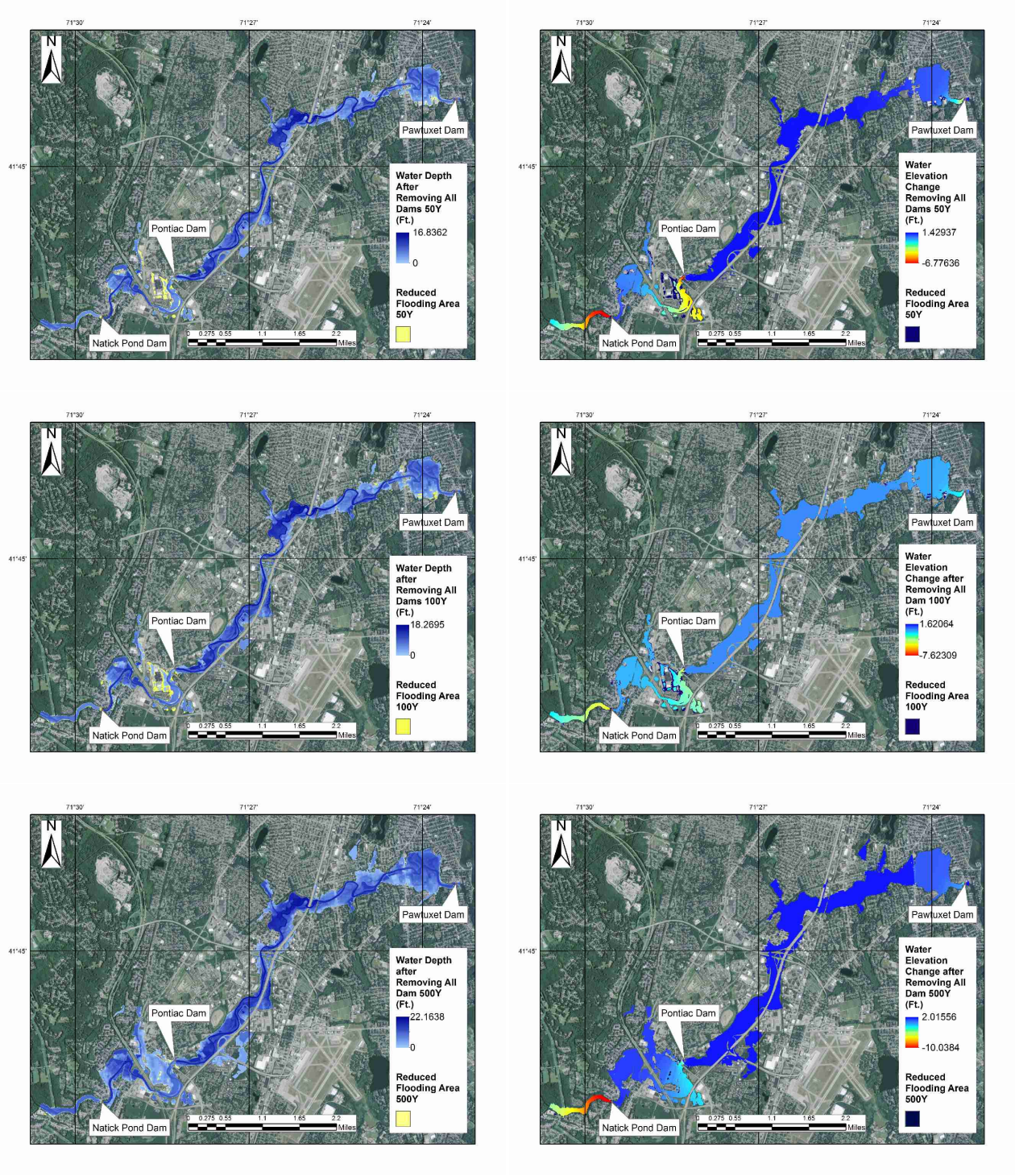

Figure 73: Removal of all dams on the Main Branch. Left column: flood water depth in blue contour (after removal) and reduced flooding areas due to dam removal in yellow. Right column shows the flood water elevation change (i.e., water elevation before removal minus water elevation after removal). The reduced flooding area due to removal is shown in dark purple in the right column. The top row shows results for a 50-year event, the middle row for a 100-year event, and the bottom row for a 500-year event.

companies in the past. Figures 74 shows the location of each of these dams in the map, and Figure 75 shows photographs of them. All of these dams were removed one by one to see the dam removal impact on their respective local flooding. As Hope Dam has the most impact on the floodplain in comparison to the other dams in the North Branch, we will only show the individual results from Hope Dam. We will also show the effect of removing all dams in the North Branch, afterward.

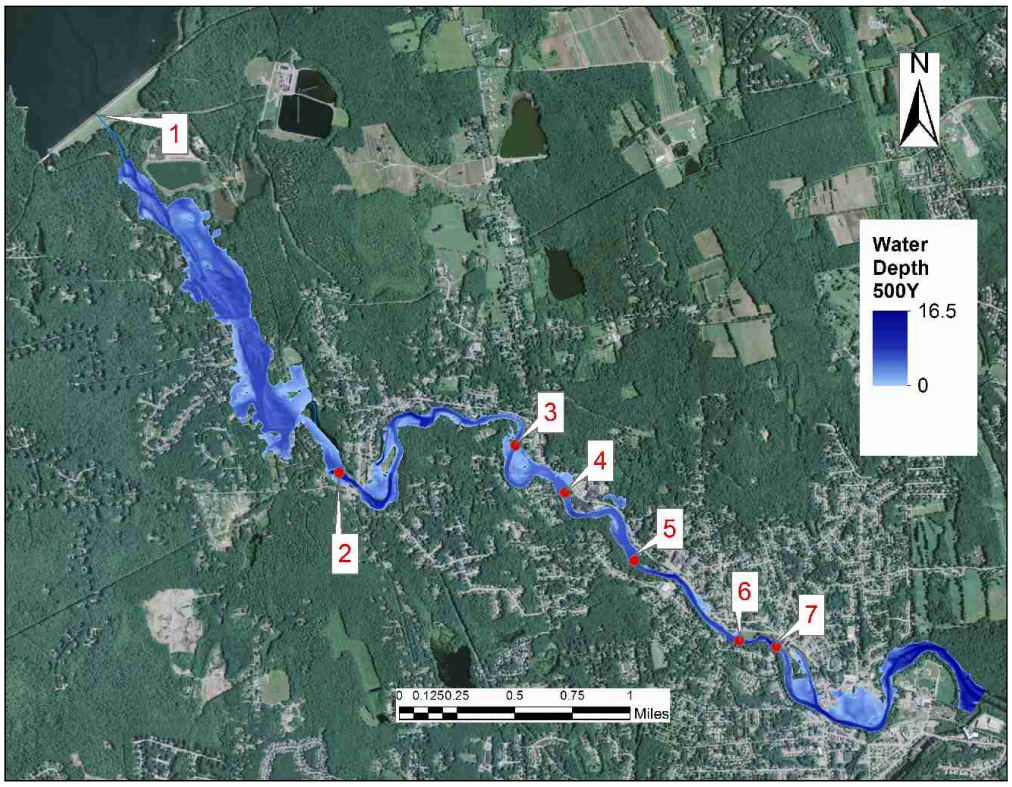

Figure 74: North Branch dam locations: 1. Scituate Reservoir Dam, 2. Hope Dam, 3. Low Head Weir, 4. Arkwright Dam, 5. Harris Pond Dam, 6. Phoenix Dam, 7. Breached Dam.

Hope Dam Removal

Hope Dam is the second dam from the upstream direction of the North Branch of the Pawtuxet River, after the Scituate Reservoir's Gainer Dam. Hope Dam has an approximate width of 140 ft and height of 10 feet. It is located at the border of Coventry and Scituate counties in the western Rhode Island. Figures 74 and 75 show the location and the photograph of Hope Dam, respectively.

For 50-, 100- and 500-year events, Figure 76 illustrates the change in water elevation and water depth of the floodplain after removing Hope Dam from the HEC-RAS river model. There is a considerable flood reduction after removing this dam. In some parts of the inun-

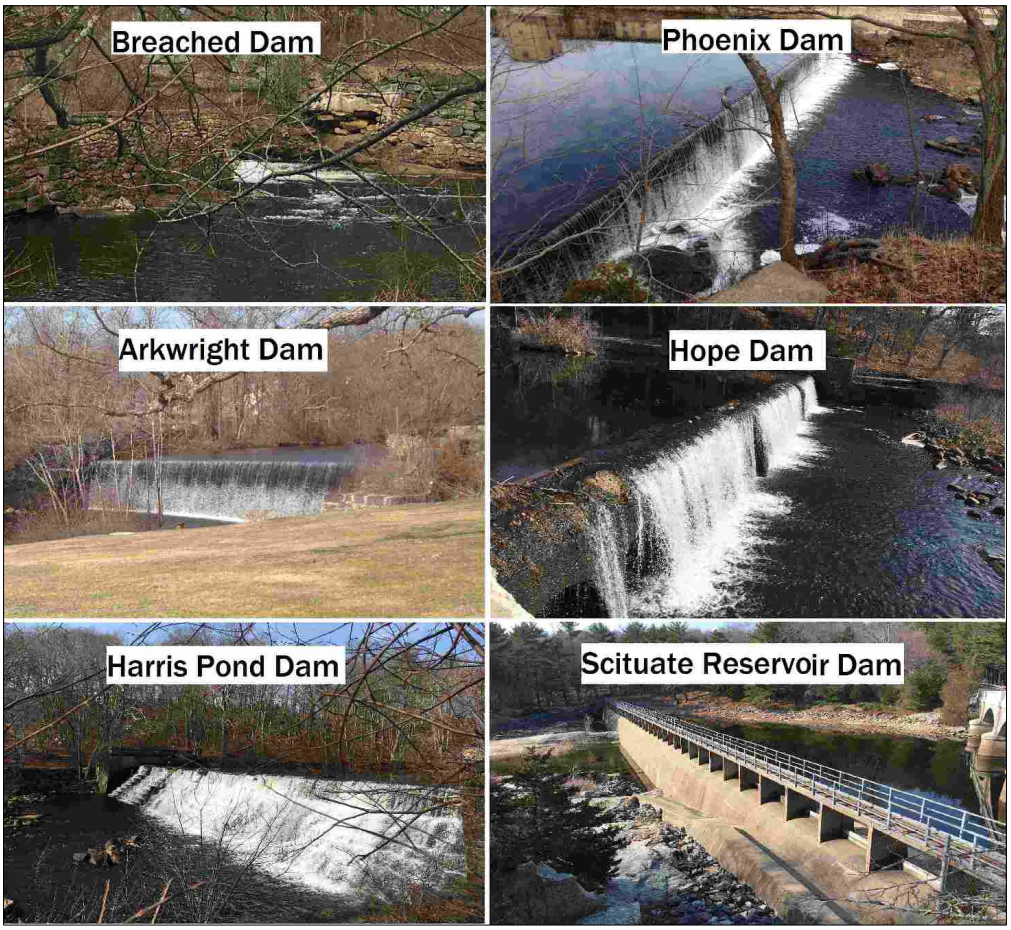

Figure 75: Photos of the 6 dams on the North Branch of the Pawtuxet River.

dation map, the flood extent is discontinuous as there was not sufficient bathymetric data at this location.

Removal of all North Branch Dams

In this scenario, all dams were removed in the North Branch to see their effects on the water elevation change. Figure 77 shows the water depth and water level changes after removing all dams in the North Branch of the Pawtuxet River. We can see from the maps that the effects of removing dams are local, and Hope dam has the largest impact.

Table 19 lists the maximum water elevation reduction in the vicinity of each dam for 50-, 100-, and 500-year events, when removing all dams in the North Branch of the Pawtuxet River. As mentioned, large change in water elevation does not necessarily mean a large impact on flooding due to topography.

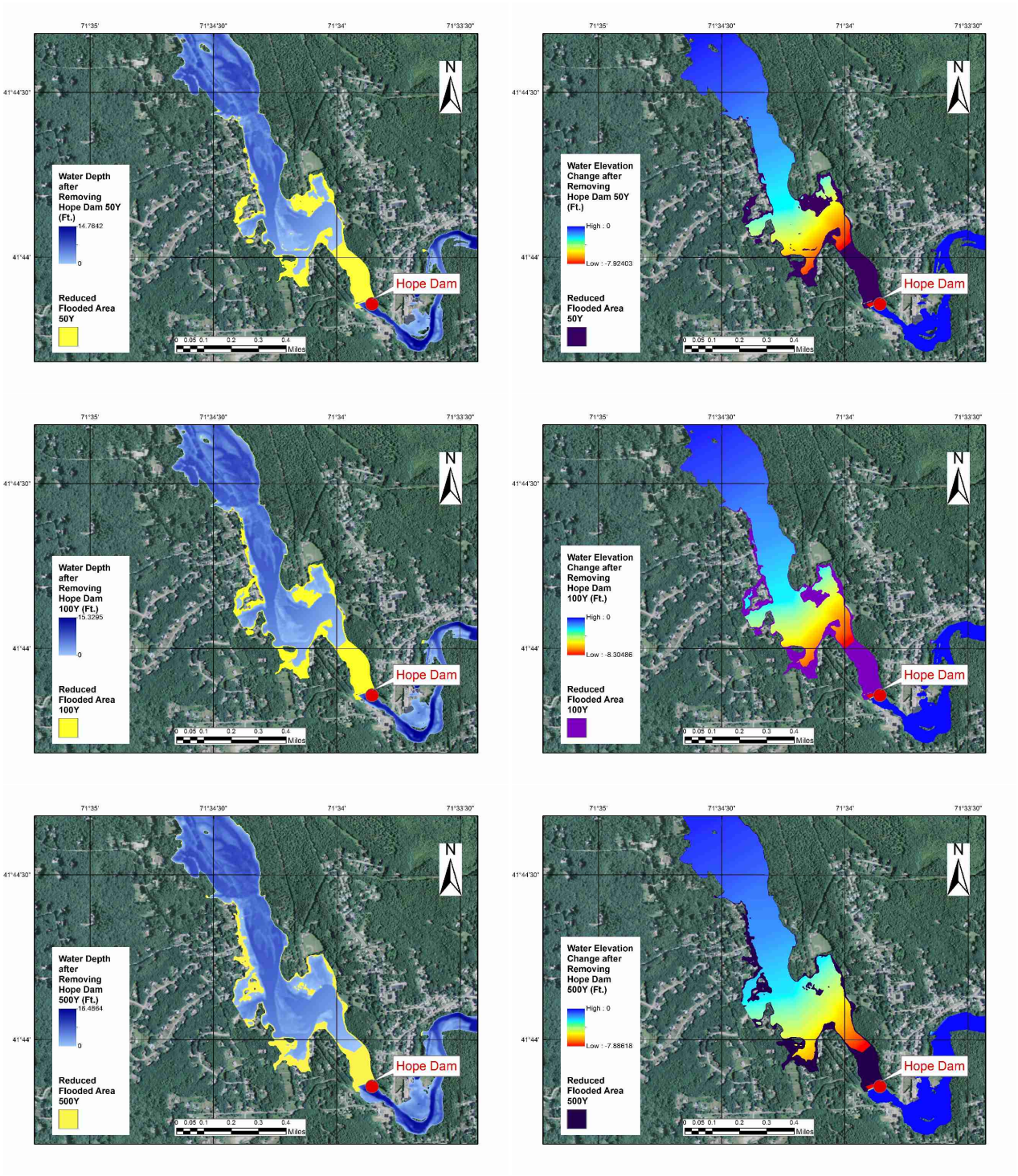

Figure 76: Removal of Hope Dam on the North Branch. Left column: flood water depth in blue contour (after removal) and reduced flooding areas due to dam removal in yellow. Right column shows the flood water elevation change (i.e., water elevation before removal minus water elevation after removal). The reduced flooding area due to removal is shown in dark purple in the right column. The top row shows results for a 50-year event, the middle row for a 100-year event, and the bottom row for a 500-year event.

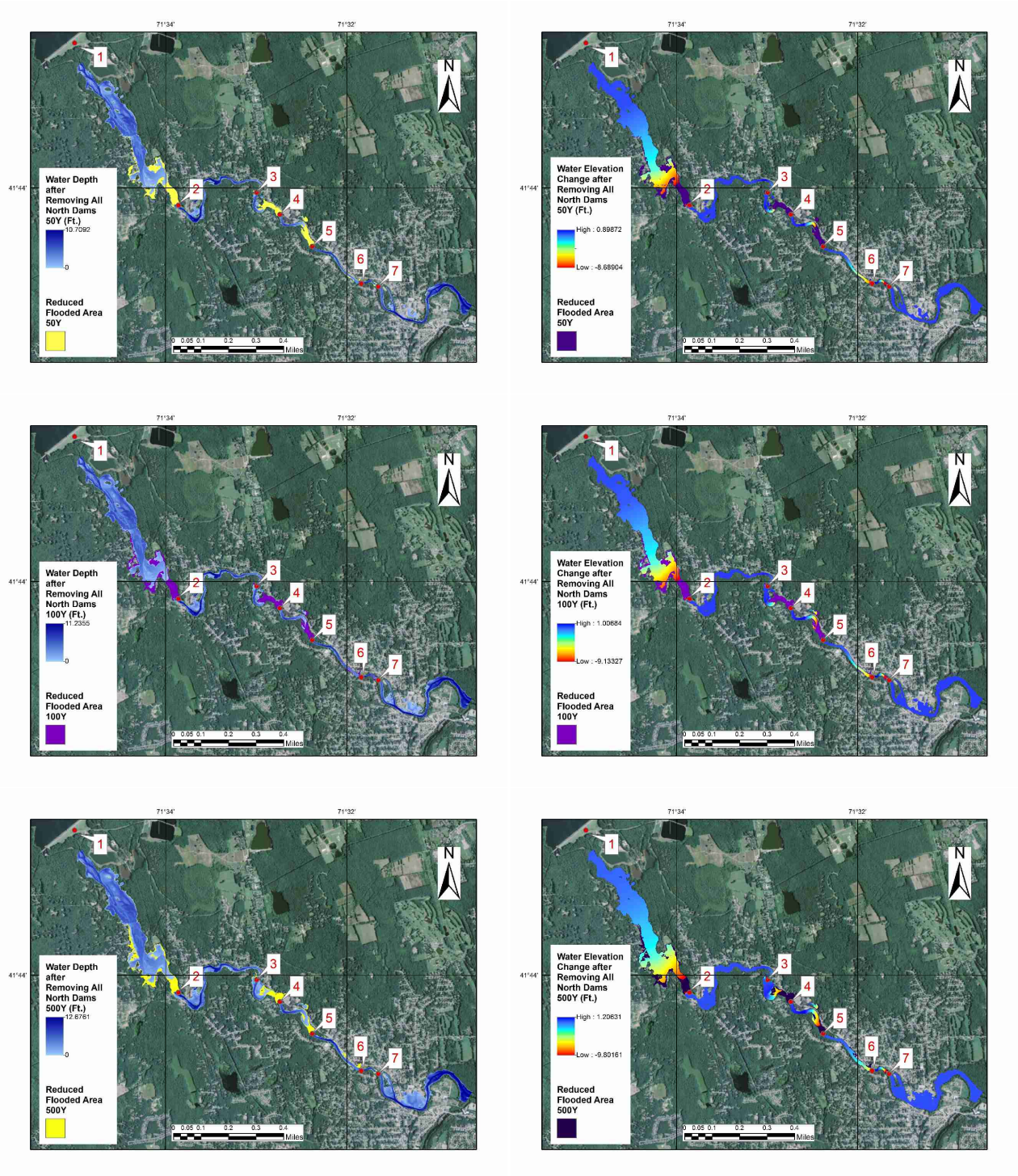

Figure 77: Removal of all dams in the North Branch. Left column: flood water depth in blue contour (after removal) and reduced flooding areas due to dam removal in yellow. Right column shows the flood water elevation change (i.e., water elevation before removal minus water elevation after removal). The reduced flooding area due to removal is shown in dark purple in the right column. The top row shows results for a 50-year event, the middle row for a 100-year event, and the bottom row for a 500-year event.

Table 19: Maximum elevation reduction by removing all dams in the North Branch of the Pawtuxet River.

North Branch Dams	River Distance from Downstream*	Max Elevation change (ft)		
		50-year	100-year	500-year
Hope Dam	24280.08	-7.92	-8.3	-7.56
Low-weir Dam	17119.872	-0.99	-0.97	-1.28
Arkwright Dam	14530.032	-9.65	-9.35	-9.5
Harris Pond Dam	11790.24	-10.7	-10.85	-11.29
Phoenix Dam	8630.16	-4.94	-5.07	-5.29
Breached Dam	7749.984	-7.81	-8.02	-8.41

* The downstream is the confluence of the North and South Branches.

6.2.4.3 Analysis of Dam Removal in the South Branch

The South Branch of the Pawtuxet River includes 11 dams, whose locations are shown in Figure 78. The Flat Reservoir Dam is the first dam upstream of the South Branch, which was discussed in Section 6.1.5. Figure 79 shows photographs of the South Branch dams. The South Branch of the Pawtuxet River runs along many residential areas, so that the impacts of removing dams in this branch is relevant to flood hazard assessment for the communities

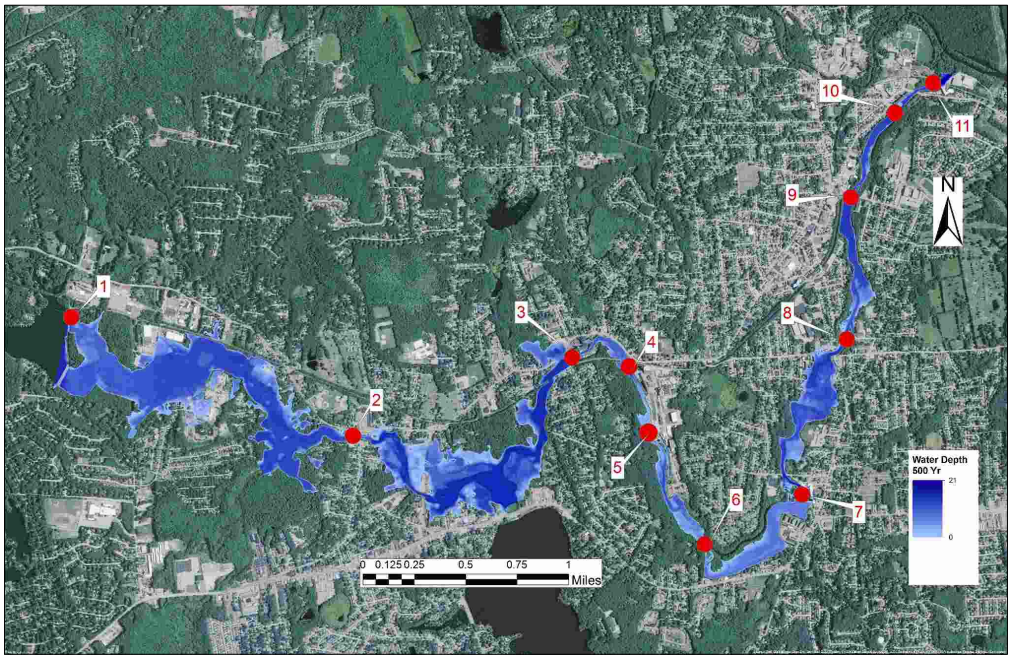

Figure 78: Location of the dams on the South Branch of the Pawtuxet River.

Figure 79: Photos of the dams in the South Branch of the Pawtuxet River.

living nearby. We removed all dams in this branch one by one in the HEC-RAS river model and found that removal of two of the dams provided the most impact. We present the results for the two dams with the most impact: Washington Pond Upper Dam, and Mill Pond Dam.

Removal of Washington Pond Upper Dam

The location of the Washington Pond Upper Dam is in Coventry, upstream of South Main Street in a residential area. It has a width of approximately 200 ft and a maximum height of approximately 12 ft. Figures 78 and 79 shows the location and the photo of the Washington Pond Upper Dam.

Figure 80 shows the water depth and water elevation change after removing the Washington Pond Upper Dam for 50, 100, and 500-year events. Figure 81 shows the water level along the river in the vicinity of the dam location, modeled with the Washington Upper Pond Dam and without the dam. Figure 82 shows the water surface elevation reduction after removing the dam for 50, 100, and 500-year event scenarios. For all three scenarios, the elevation reduction trends are similar and the elevation reduction is maximum directly upstream of the dam location.

Removal of the Mill Pond Dam

The location of Mill Pond Dam is in Coventry, upstream of Laurel Avenue in a residential area, with a width of approximately 75 ft and maximum height of approximately 12 ft. Figures 78 and 79 shows the location and the photograph of Mill Pond Dam.

After removing Mill Pond Dam from the river model, the following results were extracted. Figure 84 shows the water surface elevation reduction after removing the dam and Figure 84 shows the water level in the dam location. Figure 83 shows the water depth and water elevation change after removing the Mill Pond Dam for a 50-, 100-, and 500-year event, respectively. As these figures show, this dam has a significant impact on flooding.

Removal of All Dams in the South Branch

Table 20 gives the data for maximum water elevation reduction for removing each dam, one by one, in the South Branch of the Pawtuxet River. We saw from Figure 77 that the effects of removing an individual dam is effectively local, so our results of removing each dam individually in the South Branch is similar for combination of all dam removals.

6.2.4.4 Summary of Effect of Dams on Flooding

Table 21 lists, for each dam in the Pawtuxet River reaches, the flood extent area before removing the dam, the flood extent area after removing the dam, and the reduction of the

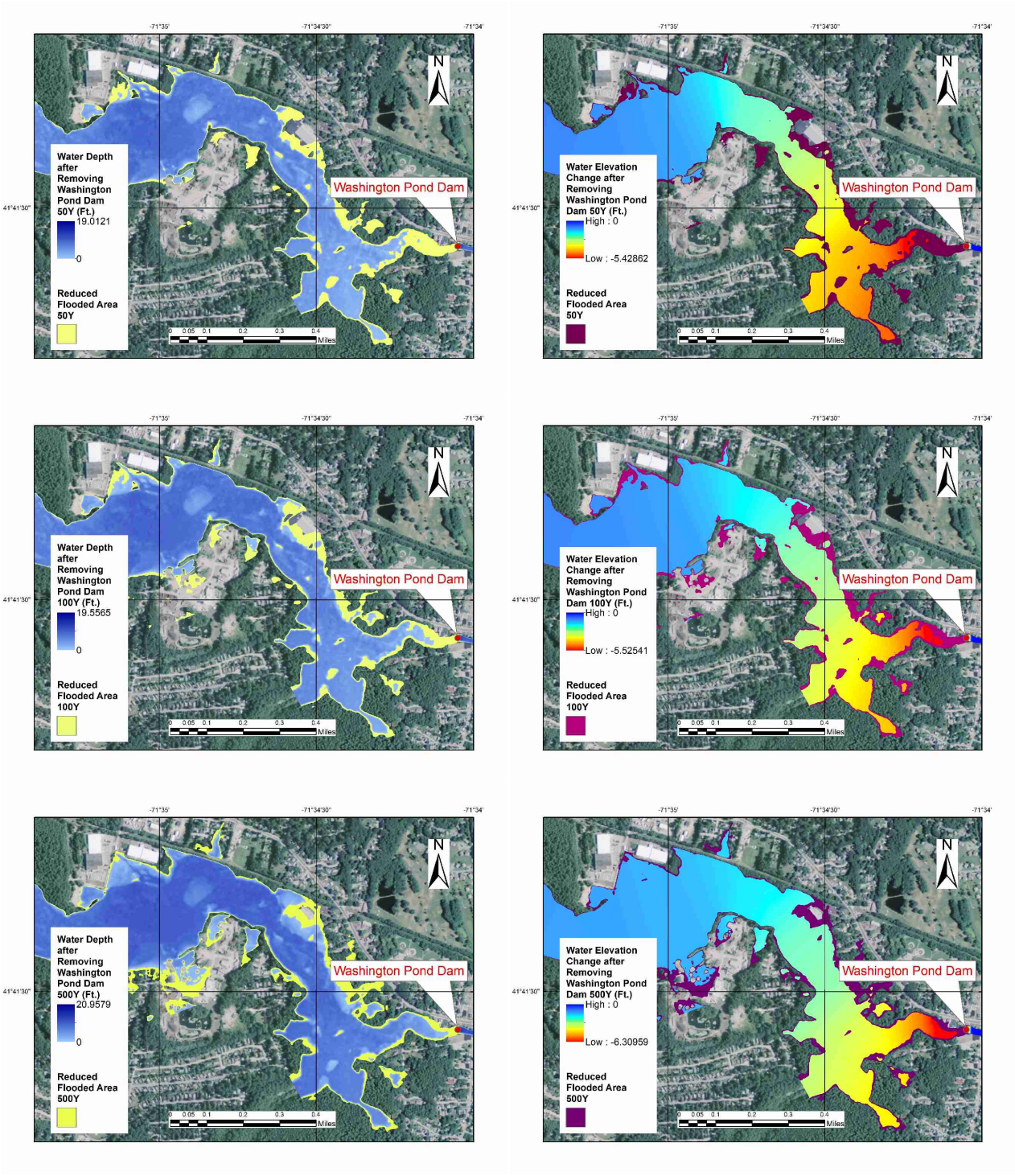

Figure 80: Removal of Washington Pond Dam on the South Branch. Left column: flood water depth in blue contour (after removal) and reduced flooding areas due to dam removal in yellow. Right column shows the flood water elevation change (i.e., water elevation before removal minus water elevation after removal). The reduced flooding area due to removal is shown in dark purple in the right column. The top row shows results for a 50-year event, the middle row for a 100-year event, and the bottom row for a 500-year event.

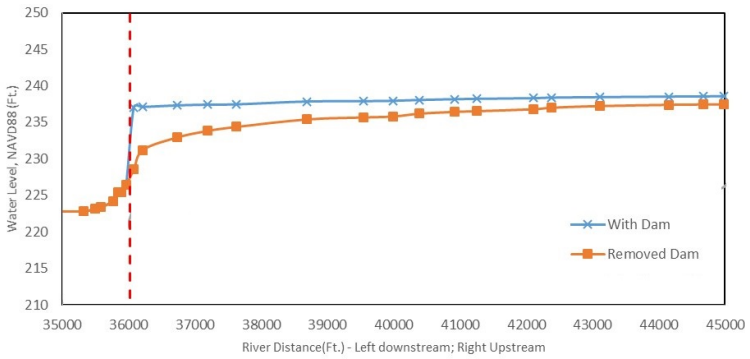

Figure 81: Modeled effect of removing Washington Upper Pond Dam on the South Branch of the Pawtuxet River profile for a 100-year event. Water levels with and without dam are shown using blue line with x markers, and in orange line with square markers, respectively. Vertical dotted red line shows the location of the dam along river length.

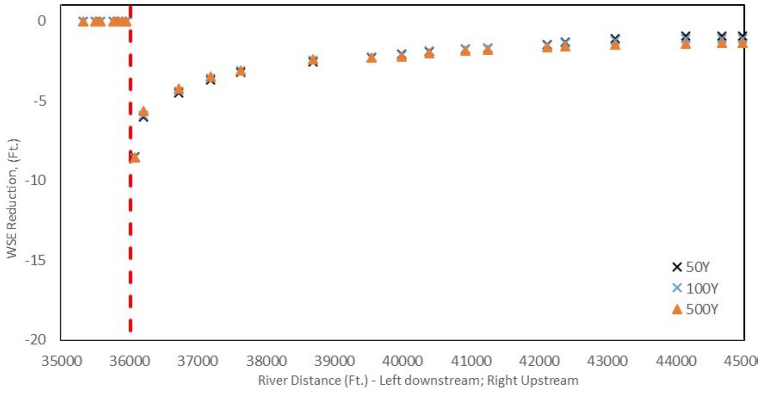

Figure 82: Water surface elevation reduction after removal of the Washington Upper Pond Dam in for 50, 100, and 500-year events. Vertical dotted red line is at location of Washington Upper Pond Dam.

flood extent areas for 50-, 100-, and 500-year return period flood scenarios. The top three rows list the values for the dams in the Main Branch, the middle 6 rows for the dams in the North Branch, and the bottom 10 rows for the dams in the South Branch. Scituate Reservoir (Gainer) Dam, and the Flat River Reservoir Dam are not included in this tabulation as it is unrealistic to remove these dams. To explore flood reduction, we looked at two parameters: flood area reduction and landuse around the dam. There are several dams that intensify flooding effects but are not in highly populated areas; hence, removing them would not lead to major reduction of the flood risk. There are also other dams such as the Natick Dam that their removal would lead to significant changes in the water level. However, the removal of

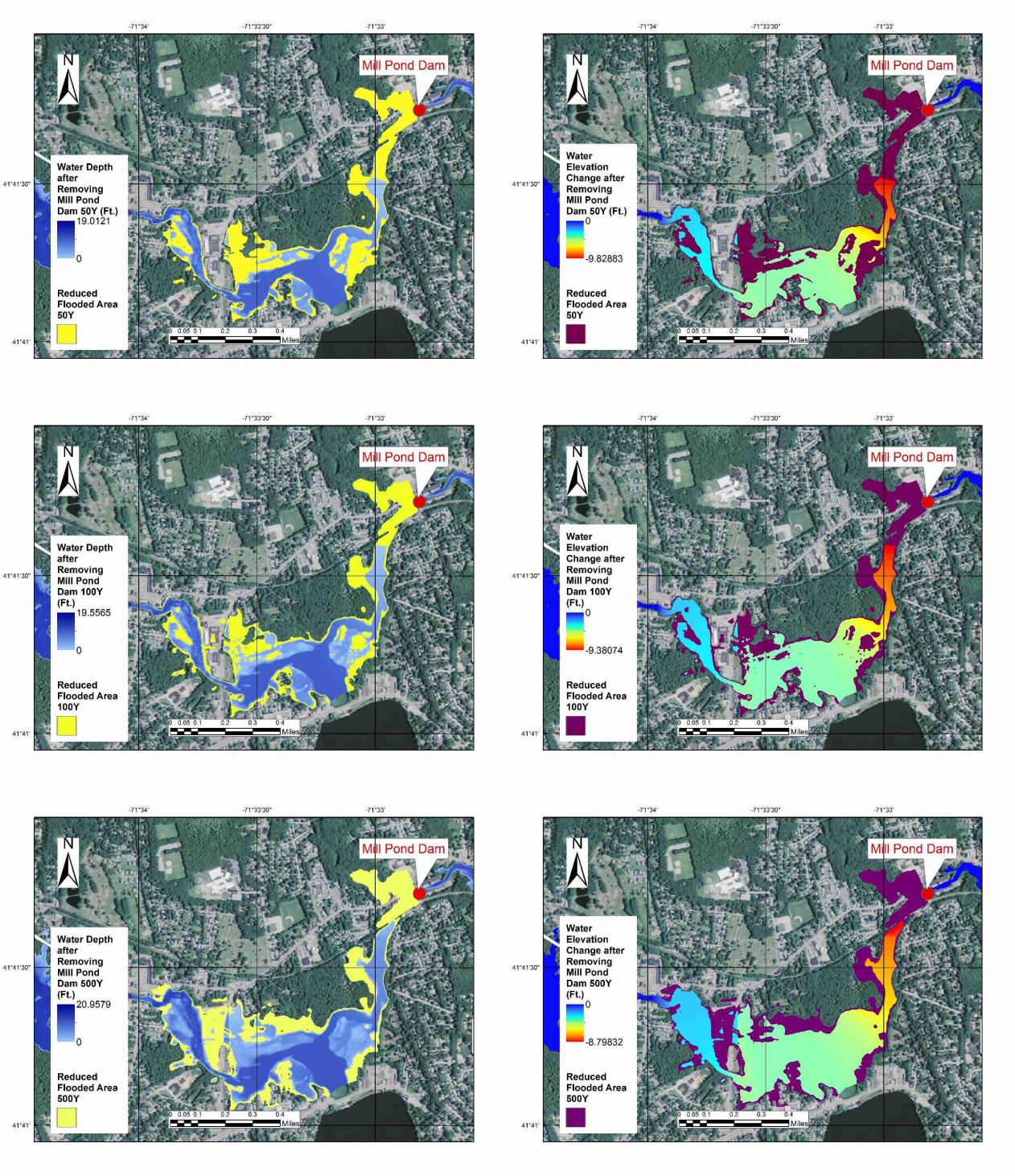

Figure 83: Removal of Mill Pond Dam on the South Branch. Left column: flood water depth in blue contour (after removal) and reduced flooding areas due to dam removal in yellow. Right column shows the flood water elevation change (i.e., water elevation before removal minus water elevation after removal). The reduced flooding area due to removal is shown in dark purple in the right column. The top row shows results for a 50-year event, the middle row for a 100-year event, and the bottom row for a 500-year event.

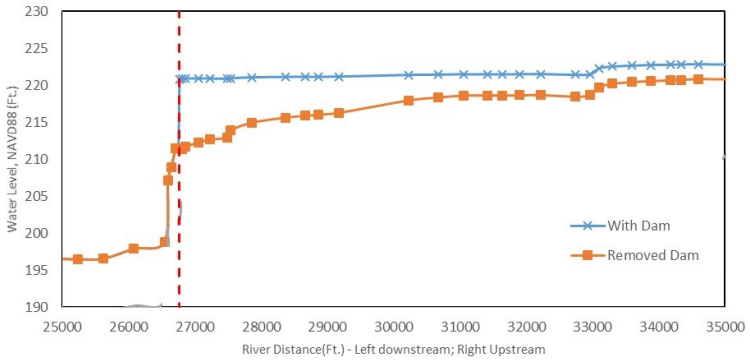

Figure 84: Modeled effect of removing Mill Pond Dam on the South Branch of the Pawtuxet River profile for a 100-year event. Water levels with and without dam are shown using blue line with x markers, and in orange line with square markers, respectively. Vertical dotted red line shows the location of the dam along river length.

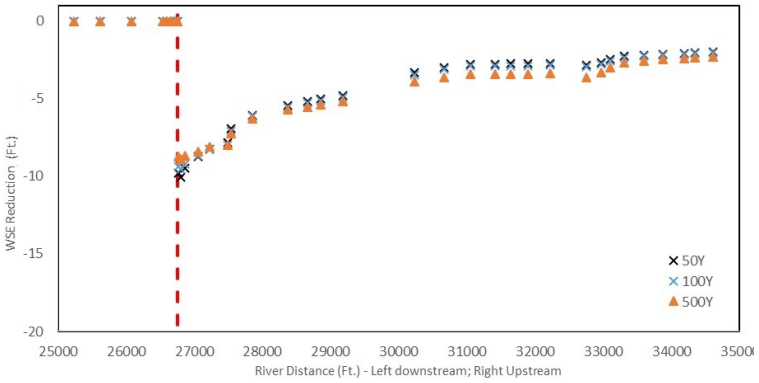

Figure 85: Water surface elevation reduction after removal of the Mill Pond Dam based on the HEC-RAS river model for 50, 100, and 500-year events. Vertical dotted red line is at location of Mill Pond Dam.

these dams would not necessarily result in a significant reduction in the flooding extent. The reason is that the channel above these dams has high banks to prevent flooding; therefore, removing these dams would not impact the risk of flooding significantly. In addition to the technical benefits of flood reduction and preventing dam breach, there are also positive and negative ecological effects of dam removal which are not in the scope of this project, such as movement of contaminants, aquatic life, and effect on fish passage.

The results in Table 21 suggest that removing the Pontiac Dam can be beneficial to control flooding in the commercial area upstream of the dam. There is significant flood extent reduction of 31.8% and 26.1% during 50 and 100-year events, signaling the importance of

Table 20: Maximum elevation reduction by removing dams in the South Branch of the Pawtuxet River.

Removed South Branch Dam	River distance from downstream*	Max Elevation change (ft) return period (years)		
		50	100	500
Washington Pond Upper Dam	36018	-8.5	-8.5	-8.5
Mill Pond Dam	26759	-10.0	-9.5	-8.8
Clarient Dam	24647	-6.0	-6.2	-6.9
Sheltra Ave Dam	22810	-3.6	-3.1	-2.0
New Dam Rd.	19102	-4.6	-4.4	-3.4
Crompton Lower Dam	14465	-7.1	-7.2	-7.3
Centreville Dam	8650	-5.0	-5.1	-5.2
Arctic Mill Dam	4890	-14.8	-15.0	-15.6
Royal Mills Dam	2300	-5.9	-6.0	-6.4
Riverpoint Lower Pond Dam	960	-4.7	-4.0	-2.1

* The downstream is the confluence of the North and South Branches.

removing the Pontiac Dam on flooding in the watershed. Its removal impacts 50- and 100-year flood scenarios that are more frequent in the watershed, in comparison with the extreme 500-year flood event scenario. We suggest further study to investigate other aspects of removing the Pontiac Dam. However, the management of the Scituate Reservoir is the most important way to mitigate flooding in this area.

In the North Branch, Hope Dam is located in an urban area. Removing this dam results in a reduction of inundated areas by 23% (in a 3.5 million ft^2 area) for the 100-year flood, and 20% for a 500-year flood. Although there are other dams in the North Branch which their removals would result in even larger reduction percentages, the areas they impact are more remote and farther from residential and commercial properties. For the South Branch, Washington Pond Upper Dam and Mill Pond Dam are also located in an urbanized area, and removing these dams would result in a significant change in the flooded area extent. More studies should be performed to compare the benefits of dam removals and using the Scituate and Flat River reservoirs for flood control, and also assess the other aspects of dam removal.

Table 21: Flood extent areas before and after dam removal, and percent reduction, for 50, 100, and 500-year return flood scenarios. Rows, separated by horizontal lines: top 3 dams located in the Main Branch, middle 6 dams in the North Branch, and bottom 10 dams in the South Branch.

	50-year Return Flood			100-year Return Flood			500-year Return Flood		
	Before (ft^2)	After (ft^2)	Reduced	Before (ft^2)	After (ft^2)	Reduced	Before (ft^2)	After (ft^2)	Reduced
Natick Dam	1,103,440	969,395	12.1%	1,124,226	1,012,242	10.0%	1,196,370	1,108,042	7.4%
Pontiac Dam	3,862,003	2,632,668	31.8%	4,857,873	3,590,463	26.1%	7,300,696	6,903,160	5.4%
Pawtuxet Dam	7,221,192	6,909,828	4.3%	7,826,496	7,539,795	3.7%	8,776,315	8,700,665	0.9%
Hope Dam	3,204,049	2,443,967	23.7%	3,387,279	2,585,299	23.7%	3,793,352	3,020,755	20.4%
Low-weir Dam	128,569	119,308	7.2%	155,002	143,180	7.6%	213,545	182,544	14.5%
Arkwright Dam	515,675	331,996	35.6%	617,241	407,907	33.9%	790,446	521,109	34.1%
Harris Pond Dam	369,885	282,607	23.6%	385,521	288,857	25.1%	421,726	324,832	23.0%
Phoenix Dam	223,051	188,011	15.7%	241,171	198,576	17.7%	333,227	257,387	22.8%
Breached Dam	71,751	56,781	20.9%	74,599	60,068	19.5%	81,371	68,551	15.8%
Washington Pond Upper Dam	150,253	101,040	32.8%	157,019	106,879	31.9%	173,360	121,412	30.0%
Mill Pond Dam	5,257,538	3,001,801	42.9%	5,650,761	3,603,542	36.2%	7,150,483	4,540,961	36.5%
Clarient Dam	294,131	215,691	26.7%	312,716	231,482	26.0%	353,330	250,580	29.1%
Sheltra Ave Dam	136,953	100,458	26.6%	143,652	102,243	28.8%	187,022	137,673	26.4%
New Dam Rd.	242,326	178,451	26.4%	262,411	226,994	13.5%	310,173	266,919	13.9%
Crompton Lower Dam	936,879	730,978	22.0%	959,286	734,332	23.5%	1,051,145	770,191	26.7%
Centreville Dam	807,401	744,550	7.8%	837,917	773,413	7.7%	952,744	873,619	8.3%
Arctic Mill Dam	210,601	191,701	9.0%	214,536	193,549	9.8%	222,672	195,819	12.1%
Royal Mills Dam	156,379	135,681	13.2%	159,887	137,904	13.7%	177,874	151,515	14.8%
Riverpoint Lower Pond Dam	83,875	75,663	9.8%	85,871	76,686	10.7%	90,366	84,242	6.8%

Main Branch

North Branch

South Branch

6.2.5 Effects of Debris on Flooding

A bridge structure comprises of a superstructure and substructure. The part on which the traffic moves (e.g. deck) is the superstructure, while the substructure transfers the traffic loading to the foundation. Piers are vertical supports in the substructure of a bridge. The most common types of bridge piers are wall type, capped pile, tee type (Hammerhead), and cap/column piers. Based on the bridge width, traffic load, river flow, and other parameters, the number of the piers are selected for a bridge. For relatively narrow sections of a river, a bridge may have no pier in the middle of the river, while for wider river sections one or more piers may be constructed in the river. Figure 89 shows the sample photos of the bridges in the Main Branch and their piers.

Figure 86: A broken tree (debris) in North Branch of the Pawtuxet River.

In many rivers such as the Pawtuxet River, where broken trees can frequently be found in the floodplains and the watershed, debris can significantly increase the risk of flooding. Floating debris can be caught at bridge piers that are located in the river channel and accumulate masses of material, which causes much larger obstruction to the flow. The additional obstruction results in decreased flow speed, reduced passage area, and increased inundation in the upstream areas of a bridge. If no pier is constructed in the river channel, debris can pass the bridge more easily as opposed to bridges which have one or several piers in the river channel. During the field visits, many broken trees and wood debris were observed in the river channel or floodplains, one example of which is shown in Figure 86. Guidelines are

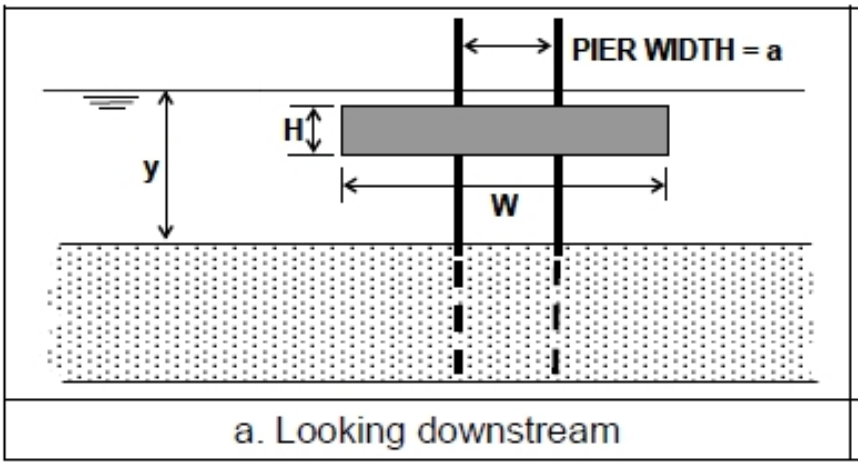

Figure 87: Idealized dimensions of rectangular modeled debris accumulations, Source: Lagasse et al. (2010).

available for calculation of debris size based on the pier dimensions (Lagasse et al., 2010).

In order to account for debris blockage effect, an option is available in the HEC-RAS model. The pier debris option blocks out a rectangular area in front of a given pier, with

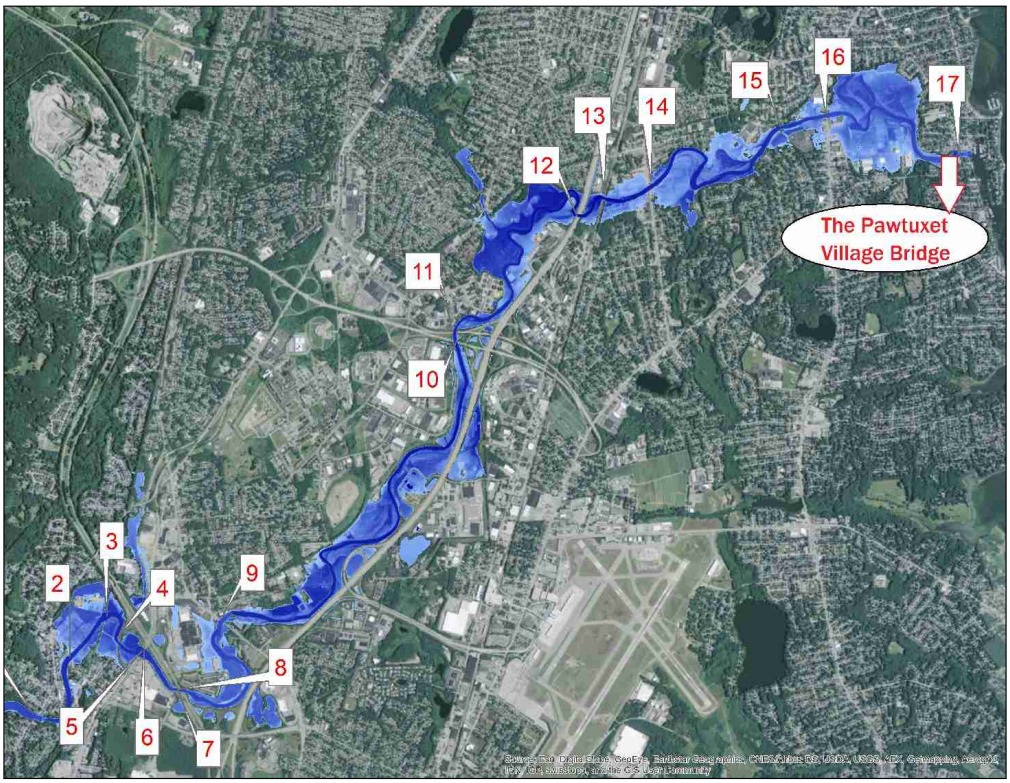

Figure 88: Location of the 17 bridges in the Main Branch of the Pawtuxet River. See Figures 89 and 90 for photos of the bridges and the names.

the height and width of the block specified by the user. HEC-RAS adjusts the area and wetted perimeter of the bridge opening to account for the upstream pier debris, with the top of the block set to be at the water surface elevation to model floating debris (Brunner, 2001). HEC-RAS changes the geometry of the bridge in order to model the pier debris (i.e., it merges the debris with the bridge geometry, then calculates the flow in the river). Figure 87 illustrates the idealized forms of a rectangular block of debris (Lagasse et al., 2010).

Earlier in Section 5.2.1, it was discussed that there are 17 bridges in the Main Branch of the Pawtuxet River. The location of each bridge is illustrated in Figure 88. Figures 89 and 90 show the photos of the corresponding bridges given in Figure 88. Among those bridges, 10 contain 1–4 piers in the river section to which we have added modeled debris. Table 22 shows the bridges with the modeled bridge, pier, and debris dimensions. Lagasse et al. (2010) reports the average width of debris to be 15 times a pier width and the height of the debris to be 0.33–0.5 of the water depth; we use the recommendations to guide our debris dimension selections.

Table 22: Debris data used in the modeling.

Symbol in Figure 88	Distance from Downstram Origin*	Location in the river	No. of Piers	Pier's Width (ft)	Debris Width (ft)	Debris Height (ft)
2	51189	East Ave	1	5	60	9
3	49524	Old RR	2	6	70	10
6	47360	Rt 2 South Ramp	4	1.5	20	10
7	45806	I-295 West	2	1.5	20	10
9	40645	Rt. 5 (Greenwich)	1	2.5	35	10
10	25987	Rt 37 South	2	4	60	7
14	14405	Elmwood Ave	2	4	60	7
15	7645	Conrail	2	2.5	35	7
16	6063	Warwick Ave	2	4	60	6
17	328	Pawtuxet Village	1	7.3	80	6

*Downstream Origin is the confluence of the Pawtuxet and the Providence Rivers.

The Pawtuxet Village Bridge (Figure 90) is one of the bridges we have modeled with debris. The Pawtuxet Village Bridge is located near the confluence of the Pawtuxet River and the Providence River. The area around the river is residential, so river flooding can be dangerous and damaging to the properties near the river.

Figure 91 shows the water depth and water elevation change after adding debris to the

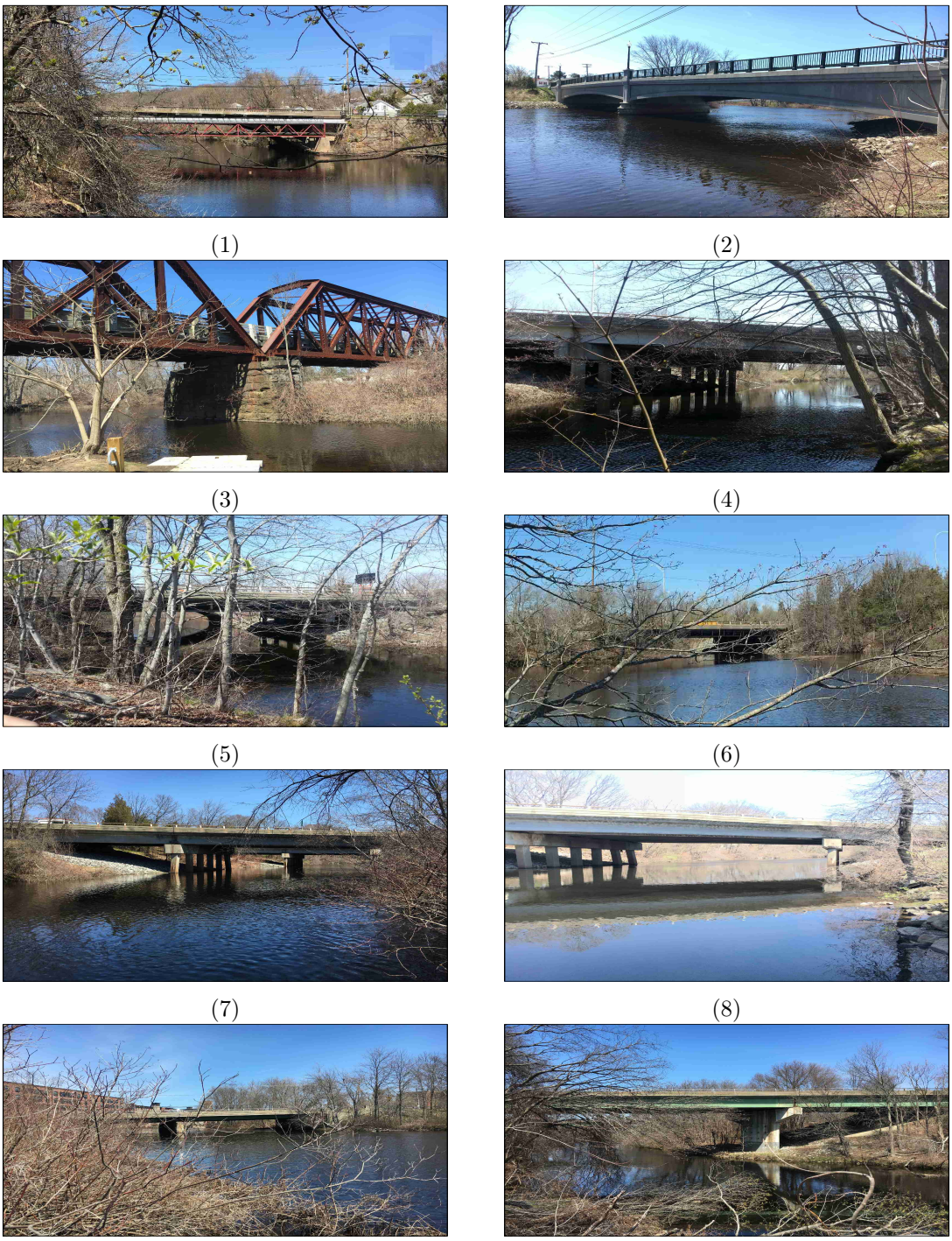

(1) (2) (3) (4) (5) (6) (7) (8) (9) (10)

Figure 89: Photos of the bridges in the Main Branch of the Pawtuxet River. See Figure 88 for location of each bridge along the Pawtuxet River. 1- Route 33 (Providence St.), 2- East Ave., 3- Washington Secondary Trail (Old Roadrail), 4- Route 2 Ramp 5- Route 2/Bald Hill Road Northwest Span, 6- Route 2/Bald Hill Road Southeast Span, 7- I-295 West Span, 8- I 295 East Span, 9- Route 5 (Greenwich Ave.), and 10- Route 37 South Span.

(11)

(12)

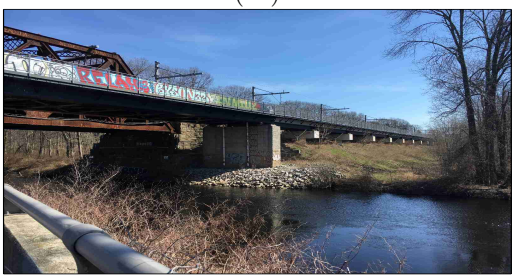

(13)

(14)

(15)

(16)

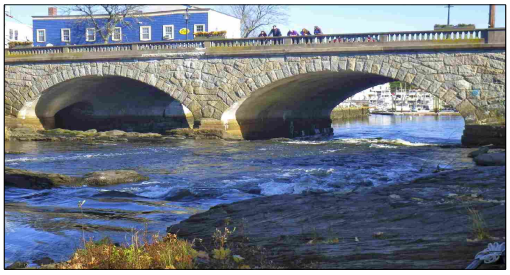

(17)

Figure 90: Photos of the bridges in the Main Branch of the Pawtuxet River (continued). See Figure 88 for location of each bridge along the Pawtuxet River. 11- Route 37 North Span, 12- I-95, 13- Conrail Bridge No. 1 (Old Railroad), 14- Elmwood Ave., 15- Conrail No. 2 (Old Roadrail), 16- Warwick Ave., and 17- Pawtuxet Village.

piers of the Pawtuxet Village Bridge for 50-, 100-, and 500-year events. In each scenario, there is a significant increase in inundated areas after the effects of debris are included in the model, with a larger increase in flooded area for the increasing return period events. We can also see from the water elevation change maps that after the debris has been modeled, the

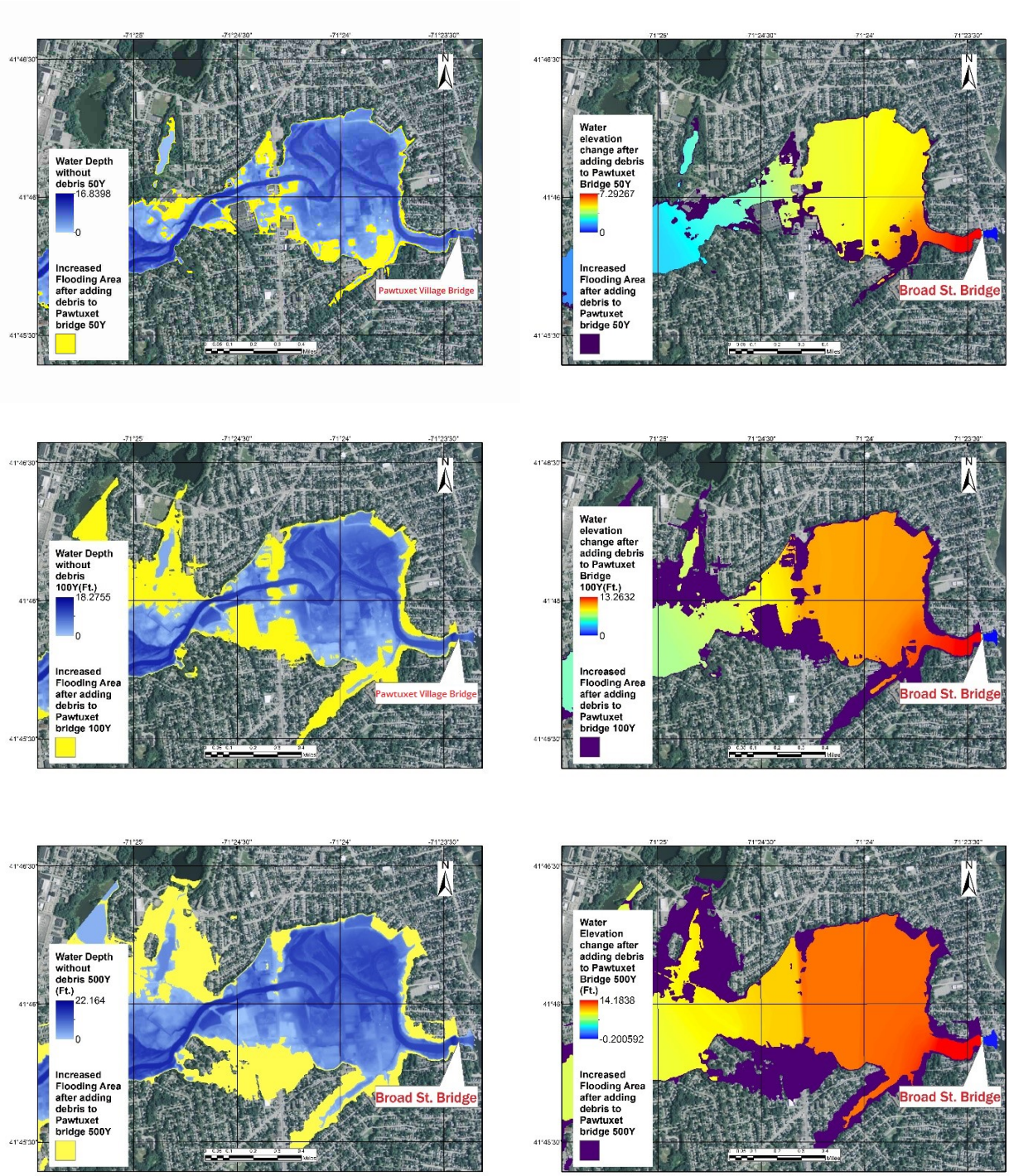

Figure 91: Flood water depth (left column) and water elevation change (right column) after adding debris to the Pawtuxet Village Bridge for 50 (top row), 100 (middle row), and 500-year (bottom row) event scenarios.

Table 23: Maximum elevation increase by adding debris to bridge piers in the Main Branch of the Pawtuxet River model.

Main Stream Pawtuxet River Bridges		Max elevation change (ft)		
Symbol in	Location in the	return period (years)		
Figure 88	watershed	50	100	500
2	East Ave	0.2	0.1	0.0
3	Old RR	0.1	0.1	0.1
6	Rt 2 South Ramp	0.2	0.2	0.0
7	I-295 West	0.3	0.5	0.7
9	Rt. 5 (Greenwich)	0.1	0.1	0.3
10	Rt 37 South	0.41	0.6	1.0
14	Elmwood Ave	2.0	1.1	0.4
15	Conrail	0.2	0.1	0.0
16	Warwick Ave	2.6	2.8	0.0
17	Pawtuxet Village	7.3	13.3	14.2

water elevation increases upstream of the Pawtuxet Village Bridge, at its maximum directly upstream of the bridge location. Further upstream, the water elevation is still increased. The effect is intensified with higher values of return periods. Table 23 shows the maximum elevation increase in the vicinity of each bridge for 50, 100, and 500-year events, having added pier debris to 10 of the bridges in the river model. Based on these results, the modeling of debris in the river adds significantly to flooding extent, and should be modeled for more accurate risk assessments.

Prediction/control of any debris upstream of the bridges is practically almost impossible. The above results show that the impact of debris on flooding is not negligible. Since there are several bridges along the Pawtuxet River, we believe that adding flooded map layers with consideration of reasonable debris estimation behind the bridges is necessary.

6.2.6 Effect of Sea Level Rise and Storm Surge on Flooding

In general, apart from the river flow over spillways and dams, the flow regime in the majority of reaches in a river is subcritical. A subcritical flow is controlled by the downstream boundary condition. As it was mentioned in Chapter 2, the Pawtuxet River empties into the Providence River in the upper Narragansett Bay. The downstream boundary condition for the Pawtuxet River HEC-RAS model is the water level in the Narragansett Bay, which is affected by tides,

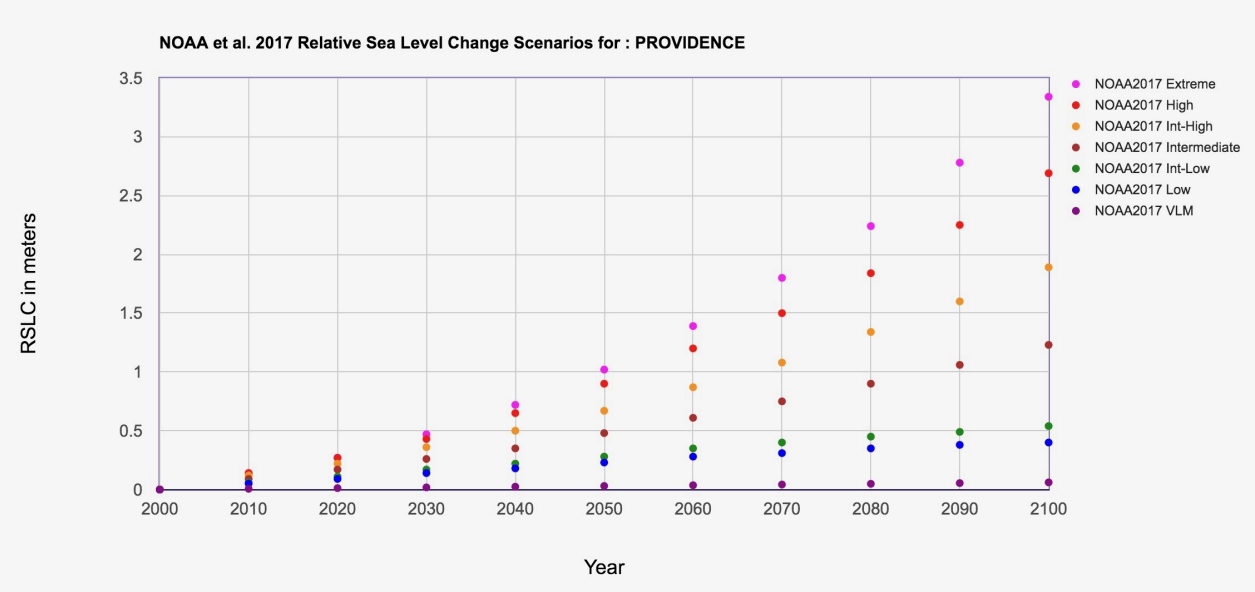

Figure 92: NOAA 2017 relative sea level change scenarios for Providence. (1 m = 3.28 ft).

surge and Sea Level Rise (SLR). Therefore, water level fluctuations in the Narragansett Bay will potentially impact the flood areas around the Main Branch of the Pawtuxet River. Figure 92 shows the projected SLR scenarios according to NOAA. As this figure shows, in the Extreme Scenario, about 12 ft (3.5 m) of SLR is projected in 2100.

Figure 93 shows the NOAA's estimated storm surge for various return periods at the Providence Station, 8454000. The upper and lower confidence intervals are also plotted in gray. To assess the combined impacts of inland and coastal flooding, a 2.2 m (7.2 ft) surge (in addition to tide) which corresponds to 50-year return period, and 2.7 m (8.8 ft) surge which corresponds to 100-year return period on the mean curve were also considered. It should be mentioned that in assessments of the impact of SLR, a future year (e.g., 2100) is usually

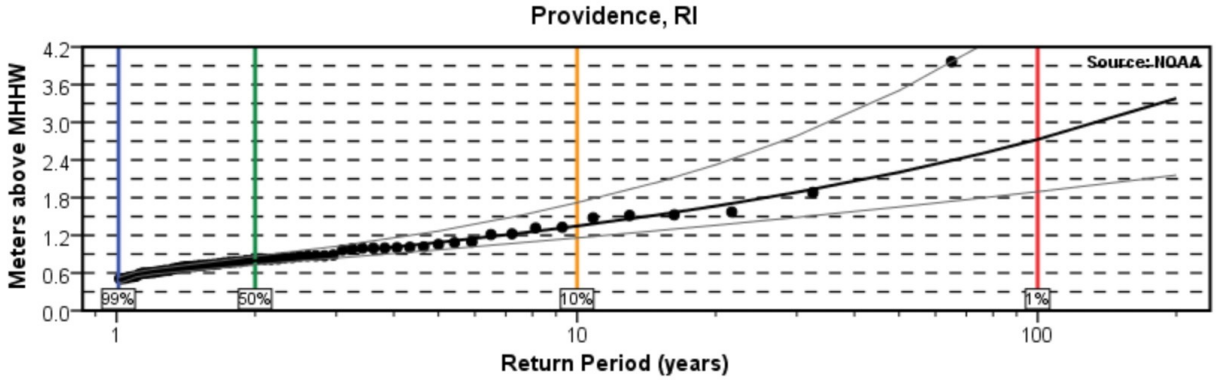

Figure 93: NOAA's estimated storm surge values for various return periods at the Providence Station.

Table 24: Tide, surge and SLR at the downstream point of the Main Branch for three extreme scenarios (1 m = 3.28 ft).

Scenario	Characteristics			
	Tide (ft)	SLR (ft)	Storm surge (ft)	River flood return period (years)
1	2.7	12	–	100
2	2.7	12	7.2 (50-year)	100
3	2.7	12	8.8 (100-year)	100

considered. It is assumed that the return periods of storm surge will not change in the future. This may not be the case as a result of climate change, but we made this assumption for simplicity. This analysis shows the impact of SLR when the sea level rises up to 3.5 m (12 ft) in the future. We assessed three scenarios to look at the effects of tides, surge, and SLR on inland flooding:

1. High tide of 0.83 m (2.7 ft) [30] relative to Mean Sea Level(or 2.5 ft in NAVD88), 12 ft (3.5 m) of SLR, and no storm surge (i.e., effect of SLR on inland flooding).

2. The first scenario when a storm surge of 2.2 m (7.2 ft; 50-year) is added (i.e., combined land and coastal flooding plus SLR)

3. The first scenario when a storm surge of 2.7 m (8.8 ft; 100-year) is added (i.e., combined land and coastal flooding plus SLR).

In all scenarios, the impact of SLR on 100-year inland flooding was investigated. These scenarios are summarized in the Table 24.

HEC-RAS simulations were performed for these scenarios. Figure 94 shows the flooding extent in the downstream of the Pawtuxet River. If we just add SLR and tides to model (i.e., Scenario 1), the impact on riverine flooding extent for this river is not that significant. However, if storm surge is added (e.g. a wet hurricane), the impact of SLR is significant (Figure 94b,c). Increased flooding extent is marked by yellow in the figure which can reach I-95 for these scenarios. Therefore, SLR can increase the risk of flooding during combined inland and coastal flooding.

[30] https://tidesandcurrents.noaa.gov/

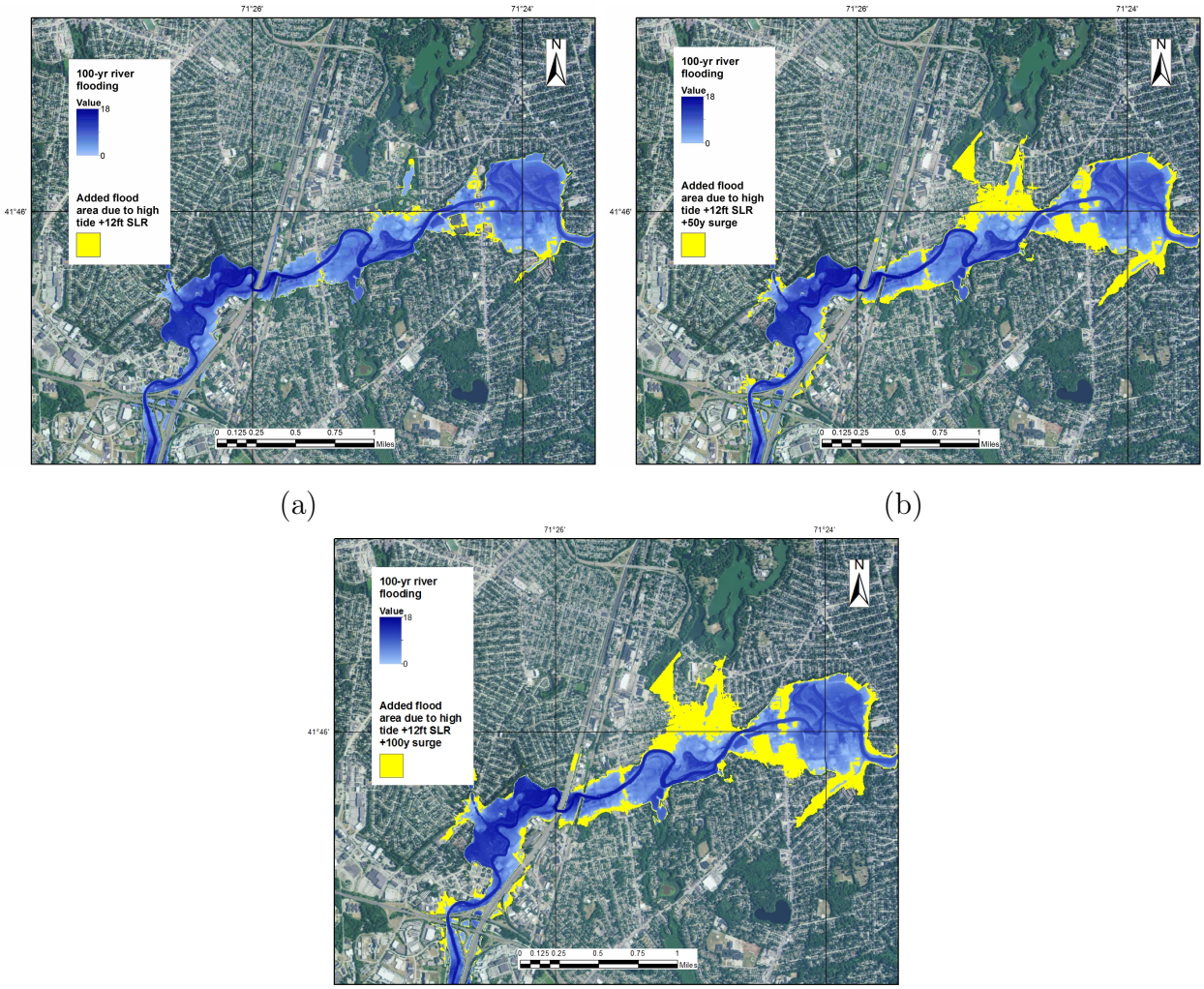

Figure 94: 100-year flood water depth and the increased extent of flooding for three scenarios in the Main Branch: 12 ft SLR plus 2.7 ft of tide (a); 12 ft SLR plus 2.7 ft tide plus 7.2 ft (50-yr) surge (b); 12 ft SLR plus 2.7 ft tide plus 8.8 ft (100-yr) surge (c). The yellow areas show the increased flooded area due to tide, SLR, and surge.

6.2.7 Flood Mitigation at the Warwick Wastewater Treatment Facility

The Warwick Wastewater Treatment Facility is located at 125 Arthur W. Devine Boulevard, Warwick, next to the I-95. It was established in 1962 to collect and treat the wastewater for the city of Warwick. The effluent of the treatment facility is discharged to the Pawtuxet River. In the March 2010 event, the Warwick Wastewater Treatment Facility and its remote pumping stations were flooded due to the high rainfall and flooding in the Pawtuxet River.

Figure 95 shows a photograph of the flooded Warwick Wastewater Treatment Facility during the March 2010 flood event. Following the March 2010 extreme events, the authorities

initiated efforts to mitigate the flooding around the facility and prevent pollution. They constructed a levee all around the facility, elevated critical pumping stations, as well as modifying impacted structures. In this section, we modeled the new levee around the Warwick Wastewater Treatment Facility to examine its effectiveness in future flood mitigation.

Figure 95: Warwick Wastewater Treatment Facility during the flood in March 2010.

In order to model the Warwick Wastewater Treatment Facility levees, we used details of levees (Figure 96). Based on these information, the elevation of the levees is 34.5 ft. with respect to NGVD 29 datum. Therefore, the levee elevation with respect to NAVD 88 is 33.66 ft (0.84 ft change due to datum).

Three of the river cross sections pass through the Warwick Wastewater Treatment Facility in the HEC-RAS river model. The location of the cross sections relative to the Warwick

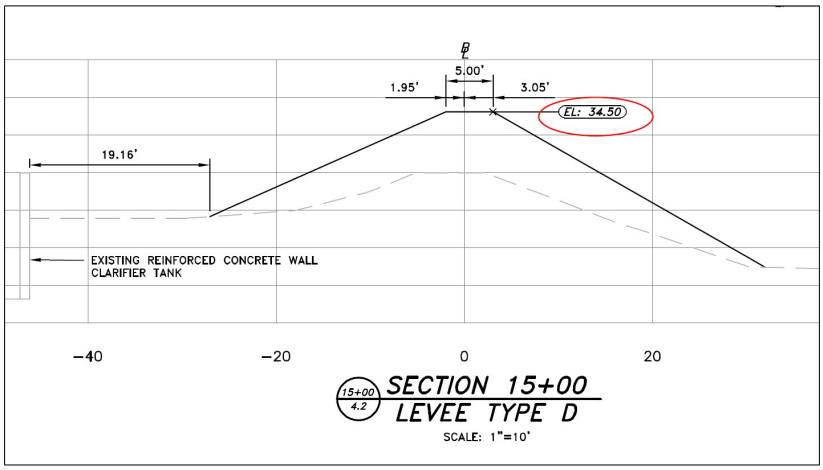

Figure 96: Warwick Wastewater Treatment Facility Levees (Pare Corporation, 2016)

31

Wastewater Treatment Facility can be seen in Figure 97; the Warwick Wastewater Treatment Facility and levee structures are within the red outline on the map, each of the river cross section 30500.50, 31385.16, and 32037.30 are drawn in green, the Pawtuxet River is outlined in blue, and the direction of flow in the river is shown with the dark blue arrow.

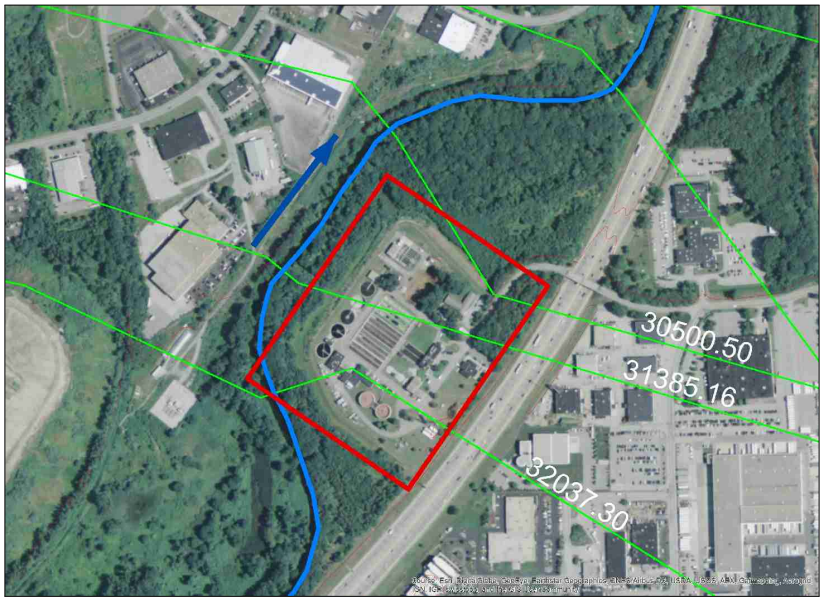

Figure 97: Location of the Warwick Wastewater Treatment Facility, outlined in red. Levee structures are within Warwick Wastewater Treatment Facility perimeter. Green lines show river cross section locations, labeled with cross section identifier numbers. Blue line outlining Pawtuxet River, dark blue arrow showing flow direction of the river.

Table 25: Maximum water elevation in the vicinity of the Warwick Warwick Wastewater Treatment Facility. The levee elevation is 33.66 ft (NAVD88).

Cross Section	Maximum water elevation (NAVD88,ft)		
	return period (years)		
	50	100	500
30500.5	25	26.5	30.5
31385.16	25	26.5	30.5
32037.3	25.4	26.9	30.8

The levee was added to each of three cross section to analyze the water level in the river in the vicinity of the Warwick Wastewater Treatment Facility. Running the model for return periods of 50-, 100-, and 500-year, Table 25 summarizes the values for water elevation around

the Warwick Wastewater Treatment Facility. From the table, we observe that the value of maximum elevation in each cross section is less than the levee height of 33.66 ft.

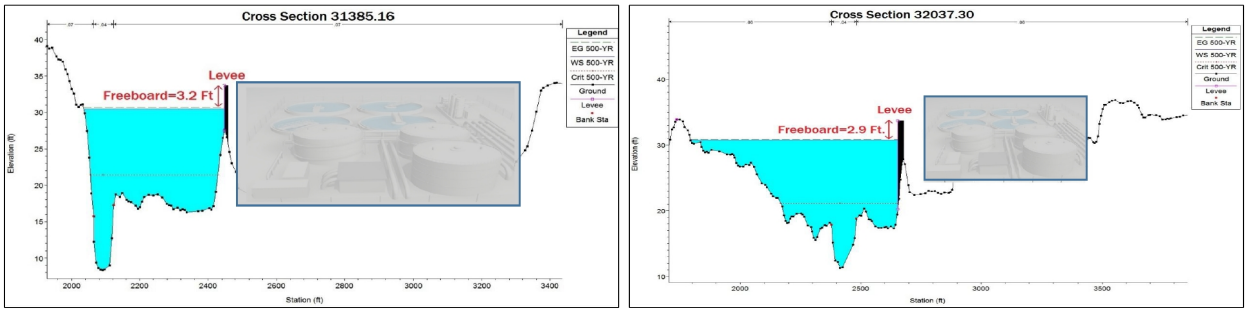

(a) *(b)*

Figure 98: Elevation plots for a 500-year flooding event, at cross sections 31385.16 and 32037.30 adjacent to the Wastewater Treatment Facility. Levee structure location marked, as well as corresponding freeboard.

Figure 98 shows the elevation plots at two of the river cross sections adjacent to the Warwick Wastewater Treatment Facility. Figure 98a shows that the freeboard with the levee in place at river cross section 31385.16 is 3.2 ft, and Figure 98b shows the freeboard for cross section 32037.30 is 2.9 ft for a 500-year flood. Therefore, based on the information provided, we have shown that the new levees mitigate the floods if the levee structure can resist the erosion caused by flood flows.

Transferring results to HEC-GeoRAS, Figure 99 shows the flooding map for 100 and 500-year events around the Warwick Wastewater Treatment Facility. As this figure shows, the

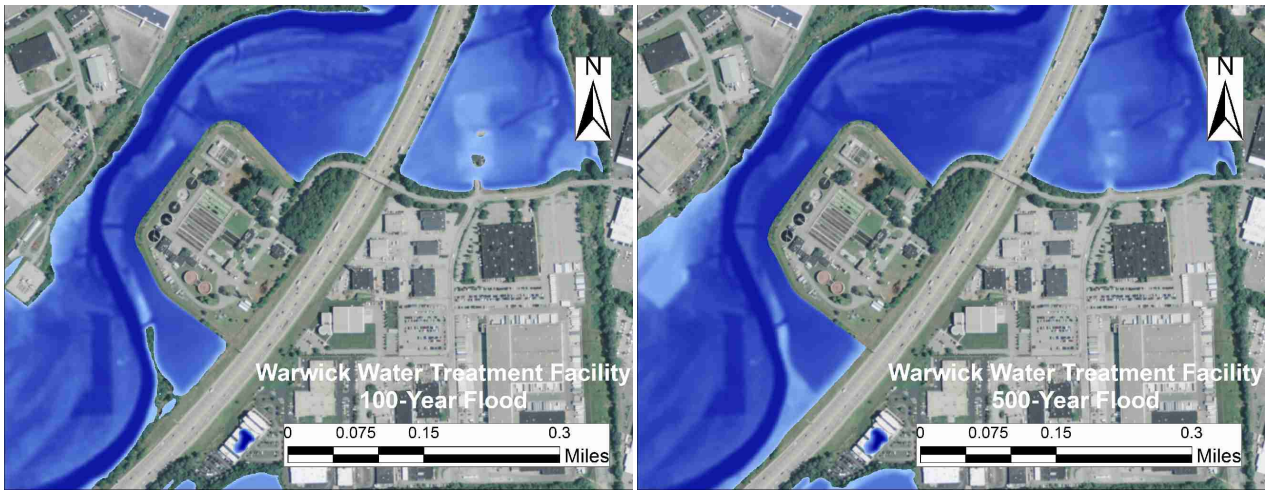

Figure 99: The Warwick Wastewater Treatment Facility is protected by its levee for a 100-year event (left) and a 500-year event (right).

Wastewater Treatment Facility is protected from flooding with the newly constructed levee for 100- and 500-year events.

7 Summary and Conclusions

7.1 Overview of the Results

This report has presented the results for the integrated watershed and river modeling of the Pawtuxet River. The project was motivated by the extreme flooding that took place in March 2010 and impacted the communities of Rhode Island, and the Mid-Atlantic and New England states in general.

The project deliverables and objectives are met: developing a validated, spatially distributed watershed/river model for the Pawtuxet River and Watershed; assessment of the impacts of watershed and river structures such as reservoirs, dams, debris, and levees on flooding.

We have presented the watershed/river, observed, and modeled data sources used in the modeling and validation processes. We have also discussed the details of HEC-HMS, HEC-RAS models, as well as the concepts behind the modeling. Model parameters and methods, calibration and validation, and an uncertainty analysis were also described. The main contributions and recommendations are summarized here.

7.2 Main Contributions

The main results and contributions from our integrated Pawtuxet River watershed and river model are listed below:

- The integrated Pawtuxet River watershed and river model developed here can predict and help mitigate flooding damages in future extreme flooding situations. The model can generate the flooding maps for any event and produce public access to them via STORMTOOLS website.

- The models and methodology provide a framework for a real-time flood forecasting tool for inland flooding. The methodology presented here is applicable to other rivers and watershed areas in Rhode Island. For forecast applications, we strongly recommend the ensemble approach to represent a rainfall event.

- The uncertainty analysis shows that the model is sensitive to errors in the input precipitation data more than other parameters; ensemble approaches give a more accurate and reliable range of model predictions. This can be extended to flooding maps by providing maps with a level of uncertainty.

- The simulation of the Scituate Reservoir in the watershed model shows that the reservoir elevation can be controlled to manage the flooding. The generated capacity by adjusting the reservoir water level to 4 ft below the spillway crest or above it by adding gates can reduce the peak discharge by about 60% in an event of a 500-year return period, for the North Branch. Regulating the discharge of water from this reservoir is the most effective way to control flooding. However, more study should be carried out to design a structure with minimum impact on the dam structure and upstream areas. Also, water supply demand which is the main function of the reservoir should be met.

- The flood inundation maps for the Pawtuxet River have been integrated into the Rhode Island STORMTOOLS coastal flood maps system. Flood maps and depths for 10-, 50-, 100-, and 500-year flood events are available in public domain.[32]

- Effect of dams on flooding are found to be largely local, not cumulative, and effect of each dam can be investigated locally.

- For flood mitigation in the area, we found that removal of the Pontiac Dam in the Main Branch of the Pawtuxet River would decrease flood area extent by 31.8%, 26.1%, and 5.4% in a 50, 100, and 500-year flood, respectively. Nevertheless, the Scituate Reservoir can mitigate flood everywhere and is more effective for flood risk management.

- The presence of debris significantly increases flooding extent. We recommend that their effects be considered in risk assessments which is not included in FEMA FIRMs.

- Flat River reservoir also affects flooding in the South and Main Branch, but it is less effective in reducing risk compared to Scituate Reservoir as its area is much smaller.

- The Warwick Wastewater Treatment Facility Levee installation is found to be effective in control of flooding in 500-year flood scenario. The levees at the Warwick Wastewater Treatment Facility are sufficient for preventing flooding at the facility for a 500-year flood event.

- The projected sea level rise can lead to increased inland flooding in the Pawtuxet River, particularly, near the Providence River during concurrent coastal and inland floods. This is an additional risk associated with hurricanes that contain considerable rain (i.e., wet hurricanes).

[32] http://edc.maps.arcgis.com/home/webmap

7.3 Recommendations

Based on our analysis and results, the following recommendations can be made:

- An operational flood forecasting model for the Pawtuxet River watershed area can be setup based on the model. The model and results here build the framework for such a real time flood forecasting tool for the entire watershed, and the methodology presented here can also be applied to other rivers and watersheds in Rhode Island. We recommend that this model be maintained and updated as a real time flood forecasting web-based tool, available to public and emergency managers.

- Study the consequences of possible catastrophic dam failures during major floods, such as effects on water quality, flooding, and negative impacts on river ecosystems and Narragansett Bay.

- Simulating the impacts of climate change on the watershed-river flooding risk. This can include assessing the risks of flooding on the communities around the river. Some studies show that the extreme rainfall events and average precipitation rate are increasing in this area due to climate change.

- Installing a stream gauge downstream of the Scituate Reservoir. We have shown that the Scituate Reservoir has a significant impact on the flooding in the watershed. A measurement station at this location would provide valuable observational data to more accurately observe the impact of this reservoir on flooding.

- Installing a meteorological station in the watershed (in upland areas). Currently, the only precipitation gauge in the Pawtuxet River watershed is located at the T.F. Green Airport in Warwick, RI. Available precipitation observations in the watershed are limited to a point measurement. Adding another gauge would allow for more accurate flooding prediction near the Scituate Reservoir, and elsewhere decrease the uncertainty.

- Effective management of the Scituate Reservoir for flood control. This may involve controlling water elevation in the reservoir with approaching large storms, or constructing a controlled spillway. The Scituate Reservoir is constructed for drinking water supply, and it is ideal to keep the current capacity at the spillway crest level. However, additional capacity can be added by gates. This requires further study to assess the impacts on the structure of the dam and upstream areas.

A Streamflow Data in Selected USGS Stations

Tables 26, 27, and 28 summarize the start dates for various available hourly, daily, and monthly data in the USGS stream gauges in the Pawtuxet River watershed. Table 26 summarizes the start dates for hourly streamflow data and annual peak data. Tables 27, and 28 summarize start dates for available temperature, discharge and specific conductance for daily, monthly, and annual data, respectively[33].

Table 26: Availability of hourly data at selected stream gauge stations. See Figure 21 for gauge locations.

Data (hourly)		
	Hourly Streamflow	Annual Peak Flow
Stations	Start Date	Start Date
1115190	Feb 10, 2009	Apr 22, 2009
1115187	Oct 1, 2007	Dec 24, 1994
1115265	Feb 5, 2009	Jul 24, 2009
1115280	May 1, 2009	Jul 24, 2009
1115275	Oct 1, 2009	Jul 24, 2009
1115110	Feb 20, 2009	Jul 24, 2009
1115114	Feb 9, 2009	Jul 24, 2009
1115098	Oct 1, 2007	Dec 24, 1994
1115170	Feb 25, 2009	Jul 24, 2009
1115183	Feb 6, 2009	Jul 24, 2009
1115630	Oct 1, 2007	Jan 25, 1964
1116000	Oct 1, 2007	Mar 3, 1936
1116500	Oct 1, 2007	Jan 15, 1940

[33] http://waterdata.usgs.gov/

Table 27: Availability of daily data at selected stream gauge stations. See Figure 21 for gauge locations.

	Data (Daily)		
	Temperature (°C)	Discharge (CFS)	Specific Conductance
Stations	Start Date	Start Date	Start Date
1115190	Feb 9, 2000	Oct 1, 2008	Feb 9, 2000
1115187	Feb 1, 2000	Mar 22, 1994	Feb 1, 2000
1115265	Feb 1, 2000	Oct 1, 2008	Feb 1, 2000
1115280	Feb 4, 2000	Oct 1, 2008	Feb 4, 2000
1115275	Jan 15, 2000	–	Jan 15, 2000
1115110	Jan 29, 2000	Oct 1, 2008	Jan 29, 2000
1115114	Feb 10, 2009	Oct 1, 2008	Jun 29, 2009
1115098	Jan 29, 2000	Jun 23, 1994	Feb 29, 2000
1115170	Mar 10, 2000	Oct 1, 2008	Mar 10, 2000
1115183	Jan 25, 2000	Oct 1, 2008	Jan 26, 2000
1115630	–	Nov 26, 19636	–
1116000	–	Oct 1, 1940	–
1116500	–	Dec 6, 1939	–

Table 28: Availability of monthly data at selected stream gauge stations. See Figure 21 for gauge locations.

	Data (Monthly Statics)		
	Temperature (°C)	Discharge (CFS)	Specific Conductance
Stations	Start Date	Start Date	Start Date
1115190	Feb 2000	Oct 2008	Feb 2000
1115187	Feb 2000	Mar 1994	Feb 2000
1115265	Feb 2000	Oct 2008	Feb 2000
1115280	Feb 2000	Oct 2008	Feb 2000
1115275	Jan 2000	–	Jan 2000
1115110	Jan 2000	Oct 2008	Jan 2000
1115114	Feb 2009	Oct 2008	Jun 2009
1115098	Jan 2000	Jun 1994	Jan 2000
1115170	Mar 2000	Oct 2008	Mar 2000
1115183	Jan 2000	Oct 2008	Jan 2000
1115630	–	Nov 1963	–
1116000	–	Oct 1940	–
1116500	–	Dec 1939	–

References

Ackerman, C. T. (2009). *HEC-GeoRAS GIS Tools for Support of HEC-RAS using ArcGIS: User's manual*. US Army Corps of Engineers, Institute for Water Resources, Hydrologic Engineering Center.

Brunner, G. W. (2001). *HEC-RAS River Analysis System: User's manual*. US Army Corps of Engineers, Institute for Water Resources, Hydrologic Engineering Center.

Brunner, G. W. (2016). *HEC-RAS River Analysis System: Hydraulic Reference Manual*. US Army Corps of Engineers, Hydrologic Engineering Center.

Chen, S.-H. (2015). *Hydraulic Strucures*. Springer.

Coleman, P. J. (1963). *The transformation of Rhode Island 1790-1860*. Brown University Press.

Demeritt, D., Cloke, H., Pappenberger, F., Thielen, J., Bartholmes, J., and Ramos, M.-H. (2007). Ensemble predictions and perceptions of risk, uncertainty, and error in flood forecasting. *Environmental Hazards*, 7(2):115–127.

Doan, J. et al. (2000). Geospatial hydrologic modeling extension HEC-GeoHMS userâĂŹs manual version 1.0. *US Army Corps of Engineers Hydrologic Engineering Center, Davis, California, USA*.

Feldman, A. D. (2000). *Hydrologic modeling system HEC-HMS: technical reference manual*. US Army Corps of Engineers, Hydrologic Engineering Center.

Halberg, H. N., Knox, C. E., Pauszek, F., et al. (1961). *Water resources of the Providence area, Rhode Island*. US Government Printing Office.

Knebl, M., Yang, Z.-L., Hutchison, K., and Maidment, D. (2005). Regional scale flood modeling using NEXRAD rainfall, GIS, and HEC-HMS/RAS: a case study for the san antonio river basin summer 2002 storm event. *Journal of Environmental Management*, 75(4):325–336.

Lagasse, P., Clopper, P., Zevenbergen, L., Spitz, W., and Girard, L. (2010). Effects of debris on bridge pier scour, NCHRP Rep. 653. *Transp. Res. Board, Washington, D. C.*

Lim, K. J., Engel, B. A., Muthukrishnan, S., and Harbor, J. (2006). Effects of initial abstraction and urbanization on estimated runoff using CN technology.

Scharffenberg, W. A. and Fleming, M. J. (2006). *Hydrologic modeling system HEC-HMS: User's manual*. US Army Corps of Engineers, Hydrologic Engineering Center.

Sordo-Ward, A., Garrote, L., Bejarano, M. D., and Castillo, L. G. (2013). Extreme flood abatement in large dams with gate-controlled spillways. *Journal of Hydrology*, 498:113–123.

Spaulding, M. L., Grilli, A., Damon, C., Crean, T., Fugate, G., Oakley, B. A., and Stempel, P. (2016). STORMTOOLS: Coastal Environmental Risk Index (CERI). *Marine Science and Engineering*.

USBR (1977). *Design of Arch Dams*. United States Department of the Interior, BUREAU OF RECLAMATION, Colorado, USA.

USDA, S. (1986). Urban hydrology for small watersheds. *Tech Release*, 55:2–6.

Zarriello, P. J., Ahearn, E. A., and Levin, S. B. (2012). Magnitude of flood flows for selected annual exceedance probabilities in Rhode Island through 2010. Technical report, US Geological Survey.

Zarriello, P. J. and Bent, G. C. (2011). Elevation of the March-April 2010 flood high water in selected river reaches in Rhode Island. Technical report, US Geological Survey.